

DOE/BC/14988-8
(DE96001265)

INCREASED OIL PRODUCTION AND RESERVES UTILIZING
SECONDARY/TERTIARY RECOVERY TECHNIQUES ON SMALL
RESERVOIRS IN THE PARADOX BASIN, UTAH

Annual Report

By
T. C. Chidsey, Jr.

February 1997

Performed Under Contract No. DE-FC22-93BC14988

Utah Geological Survey
Salt Lake City, Utah



National Petroleum Technology Office
U. S. DEPARTMENT OF ENERGY
Tulsa, Oklahoma

DISCLAIMER

This report was prepared as an account of work sponsored by an agency of the United States Government. Neither the United States Government nor any agency thereof, nor any of their employees, makes any warranty, expressed or implied, or assumes any legal liability or responsibility for the accuracy, completeness, or usefulness of any information, apparatus, product, or process disclosed, or represents that its use would not infringe privately owned rights. Reference herein to any specific commercial product, process, or service by trade name, trademark, manufacturer, or otherwise does not necessarily constitute or imply its endorsement, recommendation, or favoring by the United States Government or any agency thereof. The views and opinions of authors expressed herein do not necessarily state or reflect those of the United States Government.

This report has been reproduced directly from the best available copy.

Available to DOE and DOE contractors from the Office of Scientific and Technical Information, P.O. Box 62, Oak Ridge, TN 37831; prices available from (615) 576-8401.

Available to the public from the National Technical Information Service, U.S. Department of Commerce, 5285 Port Royal Rd., Springfield VA 22161

DOE/BC/14988-8
Distribution Category UC-122

**Increased Oil Production and Reserves Utilizing Secondary/Tertiary Recovery
Techniques On Small Reservoirs In The Paradox Basin, Utah**

Annual Report

**By
Thomas C. Chidsey, Jr.**

February 1997

Work Performed Under Contract No. DE-FC22-94BC14988

**Prepared for
U.S. Department of Energy
Assistant Secretary for Fossil Energy**

**Rhonda Lindsey, Project Manager
Bartlesville Project Office
P.O. Box 1398
Bartlesville, OK 74005**

**Prepared by:
Utah Geological Survey
Salt Lake City, Utah 84114**

CONTENTS

ABSTRACT	ix
EXECUTIVE SUMMARY	xi
ACKNOWLEDGEMENTS	xiii
1. INTRODUCTION	1-1
2. REGIONAL FACIES EVALUATION AND OUTCROP	
RESERVOIR ANALOGUES	2-1
2.1 Regional Facies Evaluation	2-1
2.1.1 Paleogeographic Setting	2-1
2.1.2 Generalized Regional Facies Belts	2-2
2.1.3 Study Results	2-3
2.2 Outcrop Reservoir Analogues	2-3
2.2.1 Field Work	2-3
2.2.2 Study Results	2-4
2.3 References	2-6
3. PROJECT FIELDS, NAVAJO NATION, SAN JUAN COUNTY, UTAH	3-1
3.1 Data Collection	3-2
3.2 Field Studies	3-2
3.2.1 Runway Field	3-4
3.2.2 Heron North	3-5
3.2.3 Mule Field	3-5
3.2.4 Blue Hogan	3-6
3.2.5 Anasazi Field	3-7
3.3 New Development Wells	3-7
3.3.1 Drilling Rationale	3-7
3.3.2 Anasazi No. 6H-1 Well, Anasazi Field	3-8
3.3.3 Results	3-9
3.4 References	3-11
4. GEOLOGICAL CHARACTERIZATION OF THE CARBONATE	
RESERVOIR IN THE DESERT CREEK ZONE	4-1
4.1 Location, Geometry, and General Stratigraphy	4-1
4.2 Reservoir Architecture	4-2
4.3 Reservoir Model Geometry	4-4
4.4 Seismic Constraints	4-12
4.5 Reservoir Model Design	4-15
4.6 References	4-16

5. ENGINEERING RESERVOIR CHARACTERIZATION OF THE CARBONATE RESERVOIR IN THE DESERT CREEK ZONE	5-1
5.1 Review of Existing Field Data and Re-evaluation of Well Test Data	5-1
5.1.1 Field Data Review	5-1
5.1.2 Well Test Data Re-Evaluation	5-2
5.2 Fluid Characterization	5-7
5.2.1 Sample Preparation and Compositional Analysis	5-7
5.2.1.1 Separator Oils.	5-8
5.2.1.2 Separator Gases.	5-8
5.2.1.3 Dead Oil.	5-8
5.2.2 Fluid Recombination and Swelling Tests	5-8
5.2.2.1 Fluid Recombination.	5-8
5.2.2.2 Swelling Tests.	5-9
5.2.3 Separator Tests	5-10
5.2.4 Summary	5-11
5.3 Rock Characterization	5-11
5.3.1 Relative Permeability Measurements	5-12
5.3.1.1 Fluid Measurements.	5-12
5.3.1.2 Experimental Procedures.	5-12
5.3.1.3 Resaturation and K_{ew} Measurements.	5-13
5.3.1.4 Initial Oil/Brine Drainage Experiment and Aging.	5-13
5.3.1.5 Brine/Oil Imbibition Capillary Pressure Test.	5-13
5.3.1.6 K_{ew} Measurements and Oil/Brine Secondary Drainage Test. .	5-13
5.3.1.7 Brine/Oil Imbibition Relative Permeability Test.	5-13
5.3.1.8 Oil/Brine Drainage Relative Permeability Test.	5-16
5.3.1.9 Gas/Oil Capillary Pressure and Relative Permeability Experiment.	5-16
5.3.1.10 Final Saturation Determination via Dean-Stark.	5-22
5.3.1.11 Gas Property Measurements.	5-22
5.3.1.12 Saturation and K_{wv}	5-22
5.3.1.13 Primary Drainage Capillary Pressure Measurements.	5-22
5.3.1.14 U.S. Bureau of Mines and Amott Wettability Indices.	5-22
5.3.1.15 Bond Number versus S_{or}/S_{oi}	5-23
5.3.1.16 Summary.	5-23
5.3.2 Rock Compressibility Measurements	5-24
5.4 References	5-26
6. MECHANISTIC RESERVOIR SIMULATION STUDIES	6-1
6.1 Introduction	6-1
6.2 Model Description	6-1
6.3 Fluid Properties and Production Data	6-1
6.4 Stimulation Study Procedure	6-2
6.5 Study Results	6-2
6.6 Future Work	6-5

7. TECHNOLOGY TRANSFER 7-1
 7.1 Utah Geological Survey Petroleum News and Survey Notes 7-1
 7.2 Workshops, Presentations, and the 1996 Paradox Basin Symposium 7-3
 7.3 Addressing Regulatory Issues 7-4

APPENDIX A: PARADOX BASIN PROJECT FIELD SUMMARIES A-1

APPENDIX B: COMPOSITIONAL ANALYSES OF OIL AND GAS B-1

APPENDIX C: SWELLING TEST DATA C-1

FIGURES

Figure 1.1. Five shallow-shelf carbonate fields (dark shading with names in bold type) on the Navajo Nation, San Juan County, Utah are targeted for geological and reservoir characterization	2-1
Figure 2.1. Generalized regional facies belts for Desert Creek zone, Pennsylvanian Paradox Formation, southeastern San Juan County, Utah.	2-2
Figure 2.2. Location of Paradox Formation outcrops in the Wild Horse Canyon area along the San Juan River, southeastern Utah.	2-4
Figure 2.3. Outcrops in the Ismay zone of the Paradox Formation, Wild Horse Canyon near the San Juan River, southeastern Utah.	2-5
Figure 3.1. Representative seismic line, shaded according to amplitude variations, across Mule field.	3-3
Figure 3.2. Three-dimensional "net" view to the southwest of the surface on top of the Mississippian Leadville Limestone and the north-bounding faults which control the localization of small algal and other carbonate buildups	3-4
Figure 3.3. Core surface view of highly productive, dolomitized, phylloidal algal plate bafflestone from the Mule No. 31-M well	3-6
Figure 3.4. Location of the first project development well, the Anasazi No. 6H-1, drilled in the Anasazi field	3-9
Figure 3.5. A set of CAT scans of two mutually perpendicular longitudinal-axial sections of each of the four core plugs taken from the Anasazi No. 6H-1 well	3-10
Figure 4.1. Gross Desert Creek isopach based on geophysical well log and seismic data, Anasazi field, sections 5 and 6, T. 42 S., R. 24 E., Salt Lake Base Line, San Juan County, Utah.	4-1
Figure 4.2. Stratigraphic cross section across Anasazi field displaying reservoir lithotypes, flooding surfaces, and facies relations within the Desert Creek platform, mound-core, and supra-mound intervals based on core.	4-3
Figure 4.3. Computed geophysical well logs and lithology plots of the Desert Creek zone ..	4-5
Figure 4.4. Photomicrographs of thin sections (plane light view) showing low-quality architectural lithotypes (24x).	4-8
Figure 4.5. Photomicrographs of thin sections (plane light view) showing high-quality architectural lithotypes (24x).	4-9
Figure 4.6. Photomicrographs of thin sections (plane light view) showing moderate- to high-quality architectural lithotypes (24x).	4-10
Figure 4.7. Photomicrograph of a thin section (plane light view) showing a phylloid algal bafflestone from the Anasazi No. 1 well	4-11
Figure 4.8. Anasazi reservoir gridded isolith map	4-12
Figure 4.9. Reservoir quality index (RQI) map with seismic data points (+), Anasazi reservoir.	4-13
Figure 4.10. Estimation of average porosity from RQI, Anasazi reservoir.	4-14
Figure 4.11. Map of average porosity derived from the RQI, Anasazi reservoir.	4-15

Figure 5.1. Anasazi No. 1 well test (1991) displaying pressure difference and pressure derivative match.	5-5
Figure 5.2. Anasazi No. 1 well test (1991) displaying superposition time vs. pressure match.	5-6
Figure 5.3. Anasazi No. 1 well test (1991) displaying pressure vs. time match.	5-6
Figure 5.4. Comparison of the (C30+) weight-percent composition measured for the flashed separator oil (cylendar W8301) and dead oil samples (6H-1-limestone, 6H-1-dolomite, and 5L-3).	5-9
Figure 5.5. Brine - oil primary imbibition capillary pressure curves from elevated temperature, automated centrifuge data for Anasazi No. 6H-1 well.	5-14
Figure 5.6. Oil - brine secondary drainage capillary pressure curves from elevated temperature, automated centrifuge data for Anasazi No. 6H-1 well.	5-15
Figure 5.7. Oil - brine relative permeability curves from elevated temperature, automated centrifuge data for Anasazi No. 6H-1 well.	5-16
Figure 5.8. Oil - brine primary drainage capillary pressure curve from elevated temperature, automated centrifuge data for Anasazi No. 6H-1 well.	5-17
Figure 5.9. Gas - oil drainage capillary pressure curve from elevated temperature, automated centrifuge data for Anasazi No. 6H-1 well.	5-18
Figure 5.10. Gas - oil relative permeability curves from elevated temperature, automated centrifuge data for Anasazi No. 6H-1 well.	5-19
Figure 5.11. Bond number vs. S_{or}/S_{oi} curves from elevated temperature, automated centrifuge data for Anasazi No. 6H-1 well.	5-23
Figure 6.1. Results of two-dimensional reservoir simulation of the Anasazi field (k_v/k_h ratio = 0.02).	6-3
Figure 6.2. Two-dimensional reservoir simulation of the Anasazi field showing gas saturation for XZ plane after 1,461 days of production on January 1, 1994.	6-4
Figure 6.3. Schematic reservoir simulator model of the Anasazi reservoir.	6-4
Figure 7.1. UGS Survey Notes and Petroleum News provide project updates, publication notices, and announcements of presentations to both industry and lay public.	7-2
Figure 7.2. Participants at the UGS-sponsored core workshop, during the 1994 AAPG Annual Convention in Denver, Colorado, examine cores representing various types of oil-producing reservoirs from the Paradox basin project fields.	7-3

TABLES

Table 3.1. Cumulative production of project fields in the Paradox basin, San Juan County, Utah.	3-1
Table 3.2. Geological and engineering data for project fields in the Paradox basin, San Juan County, Utah.	3-3
Table 4.1. Average reservoir properties of architectural lithotypes, Anasazi field.	4-7
Table 5.1. Swelling test data for the Anasazi No. 5L-3 oil at 130°F (54°C).	5-10
Table 5.2. Separator test volumetric data.	5-10
Table 5.3. Separator test-produced GOR.	5-11
Table 5.4. Brine composition.	5-12
Table 5.5. Fluid properties.	5-12
Table 5.6. Permeability and porosity data summary for the Anasazi No. 6H-1.	5-20
Table 5.7. Pre-test sample conditions and physical properties for selected samples from the Anasazi Nos. 1 and 6H-1 wells.	5-24
Table 5.8. Target pressures for simulated <i>in-situ</i> conditions.	5-25
Table 5.9. Compressibilities determined from hydrostatic compression for samples from the Anasazi Nos. 1 and 6H-1 wells.	5-25
Table 5.10. Quasi-static mechanical properties determined from triaxial compression for samples from the Anasazi Nos. 1 and 6H-1 wells.	5-26
Table 5.11. Parameters determined during uniaxial strain/pore pressure drawdown segment.	5-26
Table 6.1. Analysis of gravity drainage behavior.	6-5
Table B.1. Composition of Anasazi No. 5-L separator oil cylinder No. W8301 at 73°F (23°C) and 1,014 psia (6,992 kpa).	B-2
Table B.2. Composition of Anasazi No. 5-L separator oil cylinder No. W4635 at 73°F (23°C) and 1,014 psia (6,992 kpa).	B-4
Table B.3. Composition of Anasazi No. 5-L separator gas cylinder No. 5EK088.	B-6
Table B.4. Composition of Anasazi No. 5-L separator gas cylinder No. 6EK087.	B-7
Table B.5. Dead oil liquid composition of the Anasazi flashed separator oils and dead oils. ...	B-8
Table B.6. Composition of Anasazi No. 5-L recombined separator oil at 70°F (21°C) and 3,014 psia (20,782 kpa).	B-10
Table B.7. Composition of Anasazi No. 5-L recombined oil flashed to 2,050 psia (14,135 kpa) at 130°F (54°C).	B-12
Table B.8. Vapor compositional data for the two separator tests.	B-14
Table C.1. Swelling test CO ₂ concentration data.	C-2
Table C.2. Relative volumes of the liquid and vapor phases as a function of pressure at 130°F (54°C) (CO ₂ concentration = 20 mole percent).	C-2
Table C.3. Properties of the saturated fluid with 20 mole percent CO ₂ at 130°F (54°C).	C-3
Table C.4. Relative volumes of the liquid and vapor phases as a function of pressure at 130°F (54°C) (CO ₂ concentration = 40 mole percent).	C-3
Table C.5. Properties of the saturated fluid with 40 mole percent CO ₂ at 130°F (54°C)	C-4

Table C.6. Relative volumes of the liquid and vapor phases as a function of pressure at 130°F (54°C) (CO₂ concentration = 60 mole percent) C-4

Table C.7. Visual determination of the bubble point pressure using small pressure drops for the Anasazi oil with 60 mole percent CO₂ concentration. C-5

Table C.8. Properties of the saturated fluid with 60 mole percent CO₂ at 130°F (54°C). C-5

Table C.9. Relative volumes of the liquid and vapor phases as a function of pressure at 130°F (54° C) (CO₂ concentration = 75 mole percent). C-6

Table C.10. Properties of the saturated fluid with 75 mole percent CO₂ at 130°F (54°C). C-6

ABSTRACT

The Paradox basin of Utah, Colorado, and Arizona contains nearly 100 small oil fields producing from carbonate buildups or mounds within the Pennsylvanian (Desmoinesian) Paradox Formation. These fields typically have one to four wells with primary production ranging from 700,000 to 2,000,000 barrels of oil per field at a 15 to 20 percent recovery rate. At least 200 million barrels of oil is at risk of being unrecovered in these small fields because of inefficient recovery practices and undrained heterogeneous reservoirs. Five fields (Anasazi, Mule, Blue Hogan, Heron North, and Runway) within the Navajo Nation of southeastern Utah are being evaluated for waterflood or carbon-dioxide-miscible flood projects based upon geological characterization and reservoir modeling. The results can be applied to other fields in the Paradox basin and the Rocky Mountain region, the Michigan and Illinois basins, and the Midcontinent.

Three generalized facies belts are present in the Desert Creek zone of the Paradox Formation: (1) open-marine, (2) shallow-shelf and shelf-margin, and (3) intra-shelf, salinity-restricted facies. Conventional cores show that the five fields are located in the shallow-shelf and shelf-margin facies belt and three compositional reservoir buildup types are present: (1) phylloid algal, (2) bioclastic calcarenite, and (3) bryozoan-dominated. Outcrops of the Paradox Formation Ismay zone along the San Juan River of southeastern Utah, provide small-scale analogues of the reservoir heterogeneity, flow barriers and baffles, and lithofacies geometry observed in the fields.

Procedures for quantitatively characterizing the Anasazi field reservoir have been defined and the required data assembled from a variety of sources. To adequately represent the observed spatial heterogeneities in reservoir properties, the mound-core interval phylloid algal bafflestones and overlying supra-mound interval dolomites have been subdivided into ten architecturally distinct lithotypes, each of which exhibits a characteristic set of reservoir properties. Geometries and patterns of spatial arrangement for these lithotypes have been inferred from the outcrop analogue studies and comparison with previous work in nearby Greater Aneth field. Reservoir properties and lithotype characterizations were obtained from cores and logs from the four Anasazi wells. Model constraints on lateral variation in average reservoir porosity and permeability are imposed by data obtained from six interpreted two-dimensional seismic lines and well-test results. The initial three-dimensional reservoir model consists of 50, 2-foot (0.6-m) layers on a 30x50-cell (380 acre [154 ha]) geographic grid, comprising a total of 75,000 grid blocks. A three-stage modeling procedure has been defined and development is well underway; initial geostatistical models of the Anasazi reservoir should be available for conducting full-field simulation studies during the second project year.

The reservoir engineering component of the work completed to date included analysis of production data and well tests, comprehensive laboratory programs, and preliminary mechanistic reservoir simulation studies. Well-test analysis indicated that dual-property models may be used to interpret the pressure response behavior of the Desert Creek zone. The laboratory work completed includes gas-oil and oil-brine relative permeability and capillary pressure measurements on new preserved cores. In addition, reservoir rock wettability measurements were completed. Rock compressibility measurement on both supra-mound (dolomite) and mound-core (limestone) samples were completed and will be used to provide data to more reliably model the liquid expansion phase of Paradox basin reservoir production.

A comprehensive fluid property characterization program was completed. This work includes a suite of carbon dioxide swelling tests using Anasazi field crude oil. Data from this set of experiments, in conjunction with black oil pressure-volume-temperature data obtained on original fluid samples, will be used to calibrate an equation of state for future compositional simulation studies.

Mechanistic reservoir production performance simulation studies were also completed. These studies were used to make a preliminary assessment of the primary production mechanistic behavior of Paradox basin reservoirs. To provide some initial insight into the basic production mechanism of the Anasazi reservoir some simple one- and two-dimensional compositional simulation studies were conducted prior to developing final reservoir description models and the final three-dimensional simulation study. The results showed that despite the major portion of production being from the mound-core interval there is not a corresponding decrease in the oil in place in the mound-core interval. This behavior clearly supports the gravity drainage of oil from the supra-mound interval into the lower mound-core interval from which the producing wells major share of production arises.

The results of this project were transferred to industry and other researchers through a petroleum extension service, a core workshop, displays at national and regional professional meetings, and publications in newsletters.

EXECUTIVE SUMMARY

The primary objective of this project is to enhance domestic petroleum production by demonstration and technology transfer of an advanced-oil-recovery technology in the Paradox basin, southeastern Utah. If this project can demonstrate technical and economic feasibility, the technique can be applied to approximately 100 additional small fields in the Paradox basin alone, and result in increased recovery of 150 to 200 million barrels of oil. This project is designed to characterize five shallow-shelf carbonate reservoirs in the Pennsylvanian (Desmoinesian) Paradox Formation and choose the best candidate for a pilot demonstration project for either a waterflood or carbon-dioxide-flood project. The field demonstration, monitoring of field performance, and associated validation activities will take place within the Navajo Nation, San Juan County, Utah.

The Utah Geological Survey (UGS) leads a multidisciplinary team to determine the geological and reservoir characteristics of typical small shallow-shelf carbonate reservoirs in the Paradox basin. The Paradox basin project team consists of the UGS (prime contractor) Harken Southwest Corporation, and several subcontractors. This research is performed under the Class II Oil Program of the U.S. Department of Energy, Bartlesville Project Office. This report covers research and technology transfer activities from the pre-award period and first project year (June 10, 1995 through February 8, 1995). This work includes evaluation of regional facies belts, outcrop analogues, five selected fields, reservoir modeling, and simulation. The results can be applied to similar reservoirs in many U.S. basins.

Regionally three generalized facies belts were identified: (1) open-marine, (2) shallow-shelf and shelf-margin, and (3) intra-shelf, salinity-restricted facies. Outcrops of the Paradox Formation Ismay zone along the San Juan River of southeastern Utah, provided small-scale analogues of reservoir heterogeneity, flow barriers and baffles, and lithofacies geometry. These characteristics are being used in reservoir simulation models for secondary/tertiary recovery of oil from the small fields in the basin.

Reservoir data, cores and cuttings, geophysical logs, various reservoir maps, and other information from the project fields and regional exploratory wells are being collected. Well locations, production reports, completion tests, core analysis, formation tops, and other data were compiled and entered in a database developed by the UGS. Base maps and new isochron maps covering project fields were prepared and cores were described from selected project wells with special emphasis on bounding surfaces of possible flow units.

The project fields (Anasazi, Mule, Blue Hogan, Heron North, and Runway) have one to three wells with primary production ranging from 700,000 to 2 million barrels of oil per field at a 15 to 20 percent recovery rate. Conventional cores from these fields show that three compositional reservoir types of carbonate buildups are present: (1) phylloid algal, (2) bioclastic calcarenite, and (3) bryozoan-dominated. Production, lithologic, basic reservoir parameters, and other data describing these fields were compiled and analyzed.

The first project development well, the Anasazi No. 6H-1, was spudded on May 20, 1995 and drilled to a total depth of 5,826 feet (1,776 m) in the Anasazi field, Navajo Nation, San Juan County, Utah. The principal reservoir evaluated was the carbonate buildup in the Desert Creek zone of the Paradox Formation. Evaluation of the core suggests the well missed the main buildup or mound-core interval (algal-bafflestone reservoir) and penetrated poorer quality mound-flank deposits (mixed carbonate fabrics that are brecciated, slumped, and chaotic) instead. However, the dolomites in the

upper part of the buildup or supra-mound may be connected to the upper Anasazi reservoirs in the rest of the field. Selected plugs from the reservoir were used to determine oil/water and gas/oil relative permeability measurements; the results will be incorporated into the Anasazi reservoir flow simulation model.

A compositional simulation approach is being used to model various types of secondary/tertiary recovery processes. A compositional approach properly accounts for oil vaporization during primary depletion and provides the correct oil compositions to subsequently assess carbon dioxide flooding potential. The main components of the engineering portion of the work are: (1) review of existing field data including re-evaluation of well-test data, (2) reservoir fluid and rock characterizations via an extensive laboratory program, (3) reservoir development (history match, process design/evaluation for waterflood and carbon dioxide flood), and (4) economics. Assessment of the carbon dioxide process will require calibration of an equation of state using the following laboratory data acquired during the year: (1) compositional analysis on a recombined fluid sample, (2) a two-stage separator test, including a stock-tank condition, and (3) swelling tests. Relative permeability data, a key data set required for reservoir recovery process evaluation via simulation, was obtained. Analysis of the resulting data from these measurements provides a valid data set for future reservoir simulation studies.

The simulation study is being conducted on the Anasazi field reservoir to investigate and compare processes of interest for various operational scenarios (including well placement and well type), geologic variation (various geostatistical realizations), and process variables. Based on simulation results, economic viability can be assessed. Also, the simulation studies will provide the base design for an actual field test. The Anasazi reservoir is stratigraphically divisible into two distinctly different intervals: (1) a lower mound-core interval, consisting primarily of a thick, porous, and highly permeable phylloid algal bafflestone, and (2) an overlying supra-mound interval, a sequence of heterogeneous dolomites (mudstones, packstones, wackestones, and grainstones) with lower permeability and higher average porosity than the underlying algal bafflestones.

Results of simple two-layer, constant-property, two-dimensional numerical flow simulations indicate that although oil production rates are significantly higher in the permeable algal bafflestone of the mound-core interval, most of the oil resides in the overlying porous dolomites of the supra-mound interval. The results of these preliminary studies, along with field production data, show that as the oil is produced from the algal bafflestones, oil from the overlying dolomites continually replenishes the bafflestone pore system, resulting in a production capacity far greater than can be attributed to the mound-core interval alone.

Technology transfer for the project (pre-award period and first year) consisted of displaying project materials at the UGS booth during the national and regional conventions of the American Association of Petroleum Geologists and the regional meeting of the Society of Petroleum Engineers. Presentations were made to geological societies and government officials. A core workshop was presented to industry representatives using materials from project fields. Newsletters were published detailing project progress and results.

ACKNOWLEDGEMENTS

This research is performed under the Class II Oil Program of the U.S. Department of Energy (DOE), Bartlesville Project Office, contract number DE-FC22-95BC14988. The Contracting Officer's Representative is Rhonda P. Lindsey of the DOE Bartlesville Project Office. Additional funding is being provided by the Utah Office of Energy and Resource Planning, Jeff Burks, Director.

Project Contributors:

Principal Investigator: M.L. Allison; Utah Geological Survey, Salt Lake City, UT

Program Manager: T.C. Chidsey, Jr.; Utah Geological Survey, Salt Lake City, UT

Financial Officers: Werner Haidenthaller; Utah Geological Survey, Salt Lake City, UT
B.N. Huff; Harken Southwest Corp., Irving, TX

Task Contributing Scientists and Organizations:

R.L. Bon, T.C. Chidsey, Jr., M.D. Laine, C.D. Morgan, D.A. Sprinkel,
K.A. Waite; Utah Geological Survey, Salt Lake City, UT

Marshall Watson, Wilson Groen, Kris Hartmann; Harken Southwest Corp.,
Irving, TX

W.E. Culham, D.M. Lorenz; REGA Inc., Houston, TX

D.E. Eby; Eby Petrography & Consulting, Inc.; Littleton, CO

Lisë Brinton; LithoLogic, Inc.; Englewood, CO

The following individuals and organizations provided valuable advice and data: Herb Mosca, Bligh Petroleum, Inc., Dallas, TX; P.G. Moreland, Geologic Consultant, Denver, CO; and John Johnson, Minerals Department, Navajo Nation, Window Rock, AZ.

Thanks is given to B.G. Hill, Utah Division of Oil, Gas and Mining, Salt Lake City, UT, for providing project base maps and other services.

This report or portions of it were reviewed by Bryce Tripp of the Utah Geological Survey and Viola Rawn-Schatzinger of BDM-Oklahoma, Inc.

1. INTRODUCTION

Thomas C. Chidsey, Jr.
Utah Geological Survey

Over 400 million barrels of oil have been produced from shallow-shelf carbonate reservoirs in the Pennsylvanian (Desmoinesian) Paradox Formation in the Paradox basin of Utah, Colorado, and Arizona. With the exception of the giant Greater Aneth field, 100 plus oil fields in the basin typically contain 2 to 10 million barrels of original oil in place per field. To date, none of these small fields have been the site of secondary/tertiary recovery techniques used in large carbonate reservoirs. Most of these fields are characterized by extremely high initial production rates followed by a very short production life (primary) and hence early abandonment. At least 200 million barrels of oil is at risk of being left behind in these small fields because of inefficient recovery practices and undrained heterogeneous reservoirs. The purpose of this multi-year project is to enhance domestic petroleum production by demonstration and technology transfer of an advanced-oil-recovery technology in the Paradox basin.

The benefits expected from the project are: (1) increasing recoverable reserves by identifying untapped compartments created by reservoir heterogeneity, (2) increasing deliverability through a waterflood or carbon-dioxide- (CO₂-) miscible flood which exploits the reservoir along optimal fluid-flow paths, (3) identifying reservoir trends for field extension drilling and stimulating exploration in Paradox basin fairways, (4) causing technology to be used in other identified basins with similar types of reservoirs, (5) preventing premature abandonment of numerous small fields, (6) reducing development costs by more closely delineating minimum field size and other parameters necessary to a successful flood, (7) allowing limited energy investment dollars to be used more productively, and (8) increasing royalty income to the Navajo Nation; Federal, State, and local governments; and fee owners. These benefits also apply to other areas in the Rocky Mountain region, the Michigan and Illinois basins, and the Midcontinent.

The geological and reservoir characteristics of five fields (figure 1.1) which produce oil and gas from the Desert Creek zone of the Paradox Formation are being quantitatively determined by a multidisciplinary team. The best candidate for a pilot waterflood or CO₂-flood demonstration project will be chosen after a reservoir simulation has been completed. To evaluate these fields as models for other shallow-shelf carbonate reservoirs, the Utah Geological Survey (UGS), Harken Southwest Corporation, Eby Petrography & Consulting Inc., LithoLogic, and REGA Inc. entered into a cooperative agreement with the U.S. Department of Energy as part of its Class II Oil program.

A two-phase approach is being used to increase production and reserves from the shallow-shelf carbonate reservoirs in the Paradox basin. Phase I is the geological and reservoir characterization of the five small fields. Work during the first year and continuing into the second year of this phase includes: (a) determining regional geological setting, (b) analyzing sequence stratigraphic framework to define and predict reservoir development and continuity, (c) drilling a development well(s), (d) field-scale geologic analysis to focus on the reservoir heterogeneity, quality, and lateral continuity versus compartmentalization, (e) extensive reservoir mapping, (f) determining field reserves and recovery, (g) various laboratory tests and analogies to large scale waterfloods/CO₂ floods, (h) reservoir simulation, and (i) determining the economic viability of secondary/tertiary recovery options.

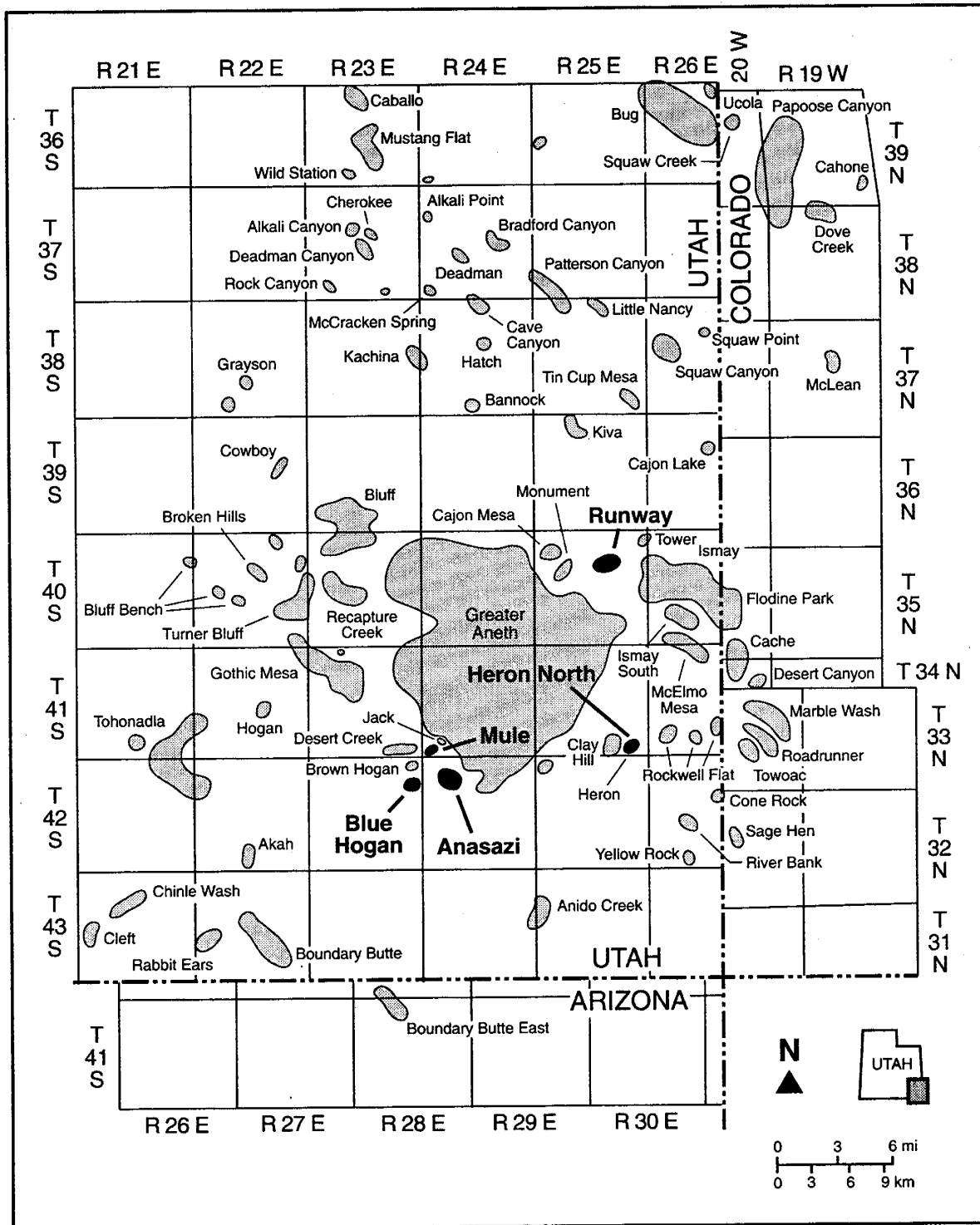


Figure 1.1. Five shallow-shelf carbonate fields (dark shading with names in bold type) on the Navajo Nation, San Juan County, Utah are targeted for geological and reservoir characterization.

Phase II will be a demonstration project on the field selected from the characterization study using the secondary/tertiary recovery techniques identified as having the greatest potential for increased well productivity and ultimate recovery. The demonstration project will include: (a) drilling a development well to facilitate sweep during the pilot flood, (b) acquiring CO₂ and/or water source for the flood project, (c) installation of CO₂ and/or waterflood injection facilities, (d) conversion of a producing well to injection, (e) flood management, monitoring, and evaluation of results, and (f) determining the application of the project to similar fields in the Paradox basin and throughout the U.S.

The results of this project are being transferred to industry and other researchers through a petroleum extension service, creation of digital databases for distribution, technical workshops and seminars, field trips, technical presentations at national and regional professional meetings, and publication in newsletters and various technical or trade journals.

This report is organized into seven sections: (1) Introduction, (2) Regional Facies Evaluation and Outcrop Analogues, (3) Project Fields, Navajo Nation, San Juan County, Utah, (4) Geological Characterization of the Carbonate Reservoir in the Desert Creek Zone, (5) Engineering Reservoir Characterization of the Carbonate Reservoir in the Desert Creek Zone, (6) Mechanistic Reservoir Simulation Studies, and (7) Technology Transfer. There three appendices: (A) Paradox Basin Project Fields Summaries, (B) Compositional Analyses of Oil and Gas, Anasazi Field, and (C) Swelling Test Data, Anasazi Field. This report presents the progress of on-going research and is not intended as a final report. Whenever possible, preliminary conclusions have been drawn based on available data.

2. REGIONAL FACIES EVALUATION AND OUTCROP RESERVOIR ANALOGUES

Thomas C. Chidsey, Jr.
Utah Geological Survey
Lisè Brinton
LithoLogic, Inc.
and
David E. Eby
Eby Petrography & Consulting, Inc.

2.1 Regional Facies Evaluation

Establishment of the general regional facies belts and stratigraphic patterns within the shallow-shelf carbonate Desert Creek zone of the Paradox Formation for the southern Paradox basin is critical to: (1) understanding reservoir heterogeneity and capacity of the five fields being evaluated for the pilot demonstration and (2) exploring areas in the basin that have the greatest petroleum potential. Generalized regional facies belts for the Desert Creek zone (figure 2.1) were mapped utilizing more than 30 conventional cores, rotary sidewall cores, cuttings descriptions, and geophysical log interpretations.

2.1.1 Paleogeographic Setting

The Paradox basin was a structural and depositional trough associated with the Pennsylvanian-age Ancestral Rocky Mountains. The subsiding basin developed a shallow-water carbonate shelf which locally contained carbonate buildups on the south and southwest margins. These carbonate buildups and the material shed from their flanks formed petroleum traps where reservoir-quality porosity and permeability have developed.

During Pennsylvanian time, the Paradox basin was in subtropical, dry climatic conditions along the trade-wind belt, 10° to 20° north of the paleo-equator. Prevailing winds were from present day north (Peterson and Hite, 1969; Heckel, 1977; Parrish, 1982). Open-marine waters flowed across the shallow cratonic shelf into the basin during transgressive periods. There are four postulated directions for normal marine access into the Paradox basin. The Cabezón accessway, which was located to the southeast, is generally accepted as the most likely normal marine-water conduit to maintain circulation on the shallow shelf (Fetzner, 1960; Ohlen and McIntyre, 1965; Hite, 1970).

Cycles in Paradox basin deposition were primarily controlled by glacio-eustatic fluctuation. The shape of the sea-level curves reflects rapid marine transgressions (rapid melting of ice caps) and slow, interrupted regression (slow ice cap buildup) (Imbrie and Imbrie, 1980; Denton and Hughes, 1983; Heckel, 1986). Irregular patterns within the cycles are predicted in response to interference of orbital parameters (Imbrie and Imbrie, 1980). These cycles were also influenced by: (1) regional tectonic activity and basin subsidence (Baars, 1966; Baars and Stevenson, 1982), (2) proximity to basin margin and evaporites (Hite, 1960; Hite and Buckner, 1981), (3) climatic variation and

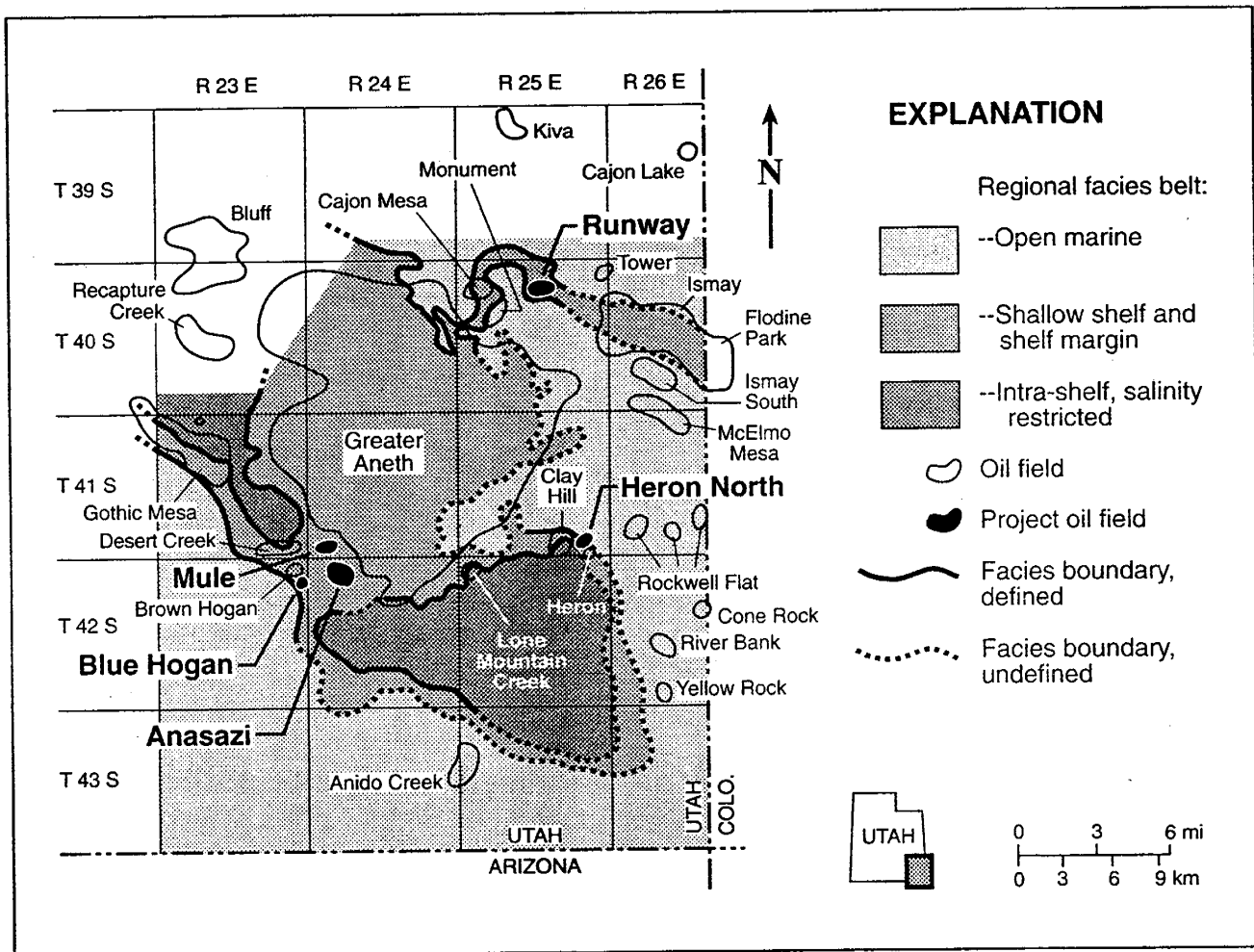


Figure 2.1. Generalized regional facies belts for Desert Creek zone, Pennsylvanian Paradox Formation, southeastern San Juan County, Utah.

episodic blockage of open marine-water conduits, and (4) fluctuations in water depth and water energy (Peterson and Ohlen, 1963; Peterson, 1966; Hite and Buckner, 1981; Heckel, 1983).

2.1.2 Generalized Regional Facies Belts

Three generalized regional facies belts are identified (figure 2.1): (1) open-marine, (2) shallow-shelf and shelf-margin, and (3) intra-shelf, salinity-restricted facies. The open-marine facies belt includes open-marine buildups (typically crinoid-rich mounds), open-marine crinoidal- and brachiopod-bearing carbonate muds, euxinic black shales, wall complexes, and detrital fans. Open-marine facies were deposited at water depths between 90 and 120 feet (27-37 m). This facies belt is the most extensive and surrounds the shallow-shelf and shelf-margin facies belt.

The shallow-shelf and shelf-margin facies belt includes shallow-shelf buildups (phylloid algal, coralline algal, bryozoan, and marine-cemented buildups [mounds]), calcarenites (beach, dune, and stabilized grain flats), and platform-interior carbonate muds and sands. These facies were deposited at water depths between 0 and 40 feet (0-12 m). Karst characteristics are occasionally present over mounds. Tubular tempestites (burrows filled with coarse sand as a result of storm pumping) are found in some carbonate muds and sands. Most oil fields which produce from the Desert Creek zone of the Paradox Formation are located within this facies belt, including the giant Greater Aneth field (figure 2.1).

The intra-shelf, salinity-restricted facies belt represents small subbasins within the shallow-shelf and shelf-margin facies belt. The water had slightly elevated salinity compared to the other facies belts. This facies belt includes platform-interior evaporites, dolomitized tidal-flat muds, bioclastic lagoonal muds, tidal-channel carbonate sands and stromatolites, and euxinic dolomites. These facies were deposited at water depths between 20 and 45 feet (6-14 m). Euxinic dolomites often display karst characteristics. Two intra-shelf subbasins have been identified in the southeastern part of the Paradox basin in Utah; each is separated from the open-marine facies belt by a fringe of the shallow-shelf and shelf-margin facies belt (figure 2.1).

2.1.3 Study Results

Mounds, tidal-channel carbonate sands, and other features often appear promising on seismic records. However, if these carbonate buildups are located within the open-marine and intra-shelf, salinity-restricted facies belts, the reservoir quality is typically poor. Porosity and permeability development is limited or, if present, plugged with anhydrite in these respective facies belts. Mounds and calcarenite in the shallow-shelf and shelf-margin facies belt can have excellent reservoir properties; all five project fields are located within this facies belt.

2.2 Outcrop Reservoir Analogues

2.2.1 Field Work

Outcrops of the Paradox Formation Ismay zone in the Wild Horse Canyon area along the San Juan River of southeastern Utah (figure 2.2), provide small-scale analogues of reservoir heterogeneity, flow barriers and baffles, and lithofacies geometry. These characteristics can be used in reservoir simulation models for secondary/tertiary recovery of oil from small fields in the basin. Quantitative data was gathered from several selected outcrops. These data included: (1) the sizes, shapes, orientations, and stratigraphic positions of units within the mounds, (2) facies relationships, and (3) gross reservoir properties of the key mound storage units, flow units, and permeability barriers. The outcrop work involved: (1) photographing mounds to create interpretive photomosaics, (2) measuring and describing stratigraphic sections, (3) mapping the areal extent of the mounds and associated facies, and (4) collecting representative samples for thin-section analysis. Major elements of reservoir architecture, lateral variations in reservoir properties, and definition of an internal "representative elementary volume" for modeling fluid storage and flow in each key facies were particularly emphasized.

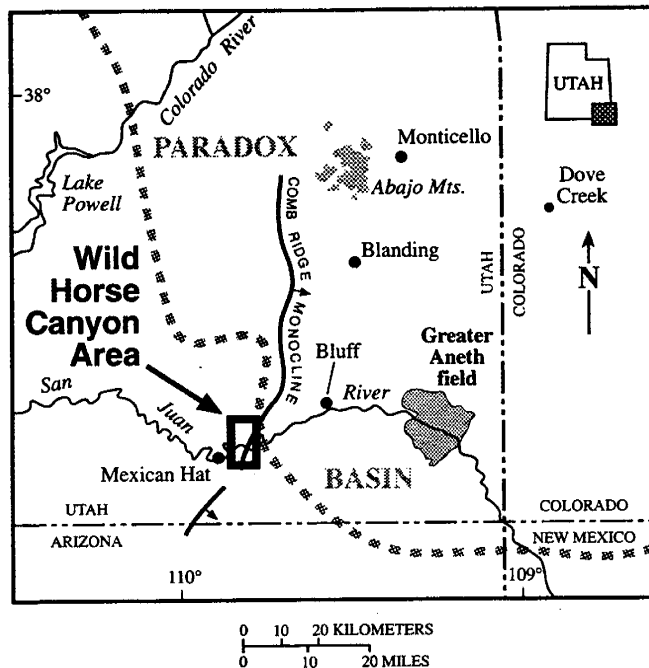


Figure 2.2. Location of Paradox Formation outcrops in the Wild Horse Canyon area along the San Juan River, southeastern Utah.

2.2.2 Study Results

From this work, it was determined that exposures of the Ismay zone (figure 2.3A) display lateral facies changes from phylloid algal mounds to off-mound detrital wedges or fans bounded at the top by a flooding surface. The phylloid mounds are composed of bafflestone (figure 2.3B), skeletal grainstone, packstone, and cementstone. Algal plates, brachiopods, bryozoans, and rugose corals are commonly found in the phylloid mounds. The mound wall is composed of rudstone, lumpstone, and cementstone. The detrital fan consists of transported algal material, grainstone, and mudstone with open-marine fossils. Within the mound complex are inter-mound troughs tentatively interpreted to be tidal channels. The geometry and composition of the rocks in the troughs significantly add to the overall heterogeneity of the mounds.

The results of these field investigations have been incorporated into the geological constraints on facies distributions in the geostatistical models. Reservoir models are being developed for possible water and CO₂ floods of small Paradox basin fields to determine the most effective secondary/tertiary recovery method. The models will include lithologic fabrics, flooding surfaces, and inter-mound troughs, based on the mound complex exposed at Wild Horse Canyon.

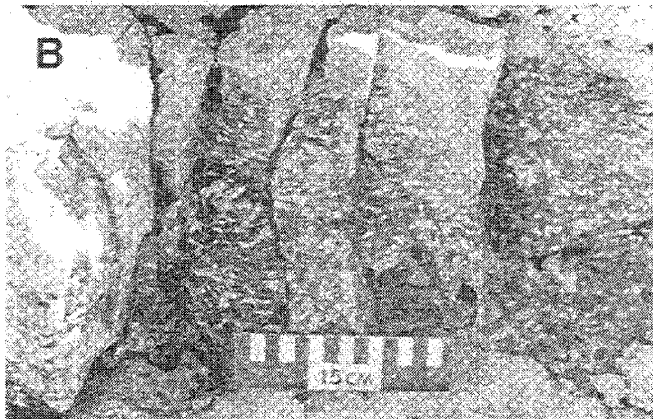
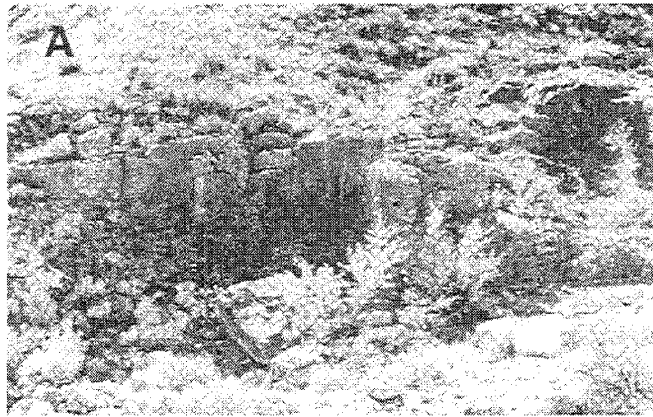


Figure 2.3. Outcrops in the Ismay zone of the Paradox Formation, Wild Horse Canyon near the San Juan River, southeastern Utah. (A) Typical phylloid mound composed of algal bafflestone, skeletal grainstone, and packstone. A flooding surface is present at the top of the mound. (B) Cement-rich algal bafflestone exposed in a phylloid mound. Original sheltered pore spaces were filled with mud; cement rinds are developed around algal plates.

2.3 References

- Baars, D.L., 1966, Pre-Pennsylvanian paleotectonics-key to basin evaluation and petroleum occurrences in Paradox basin, Utah and Colorado: American Association of Petroleum Geologists Bulletin, v. 50, no. 10, p. 2082-2111.
- Baars, D.L., and Stevenson, G.M., 1982, Subtle stratigraphic traps in Paleozoic rocks of Paradox basin, *in* Halbouty, M.T., editor, The deliberate search for the subtle trap: American Association of Petroleum Geologists Memoir 32, p. 131-158.
- Denton, G.H., and Hughes, T.J., 1983, Milankovitch theory of ice ages: hypothesis of ice-sheet linkage between regional insolation and global climate: Quaternary Research, v. 20, p. 125-144.
- Fetzner, R.W., 1960, Pennsylvanian paleotectonics of the Colorado Plateau: American Association of Petroleum Geologists Bulletin, v. 44, no. 8, p. 1371-1413.
- Heckel, P.H., 1977, Origin of phosphatic black shale facies in Pennsylvanian cyclothems of Mid-Continent North America: American Association of Petroleum Geologists Bulletin, v. 61, no. 7, p. 1045-1068.
- Heckel, P.H., 1983, Diagenetic model for carbonate rocks in midcontinent Pennsylvanian eustatic cyclothems: Journal of Sedimentary Petrology, v. 53, p. 733-759.
- Heckel, P.H., 1986, Sea-level curve for Pennsylvanian eustatic marine transgressive-regressive depositional cycles along midcontinent outcrop belt, North America: Geology, v. 14, p. 330-334.
- Hite, R.J., 1960, Stratigraphy of the saline facies of the Paradox Member of the Hermosa Formation of southeastern Utah and southwestern Colorado, *in* Geology of the Paradox basin: Four Corners Geological Society, Third Field Conference, p. 86-89.
- Hite, R.J., 1970, Shelf carbonate sedimentation controlled by salinity in the Paradox basin, southeast Utah, *in* Ran, J.L., and Dellwig, L.F., editors, Third symposium on salt: Northern Ohio Geological Society, v. 1, p. 48-66.
- Hite, R.J., and Buckner, D.H., 1981, Stratigraphic correlation, facies concepts and cyclicity in Pennsylvanian rocks of the Paradox basin, *in* Wiegand, D.L., editor, Geology of the Paradox basin: Rocky Mountain Association of Geologists 1981 Field Conference, p. 147-159.
- Imbrie, John, and Imbrie, J.Z., 1980, Modeling the climatic response to orbital variations: Science, v. 207, p. 943-953.

- Ohlen, H.R., and McIntyre, L.B., 1965, Stratigraphy and tectonic features of Paradox basin, Four Corners area: American Association of Petroleum Geologists Bulletin, v. 49, no. 11, p. 2020-2040.
- Parrish, J.T., 1982, Upwelling and petroleum source beds, with reference to the Paleozoic: American Association of Petroleum Geologists Bulletin, v. 66, no. 6, p. 750-774.
- Peterson, J.A., 1966, Stratigraphic vs. structural controls on carbonate-mound accumulation, Aneth area, Paradox basin: American Association of Petroleum Geologists Bulletin, v. 50, no. 10, p. 2068-2081.
- Peterson, J.A., and Hite, R.J., 1969, Pennsylvanian evaporite-carbonate cycles and their relation to petroleum occurrence, southern Rocky Mountains: American Association Petroleum Geologists Bulletin, v. 53, no. 4, p. 884-909.
- Peterson, J.A., and Ohlen, H.R., 1963, Pennsylvanian shelf carbonates, Paradox basin, *in* Bass, R.O., editor, Shelf carbonates of the Paradox basin: Four Corners, Geological Society Symposium, 4th Field Conference, p. 65-79.

3. PROJECT FIELDS, NAVAJO NATION, SAN JUAN COUNTY, UTAH

Thomas C. Chidsey, Jr.
 Utah Geological Survey
 Marshall Watson, Wilson Groen, and Kris Hartmann
 Harken Southwest Corp.
 and
 David E. Eby
 Eby Petrography & Consulting, Inc.

The five Paradox basin fields being evaluated in Phase I of the project are Runway, Heron North, Anasazi, Mule, and Blue Hogan located within the Navajo Nation of southeast Utah (figure 1.1); they are five of several satellite carbonate mounds around the giant Greater Aneth field. This evaluation included data collection, core analysis and description, reservoir mapping, and drilling the first of possibly three development wells.

Eby and others (1993) have identified from core, five different types of carbonate buildups or mounds in the Desert Creek zone of the Paradox Formation: (1) crinoid/sponge mounds, (2) coralline algal "reefs" mounds, (3) bryozoan-dominated mounds, (4) phylloid algal mounds, and (5) bioclastic calcarenites "beach" mounds. The controls on the development of each mound type were water depth, prevailing wave energy, and paleostructural position. Examination of core from the five project fields shows that three mound types are present (table 3.1), making them good representatives of Desert Creek zone reservoirs. The geological and reservoir characterization of these fields and resulting models can applied to similar fields in the basin (and other basins as well) where data might be limited. The following presents the initial results of these efforts.

Table 3.1. Cumulative production of project fields in the Paradox basin, San Juan County, Utah.

Field	Active Wells	Cumulative Production*			Buildup Type
		Oil (bbls)	Gas (MCF)	Water (bbls)	
Anasazi	4	1,650,133	1,281,713	25,274	Phylloid Algal
Blue Hogan	1	282,718	256,006	1,699	Phylloid Algal
Mule	2	343,180	203,116	17,930	Phylloid Algal
Heron North	1	200,759	305,669	23,578	Bioclastic Calcarenite
Runway	3	750,772	2,268,636	3,036	Bryozoan-dominated/ Phylloid Algal

*As of January 1, 1996 (Utah Division of Oil, Gas and Mining, 1996).

3.1 Data Collection

Reservoir data, cores and cuttings, geophysical logs, various reservoir maps, and other information from the project fields and regional exploratory wells are being collected by the UGS. Well locations, production reports, completion tests, core analysis, formation tops, and other data were compiled and entered in a database developed by the UGS. This database, *INTEGRAL*gim*, is a geologic-information database that links a diverse set of geologic data to records using *PARADOX™* for DOS software. The database is designed so that geological information, such as lithology, porosity, or depositional environment can be exported to software programs to produce strip logs, lithofacies maps, various graphs, statistical models, and other types of presentations. The UGS acquired information for 51 project wells. Production data, geophysical log types, and well cutting information for these project wells were entered into the UGS *INTEGRAL*gim* database. In addition, completion test data and formation tops were also entered into the database for 33 of these wells. The database containing information from the project will be available as a UGS open-file (digital format) report at the conclusion of Phase I (the geological and reservoir characterization study).

Base maps and new isochron maps covering project fields were prepared and cores were described from selected project wells with special emphasis on bounding surfaces of possible flow units. The core descriptions follow the guidelines of Bebout and Loucks (1984) which include: (1) basic porosity types, (2) mineral composition in percentage, (3) nature of contacts, (4) carbonate structures, (5) carbonate textures in percentage, (6) carbonate fabrics, (7) grain size (dolomite), (8) fractures, (9) color, (10) fossils, (11) cement, and (12) depositional environment. Carbonate fabrics were determined according to Dunham's (1962) and Embry and Klován's (1971) classification schemes.

3.2 Field Studies

Geologic, reservoir, and production data for each project field are summarized in Appendix A. Oil and gas are produced from the Pennsylvanian (Desmoinesian) Desert Creek and Ismay zones of the Paradox Formation. The fields were discovered in 1990 and 1991 as part of an ambitious exploration program conducted within the Navajo Nation by Chuska Energy Company (now Harken Southwest Corporation) and several Australian companies. Seismic surveys and subsurface geology were used to identify prospects. Each carbonate mound is expressed on seismic coverage (figure 3.1) by isochron thickening of the Desert Creek zone, isochron thinning of the overlying Ismay zone, amplitude dimming of the Desert Creek reflector, and a "doublet" development of the Desert Creek event (Johnson and Groen, 1993).

Each field consists of one to four wells. Development wells are drilled on either 40-acre (16-ha) spacing or under the 80-acre-(32-ha-)spacing rules established at Greater Aneth field. Completion practices consist of selective perforation and treatment with varying amounts of acid. The reservoir drive is gas expansion. Primary production ranges from 700,000 to 2,000,000 barrels of oil (BO [111,300-318,000 m³]) per field at a 15 to 20 percent recovery rate. Geological and engineering data for each field are summarized on table 3.2.

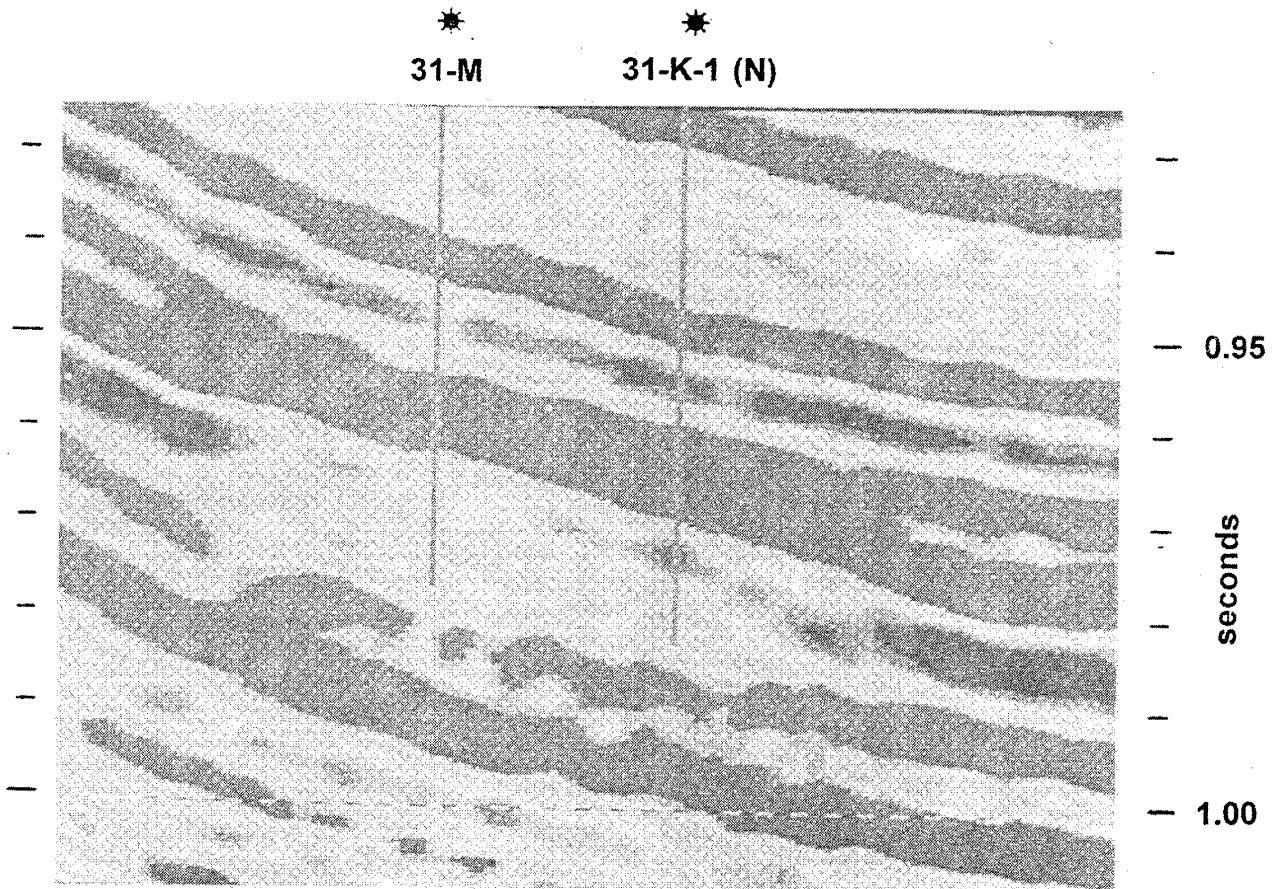


Figure 3.1. Representative seismic line, shaded according to amplitude variations, across Mule field. In general, the lighter the shades the more porous the reservoir rock within the carbonate buildup. The reservoir rock in the non-commercial Mule No. 31-K-1 (N) well is tight while the reservoir rock in the Mule No. 31-M well is more porous, resulting in excellent production. Both wells are located in section 31, T. 41 S., R. 24 E., Salt Lake Base Line, Navajo Nation, San Juan County, Utah.

Table 3.2. Geological and engineering data for project fields in the Paradox basin, San Juan County, Utah.

Field	Depth* (ft)	Area (ac)	Pay (ft)	Porosity (%)	Permeability (md)	Water Saturation (%)	Reservoir Temperature (°F)	Initial Reservoir Pressure (psi)
Runway	5,896	193	72	11.8	10.0	25.2	126	2,162
Heron North	5,584	110	60	15.0	17.7	32.2	126	1,934
Anasazi	5,574	165	57	14.1	135.3	28.1	138	1,945
Mule	5,655	48	47	13.0	20.1	31.0	128	2,050
Blue Hogan	5,400	89	82	9.1	33.6	29.0	128	1,800

*Average depth to the top of the reservoir.

3.2.1 Runway Field

Runway field (figure 1.1) consists of three wells with the discovery well, the Runway No. 10-G-1, completed in 1990 at an initial potential flow (IPF) of 825 bbls of oil per day (BOPD [131 m³/d]) and 895,000 cubic feet of gas per day (MCFGPD [25,000 m³/d]) from commingled Desert Creek and upper Ismay zones. The Runway prospect was identified as a high-resolution, common-depth point seismic anomaly in the northern Aneth platform area. This anomaly, east of the Greater Aneth field (figure 3.2), is located on the upthrown edge of a basement-involved, Mississippian-age normal fault which was a topographic high during Paradox Formation time.



Figure 3.2. Three-dimensional "net" view to the southwest of the surface on top of the Mississippian Leadville Limestone and the north-bounding faults which control the localization of small algal and other carbonate buildups such as at the Runway field. This computerized presentation was produced from a closely spaced seismic grid.

The Runway field is a lenticular, west to east-northeast trending lobate mound, 0.9 miles (1.5 km) long and 0.5 miles (0.8 km) wide. The reservoir consists of a bryozoan-dominated mound with phylloid algal mound intervals. The presence of two mound types at Runway field suggests that the water depth changed as the carbonate deposits built up over the fault-controlled paleohigh. The principal Desert Creek reservoir rocks in the field are bindstone and framestone, rarely dolomitized, in the bryozoan-dominated interval and porous bafflestone (calcified plates of the green algae *Ivanovia*) with some grainstone and occasional dolomitization in the phylloid algal mound interval. The Ismay reservoir rock is sucrosic dolomite. Both carbonate buildups are interbedded with low permeability wackestone and mudstone.

The Runway field lies along a generally gas-rich trend east and north of Greater Aneth field. Cumulative production from Runway field is 750,772 BO (119,373 m³) and 2.27 billion cubic feet of gas (BCFG [0.06 billion m³]) as of January 1, 1996 (Utah Division of Oil, Gas and Mining [UDOGM], 1996). Estimated primary recovery is 800,000 BO (127,200 m³) and 2.99 BCFG (0.09 billion m³).

3.2.2 Heron North

Heron North field (figure 1.1), southeast of the Greater Aneth field, consists of one well, the North Heron No. 35-C, completed in 1991 at an IPF of 605 BOPD (96 m³/d) and 230 MCFGPD (6,500 m³/d) from the Desert Creek zone. The North Heron prospect was identified as a seismic anomaly.

The Heron North field is a lenticular, northwest to southeast trending linear mound/beach complex, 0.8 miles (1.3 km) long and 0.5 miles (0.8 km) wide. The reservoir consists of a bioclastic calcarenite mound above a anhydrite- and salt-plugged phylloid algal mound. This calcarenite mound type, which is also productive in the Heron 35-H well 0.5 miles (0.8 km) southeast of Heron North, developed in a carbonate beach to foreshore environment with moderately high wave energy. Trough cross-bedding is often present. The reservoir consists of alternating 2- to 4-ft-(0.6-1.2-m-) thick packages of uniform beach calcarenite and poorly sorted foreshore and storm lag rudstone or breccia deposits. An 8-ft-(2.4-m-) thick anhydrite lies immediately above the reservoir interval and creates an effective seal. The principal reservoir rocks in the field are porous, sucrosic, dolomitized grainstone and packstone (calcarenite) above tight bafflestone composed of algal stromatolithic mats. The calcarenite and bafflestone intervals are separated by low permeability, dolomitized wackestone and mudstone. Stylolitization, secondary cementation, and evaporite plugging are minor in the upper portion of the reservoir, but increase with depth. Pores are often lined with bitumen which in many instances plugs pore throats.

Cumulative production from Heron North field is 200,759 BO (31,921 m³) and 0.31 BCFG (0.009 billion m³) as of January 1, 1996 (UDOGM, 1996). Estimated primary recovery is 990,000 BO (157,410 m³) and 2.65 BCFG (0.08 billion m³).

3.2.3 Mule Field

Mule field (figure 1.1) consists of two wells, the Mule No. 31-K-1 (N) discovery well and the Mule No. 31-M well, completed in 1991 and 1992 respectively. The Mule No. 31-K-1 (N) well tested approximately 10 BO (1.6 m³) per hour (based on several swab tests) with water cut increasing on each test and produced only 283 BO (45 m³) before being shut-in. The Mule No. 31-M offset well had an IPF of 735 BOPD (117 m³/d) and 97 MCFGPD (3,000 m³/d) from the Desert Creek zone. The Mule prospect, near the southwestern edge of the Greater Aneth field, was identified as a seismic anomaly (figure 3.1). A seismic program was designed for the field, and new seismic interpretations and mapping commenced.

The Mule field is a lenticular, northeast to east trending linear mound/mound flank deposit, 0.5 miles (0.8 km) long and 900 feet (274 m) wide. The reservoir consists of a phylloid algal mound combined with mound flank detrital deposits. This mound type, which dominates the area southwest of Greater Aneth field, developed where shallow water depth and low wave energy allowed establishment of phylloid algal colonies on paleohighs. Several beds in the Mule 31-K-1 (N) well

core exhibit characteristics of mound flank deposits such as downslope gravity transport and sharp erosional basal contacts. The top of the phylloid algal interval is highly irregular with several cross-cutting zones of dissolution cavities possibly from karst development during subaerial exposure. The principal reservoir rock in the field is porous algal bafflestone (figure 3.3), crinoidal packstone, and dolomitized zones interbedded with low permeability wackestone, mudstone, and dolomite. Incomplete dolomitization and secondary anhydrite replacement have resulted in poor reservoir properties in some intervals.

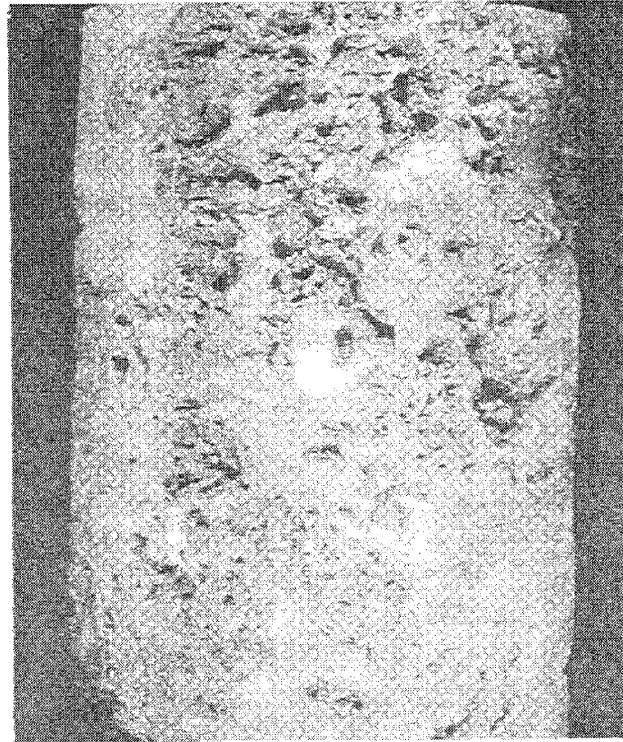


Figure 3.3. Core surface view of highly productive, dolomitized, phylloidal algal plate bafflestone from the Mule No. 31-M well, Mule field (see figure 3.1 for seismic line through well). Note good visual shelter porosity. Core diameter = 3.5 inches (8.9 cm).

Cumulative production from Mule field is 343,180 BO (54,566 m³) and 0.2 BCFG (0.006 billion m³) as of January 1, 1996 (UDOGM, 1996). Estimated primary recovery is 430,603 BO (68,466 m³) and 0.288 BCFG (0.008 billion m³).

3.2.4 Blue Hogan

Blue Hogan field (figure 1.1) consists of one well, the Blue Hogan No. 1-J-1, completed in 1991 at an IPF of 1,167 BOPD (186 m³/d) and 722 MCFGPD (20,447 m³/d) from the Desert Creek zone. The Blue Hogan prospect, near the southwest edge of the Greater Aneth field, was identified as a seismic anomaly along the east flank of the Desert Creek anticline.

Blue Hogan field is a lenticular, northwest to southeast trending linear mound, 0.5 miles (0.8 km) long and 1,000 feet (305 m) wide. The reservoir consists of a cement-rich phylloid algal mound. The principal reservoir rock in the field is porous algal bafflestone and dolomitized zones interbedded with low permeability wackestone and mudstone.

Cumulative production from Blue Hogan field is 282,718 BO (44,952 m³) and 0.26 BCFG (0.007 billion m³) as of January 1, 1996 (UDOGM, 1996). Estimated primary recovery is 645,000 BO (102,555 m³) and 0.968 BCFG (0.03 billion m³).

3.2.5 Anasazi Field

Anasazi field (figure 1.1) consists of four wells. The discovery well, the Anasazi No. 1, was completed in 1990 at an IPF of 1,705 BOPD (271 m³/d) and 833 MCFGPD (23,591 m³/d) from the Desert Creek zone. The Anasazi prospect, near the southwest edge of Greater Aneth field, was identified as a seismic anomaly along the east flank of the Desert Creek anticline. A modified seismic interpretation was completed for the field and converted into a gross Desert Creek isopach map to evaluate the area for additional drilling.

Anasazi field is a lenticular, west to northeast trending lobate mound, 0.9 miles (1.5 km) long and 2,000 to 3,000 feet (610-914 m) wide. The reservoir consists of a phylloid algal mound. The principal reservoir rock in the field is porous algal bafflestone, some grainstone, and dolomitized zones interbedded with low permeable wackestone and mudstone. Extensive fresh water dissolution and early dolomitization has resulted in good to excellent porosity development and permeability modification.

Cumulative production from Anasazi field is 1,650,133 BO (262,371 m³) and 1.28 BCFG (0.04 billion m³) as of January 1, 1996 (UDOGM, 1996). Estimated primary recovery is 2,069,392 BO (329,033 m³) and 1.89 BCFG (0.05 billion m³). Preliminary analysis of Anasazi field indicates the Desert Creek reservoir is a prime candidate for a waterflood or CO₂-miscible flood demonstration.

3.3 New Development Wells

3.3.1 Drilling Rationale

A team of geologists, reservoir engineers, and geophysicists from Harken evaluated potential development locations for the project fields. Project development wells are designed to increase the well density from 80 acres (32.3 ha) per well to 30 to 40 acres (12-16 ha) per well. During the first project year, one development well was drilled in the Anasazi field and permitting began for a second well, a horizontal lateral from the Mule No. 31-K-1 (N) well in Mule field. The length and orientation of the lateral will be determined upon completion and evaluation of the new seismic data.

The data obtained from these new wells will enable the project team to assess: (1) the frequency of reservoir compartment changes (reservoir heterogeneity) in a given area, (2) the amount of communication between compartments, (3) how a waterflood or CO₂ flood will flow from one compartment to another, and (4) the areal extent of an average compartment. The following new well information will be used in the geologic and reservoir characterization:

1. more accurate descriptions of the general reservoir geology and reservoir compartmentalization/continuity,
2. pressure data in drawn down areas from current producers,
3. wettability and relative permeability data from fresh cores,
4. pressure transient data to determine communication with other fields (determine communication with adjacent reservoirs previously thought separate), and
5. increased data for the reservoir simulation history match to allow for better construction of models used in CO₂/water flow simulations.

3.3.2 Anasazi No. 6H-1 Well, Anasazi Field

The first project development well, the Anasazi No. 6H-1, was spudded on May 20, 1995 and drilled to a total depth of 5,826 feet (1,776 m) in the Anasazi field, SE1/4NE1/4 section 6, T. 42 S., R. 24 E., Salt Lake Base Line, Navajo Nation, San Juan County, Utah (figure 3.4). The principal reservoir evaluated, a carbonate buildup in the Desert Creek zone of the Paradox Formation, was penetrated at 5,624 feet (1,714 m). The buildup was cored (120 feet [37 m] of conventional core recovered) and described. Geophysical logs run consisted of the dual laterolog, spectral density, dual-spaced neutron, gamma ray, and long-spaced sonic. The wireline formation tester obtained reservoir pressures throughout the Desert Creek zone ranging from 300 to 1,200 pounds per square inch (psi [2,069-8,274 kpa]). The main pay intervals held 15 to 25 percent of the original reservoir pressure.

The Anasazi No. 6H-1 well was completed on September 15, 1995 for an IPF of 31.3 BOPD (5.0 m³/d), 25 MCFGPD (708 m³/d), and 7.5 bbls (1.2 m³) of water per day in the Desert Creek and Ismay zones. A grainstone/packstone interval in the Desert Creek zone was perforated from 5,723 to 5,730 feet (1,744-1,746 m) and acidized with 350 gallons (gal [1,325 L]) of 15 percent hydrochloric acid (HCl). The resulting test indicated the pressure and permeability in the interval were too low to yield any meaningful data. A dolomite interval in the upper section of the Desert Creek was perforated from 5,680 to 5,694 feet (1,731-1,735 m). This interval was subsequently acidized with 30 gal (114 L) of HCl and swab tested for 2 BOPD (0.3 m³/d). After the swab test, a 200-hour pressure buildup test was run. A skin factor and permeability of +13 and 1.2 millidarcies (md) respectively were derived from the pressure buildup test. Because of the high skin damage, the zone was re-acidized. Several additional intervals were perforated and acidized including the upper Ismay zone from 5,526 to 5,531 feet (1,684-1,686 m). Production facilities were installed and the well flow rate stabilized at 17 BOPD (3 m³/d) from a gross perforated Desert Creek interval of 5,664 to 5,741 feet (1,726-1,750 m) and a Ismay interval of 5,526 to 5,531 feet (1,684-1,686 m).

Selected plugs from the reservoir were used to determine oil/water and gas/oil relative permeability (see Section 5, Engineering Reservoir Characterization of the Carbonate Reservoir in the Desert Creek Zone). These data will be incorporated into the Anasazi reservoir flow-simulation model. Whole core intervals were scanned using computerized axial tomography (CAT) techniques to ensure that permeability measurements are based on comparable pore systems. The three most homogeneous intervals were selected for additional analysis. Upon further examination and CAT

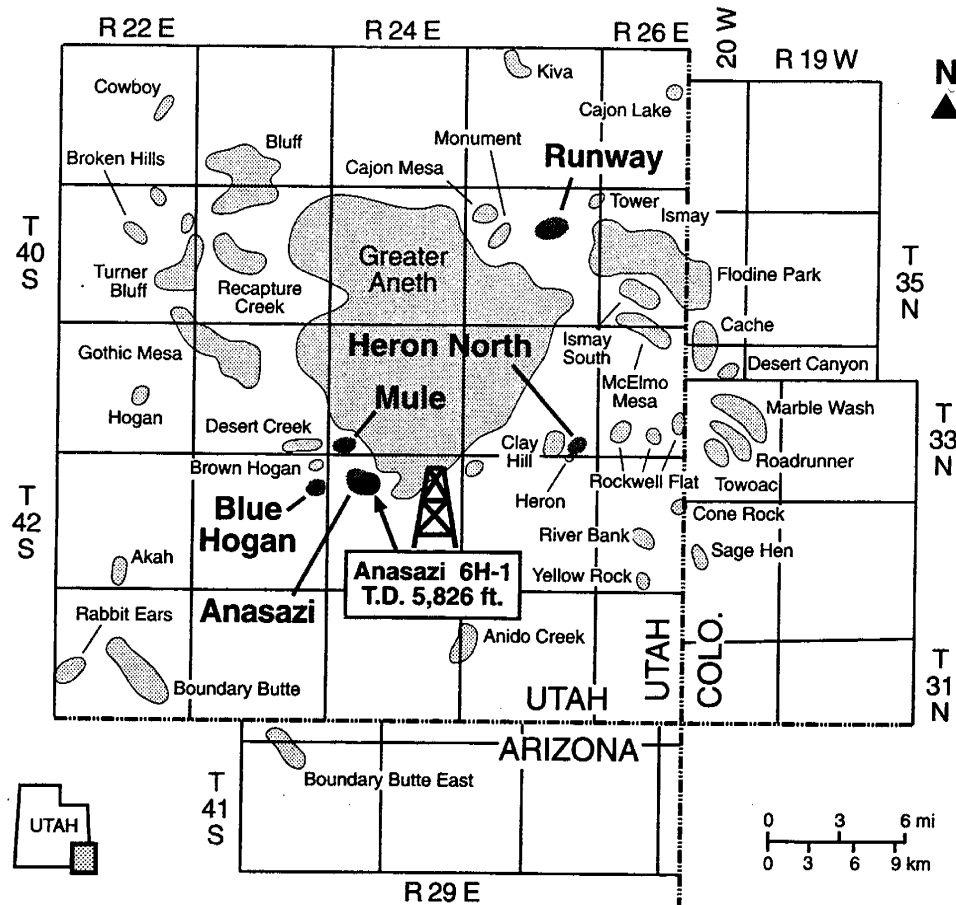


Figure 3.4. Location of the first project development well, the Anasazi No. 6H-1, drilled in the Anasazi field, SE1/4NE1/4 section 6, T. 42 S., R. 24 E., Salt Lake Base Line, Navajo Nation, San Juan County, Utah.

scans, one interval (5,691 feet [1,735 m]) appeared as the most homogeneous and contained the highest porosity. Four transverse plugs were taken from this interval for detailed CAT scans, and porosity and relative permeability measurements (figure 3.5). A variety of features were observed using these techniques including anhydrite-filled vugs, both micro-vuggy and intercrystalline porosity, patches of bitumen-filled pores, and areas of nonporous carbonate mudstone.

The pressure buildup tests are being used to determine average reservoir pressure, boundaries, and flow properties. Fluid samples taken from these intervals were used for extensive compositional studies.

3.3.3 Results

Conventional core was obtained from the Desert Creek zone of the Anasazi 6H-1 well. Evaluation of the core suggests the well missed the main buildup or mound-core interval (algal bafflestone reservoir) and penetrated poorer quality mound-flank deposits (mixed carbonate fabrics that are brecciated, slumped, and chaotic). However, the dolomites in the upper part of the buildup or supra-mound may be connected to the upper Anasazi reservoirs in the rest of the field.

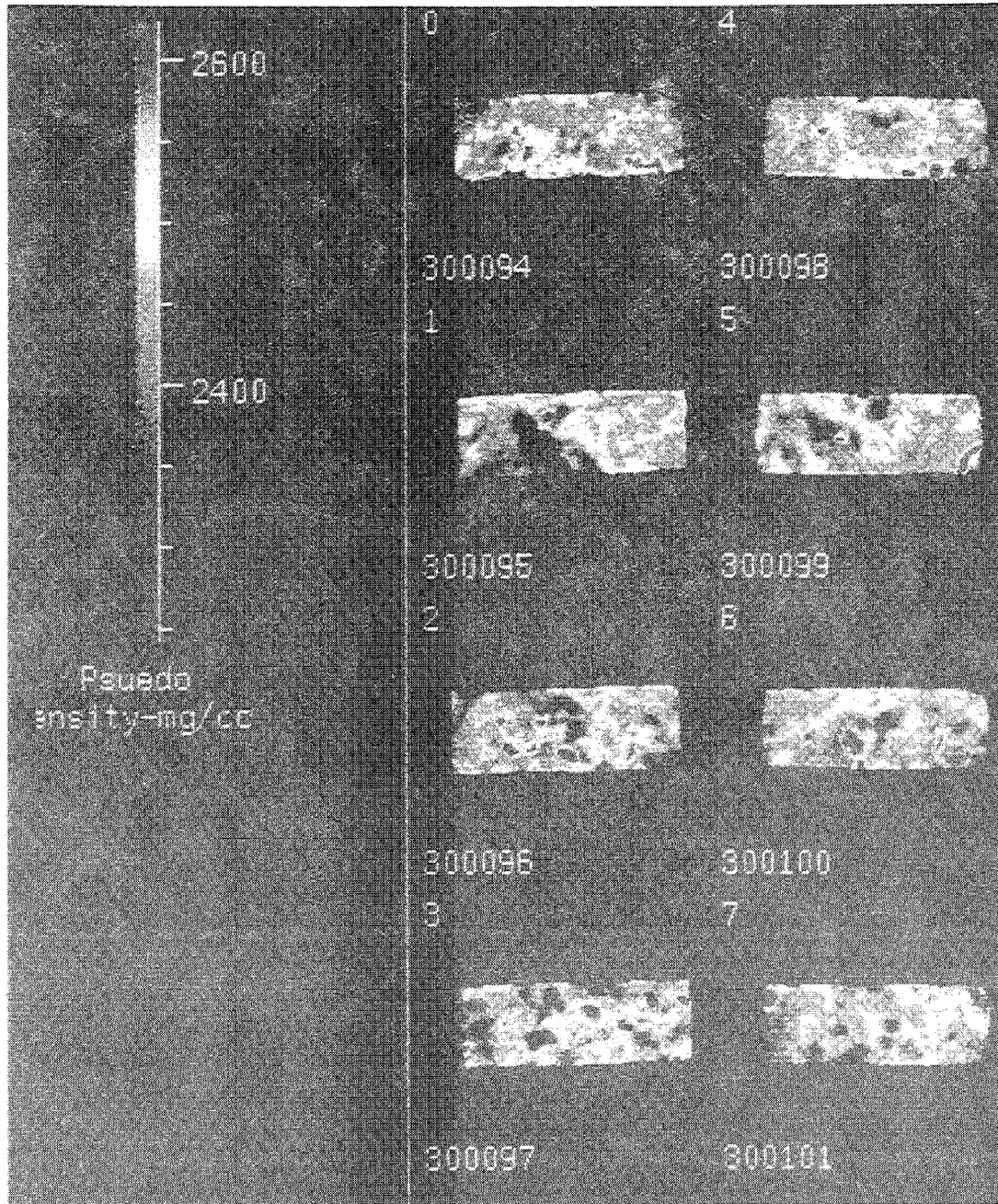


Figure 3.5. A set of CAT scans of two mutually perpendicular longitudinal-axial sections of each of the four core plugs taken from the Anasazi No. 6H-1 well to assess heterogeneity and select the most consistent intervals for measuring porosity and relative permeability in the Anasazi reservoir. The relative shades indicate pseudo density (mg/cc); the reference numbers pertain to the CAT scan locations on the core.

3.4 References

- Bebout, D.G., and Loucks, R.G., 1984, Handbook for logging carbonate rocks: Bureau of Economic Geology, University of Texas at Austin, Handbook 5, 43 p.
- Dunham, R.J., 1962, Classification of carbonate rocks according to depositional texture, *in* Ham, W.E., editor, Classification of carbonate rocks: American Association of Petroleum Geologists Memoir 1, p. 108-121.
- Eby, D.E., Groen, W.G., and Johnson, J.F., 1993, Composition of seismically identified satellite mounds surrounding Greater Aneth field, southeast Utah [abs.]: American Association of Petroleum Geologists Bulletin, v. 77, no. 8, p. 1446-1447.
- Embry, A.R., and Klovan, J.E., 1971, A Late Devonian reef tract on northeastern Banks Island, Northwest Territories: Canadian Petroleum Geologists Bulletin, v. 19, p. 730-781.
- Johnson, J.F., and Groen, W.G., 1993, Seismic structure and seismic stratigraphy of the giant Aneth field and its satellite fields of southeast Utah [abs.]: American Association of Petroleum Geologists Bulletin, v. 77, no. 8, p. 1452-1453.
- Utah Division of Oil, Gas and Mining, 1996, Oil and gas production report, December 1995: non-paginated.

4. GEOLOGICAL CHARACTERIZATION OF THE CARBONATE RESERVOIR IN THE DESERT CREEK ZONE

Douglas M. Lorenz
REGA Inc.

4.1 Location, Geometry, and General Stratigraphy

Of the five carbonate buildup fields in the Desert Creek zone originally identified as candidates for detailed study, the Anasazi field was selected for the initial investigation (figure 1.1). This mound complex has the longest production history (more than six years) and largest amount of hard data for reservoir characterization (four logged wells, three of which are also cored through the Desert Creek zone), has the most seismic coverage (six two-dimensional lines), and was considered the most promising candidate for enhanced recovery.

A detailed carbonate isolith map of the Desert Creek zone in the Anasazi area (figure 4.1) shows two mound buildups of more than 60 feet (18 m) thick, based on well log and seismic information. Three peripheral dry holes (Navajo No. 4-D [section 5, T. 42 S., R. 24 E., Salt Lake Base Line], Navajo No. D-1 [section 6, T. 42 S., R. 24 E., Salt Lake Base Line], and Navajo No. B-7 [section 32, T. 41 S., R. 24 E., Salt Lake Base Line]) do not penetrate any mound buildup facies in the Desert Creek zone, and serve to define the average non-mound Desert Creek thickness (110 feet [34 m]) in the vicinity of the Anasazi field.

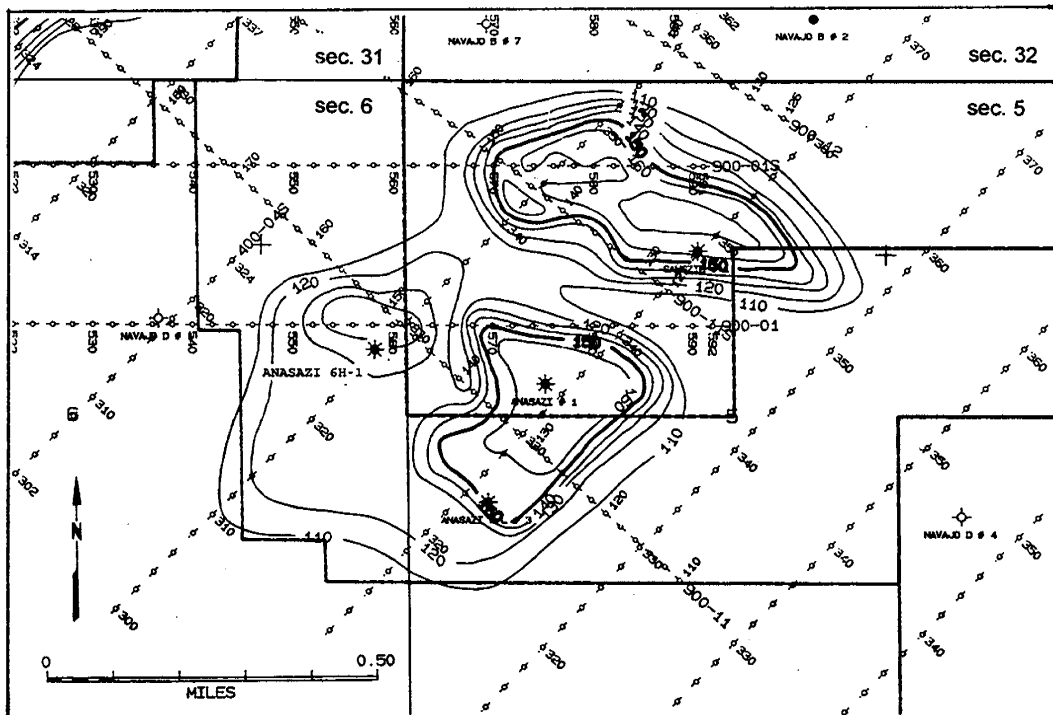


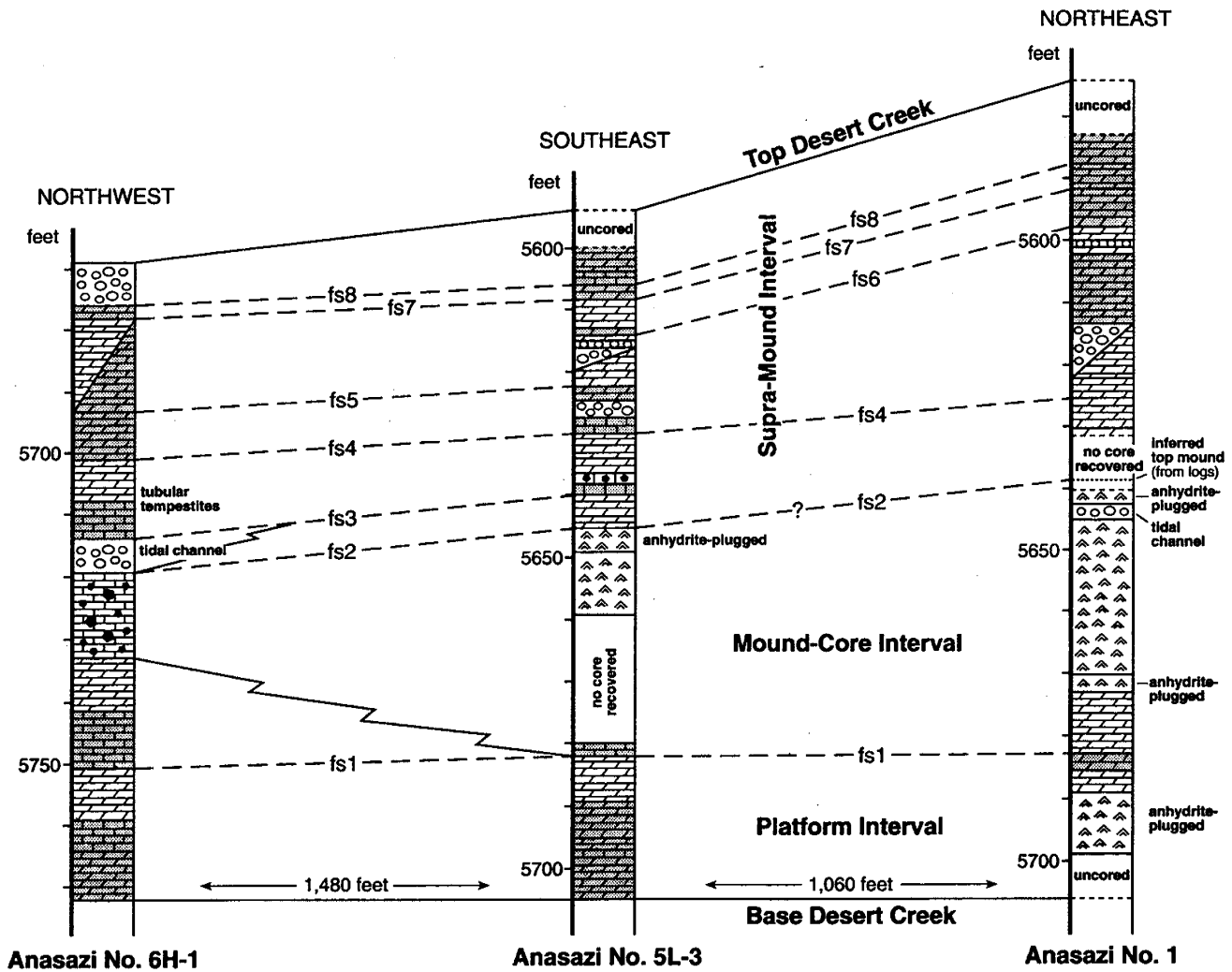
Figure 4.1. Gross Desert Creek isopach based on geophysical well log and seismic data, Anasazi field, sections 5 and 6, T. 42 S., R. 24 E., Salt Lake Base Line, San Juan County, Utah. Contour interval = 10 feet. Dotted lines are seismic shot points.

A variety of carbonate facies is encountered in all four Anasazi wells which causes a high degree of spatial heterogeneity in reservoir properties. To adequately represent the effects of this heterogeneity on reservoir behavior, detailed characterizations of these heterogeneous facies and their joint distributions within the reservoir volume must be developed.

In the mound buildup area, the Desert Creek zone is stratigraphically subdivided into three intervals. The lowest interval, averaging 25 feet (8 m) in thickness, consists largely of tight dolomudstones, with some slightly enhanced porosity (up to 10 percent) and interbedded dolomitized packstones and wackestones. A middle interval or mound core (30 to 50 feet [9-15 m] thick) is comprised almost entirely of phylloid algal bafflestone. These mound-building limestones exhibit substantial porosity (up to 22 percent locally) and permeability (generally 150 to 300 md; locally greater than 1,000 md). Thin dolomudstones, packstones, wackestones, and a few grainstones are found in flanking peripheral areas. The upper interval (55 to 65 feet [17-20 m] thick) contains largely dolomitized mudstones, packstones, wackestones, and grainstones in which each lithotype shows a wide range of secondary pore system alteration from slight (porosity less than 2 percent and permeability less than 0.1 md) to significant (porosity greater than 24 percent and permeability up to 50 md). Based on detailed core and log interpretations of the Anasazi wells and on geological studies of nearby analogous Pennsylvanian carbonate mound buildups (see Section 2.2, Outcrop Reservoir Analogues), these three successive stratigraphic intervals are identified as distinct time-equivalent sequences, termed the "platform interval", the "mound-core interval" and the "supra-mound interval", respectively. Detailed correlation of flooding surfaces (figure 4.2) demonstrates their lateral continuity within the Anasazi mound complex. The mound-core and supra-mound intervals together constitute the Anasazi reservoir; the platform interval is tight and does not yield commercial hydrocarbons.

4.2 Reservoir Architecture

The lower mound-core interval of the Anasazi reservoir is porous and highly permeable. The overlying supra-mound interval has lower permeability and higher average porosity than the underlying algal bafflestones of the mound-core interval. Results of simple two-layer constant-property, two-dimensional numerical flow simulations (see Section 6, Mechanistic Reservoir Simulation Studies) indicate that although oil production rates are significantly higher in the permeable algal bafflestone of the mound-core interval, most of the oil resides in the overlying porous dolomites of the supra-mound interval. The results of these preliminary studies, along with field production data, show that as the oil is produced from the algal bafflestones, oil from the overlying dolomites continually replenishes the bafflestone pore system, resulting in a production capacity far greater than can be attributed to the mound-core interval alone. In addition, drilling history in the Anasazi field strongly suggests that the entire reservoir has been on pressure decline since the first well was drilled in 1989 (see Appendix A, Anasazi field summary). Thus, despite the apparent heterogeneity in reservoir properties, the mound-core interval bafflestones and the supra-mound interval dolomites apparently are in pressure communication throughout the reservoir.



EXPLANATION

- Mound-core phylloid algal bafflestone with fair to good porosity and excellent permeability (except near mound top where anhydrite plugging is common)- **excellent reservoir quality**
- Grainstones with enhanced porosity- **good to excellent reservoir quality**
- Dolomitized mudstones/packstones/wackestones with enhanced porosity- **fair to good reservoir quality**
- Mound-flank mixed carbonates, brecciated/slumped/chaotic with fair porosity and permeability- **fair reservoir quality**
- Tight mudstones/packstones/wackestones and cemented grainstones- **poor reservoir quality**
- Flooding surfaces (fs1-fs8)

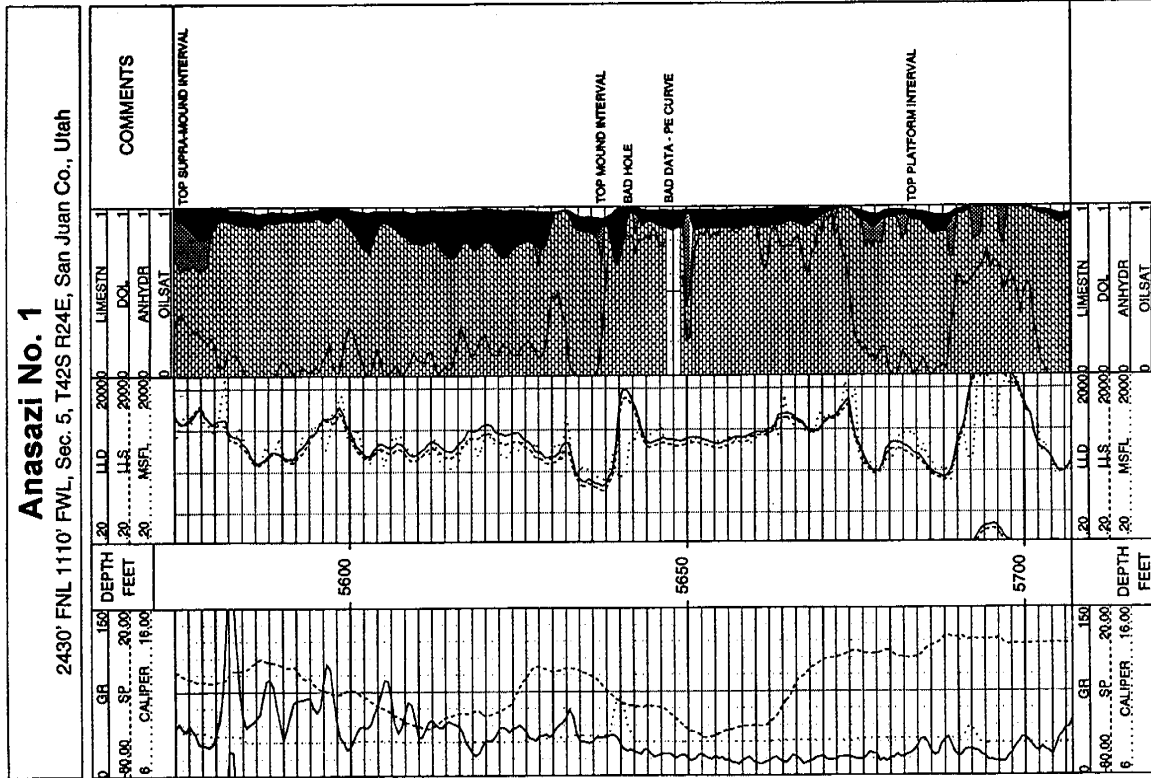
Figure 4.2. Stratigraphic cross section across Anasazi field displaying reservoir lithotypes, flooding surfaces, and facies relations within the Desert Creek platform, mound-core, and supra-mound intervals based on core.

To represent the vertical and lateral heterogeneity known to be present in the Anasazi reservoir, yet ensure that the well-documented lateral and vertical communication also is realistically modeled, a detailed facies interpretation of the conventional core from three Anasazi wells (Anasazi Nos. 1, 5L-3, and 6H-1) was undertaken. From these results, together with the log interpretations (figure 4.3), conventional core analysis, and geologically inferred lateral facies relationships based on the outcrop studies, a reservoir modeling procedure was designed to incorporate the major facies types as individual architectural entities, each exhibiting internal heterogeneities in reservoir properties but contrasting sharply between the individual lithotypes. Ten architecturally distinct lithotypes were identified in the mound core interval, eight of which also comprise the supra-mound interval in the Anasazi reservoir (table 4.1). They include the tight mudstones, packstones, wackestones, and grainstones characteristic of the off-mound areas in both intervals (figure 4.4); similar facies exhibiting enhanced porosity resulting from dolomitization and/or leaching found in the buildup areas of the supra-mound interval (and also scattered throughout off-mound areas; figures 4.5 and 4.6); and the porous, highly permeable phylloid algal bafflestones and associated mound-flank breccias (figure 4.7) which are almost entirely restricted to the buildup areas of the mound-core interval.

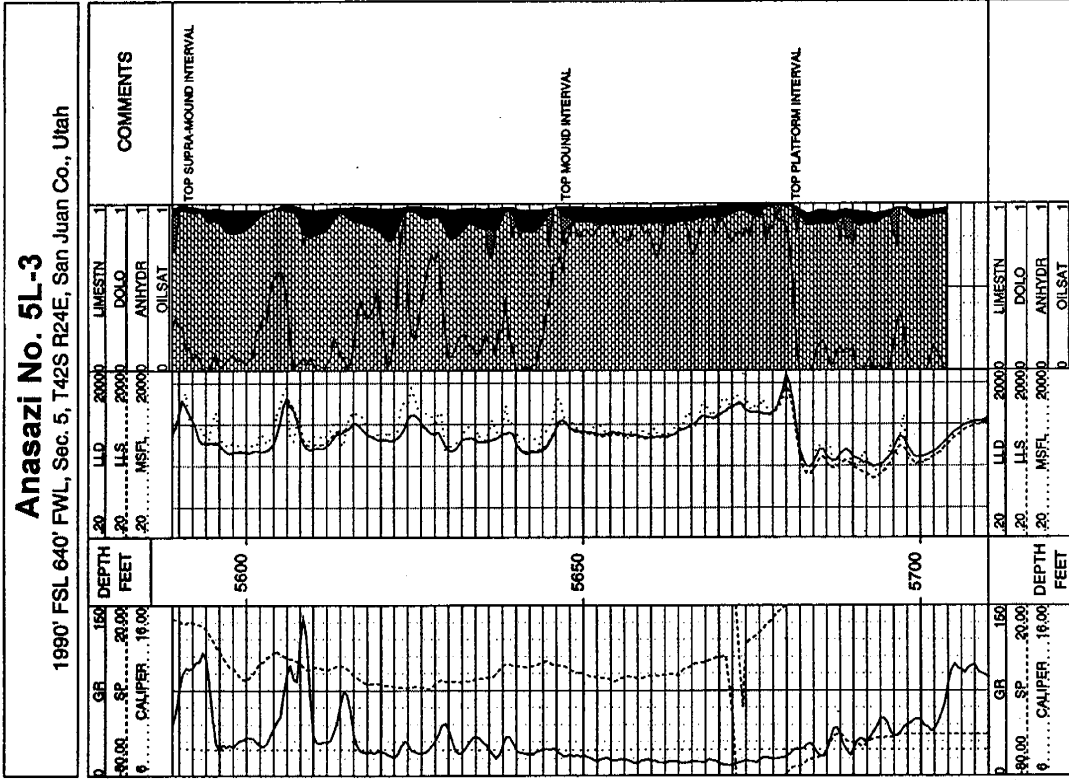
4.3 Reservoir Model Geometry

The overall Desert Creek zone in the Anasazi field represented by the isopach in figure 4.1 includes not only the reservoir interval, but also: (1) the underlying non-reservoir platform interval and (2) a sequence of overlying anhydrites. However, the aggregate non-reservoir thickness in all four Anasazi wells is remarkably constant, measuring within two feet (0.6 m) of the average thickness of 62 feet (19 m). Consequently, an isolith map of the reservoir (mound-core plus supra-mound) intervals can be obtained (figure 4.8) by subtracting 62 feet (19 m) from the Desert Creek isopach. This isolith map is used in the model to define the upper boundary of the Anasazi reservoir. The base of the reservoir (= top of the platform interval) is approximately co-planar in the four Anasazi wells, and is represented in the model as a surface of uniform slope, dipping at 0.7° to the southeast. Figure 4.8 also shows the x-y map grid defined in the model, which consists of a 30 X 50 grid block array, with individual block dimensions of 105 feet (32 m) square.

Based on the observed bedding frequencies, an average layer thickness of two feet (0.6 m) in the mound buildup areas was selected for the initial reservoir model. Although the total reservoir thickness varies considerably (figure 4.8), the relative proportions of mound-core and supra-mound interval thicknesses in the four Anasazi wells are all about 0.4 and 0.6, respectively (figure 4.3). Thus, the mound-core and supra-mound intervals are subdivided into 20 and 30 equal-thickness layers, which yield approximately two-foot (0.6-m) layers within and over the mound buildups, thinning to about half that in the peripheral areas. Consequently, the initial Anasazi model consists of 50 layers, each divided geographically into 1,500 x-y blocks, for a total of 75,000 grid blocks, representing an overall volume of 57.8 million cubic feet (17.6 million m^3).

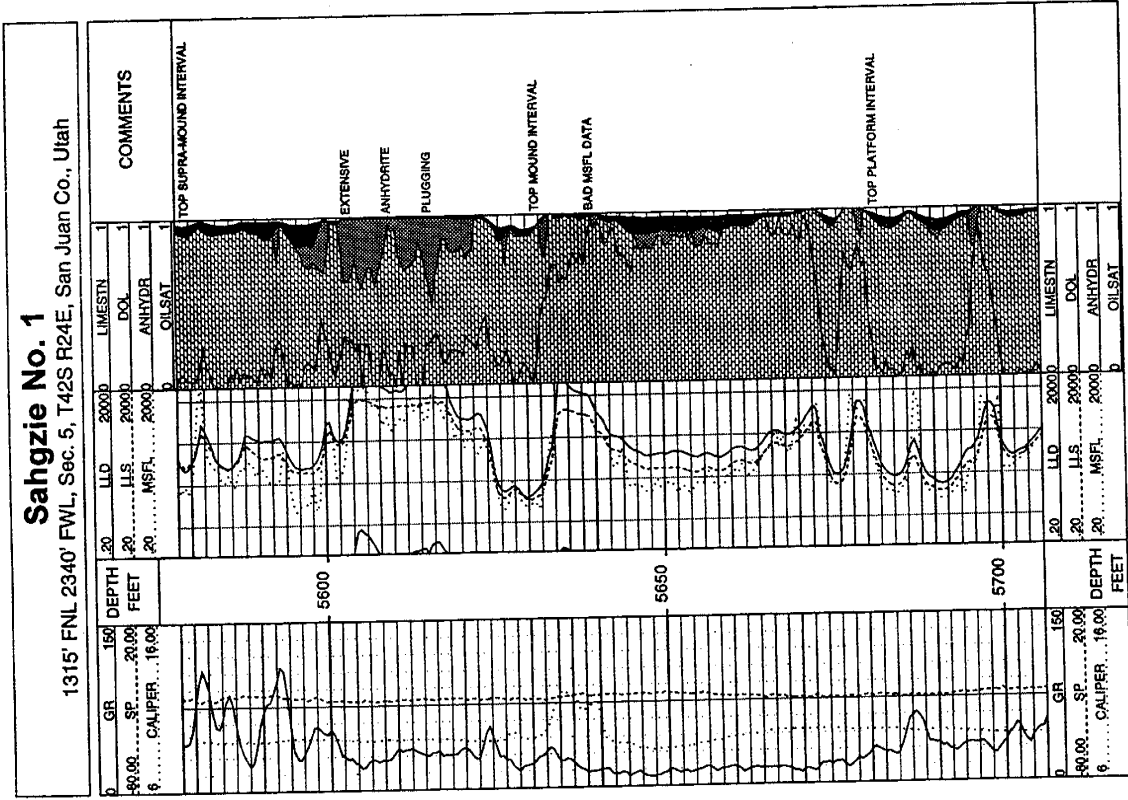


(A)

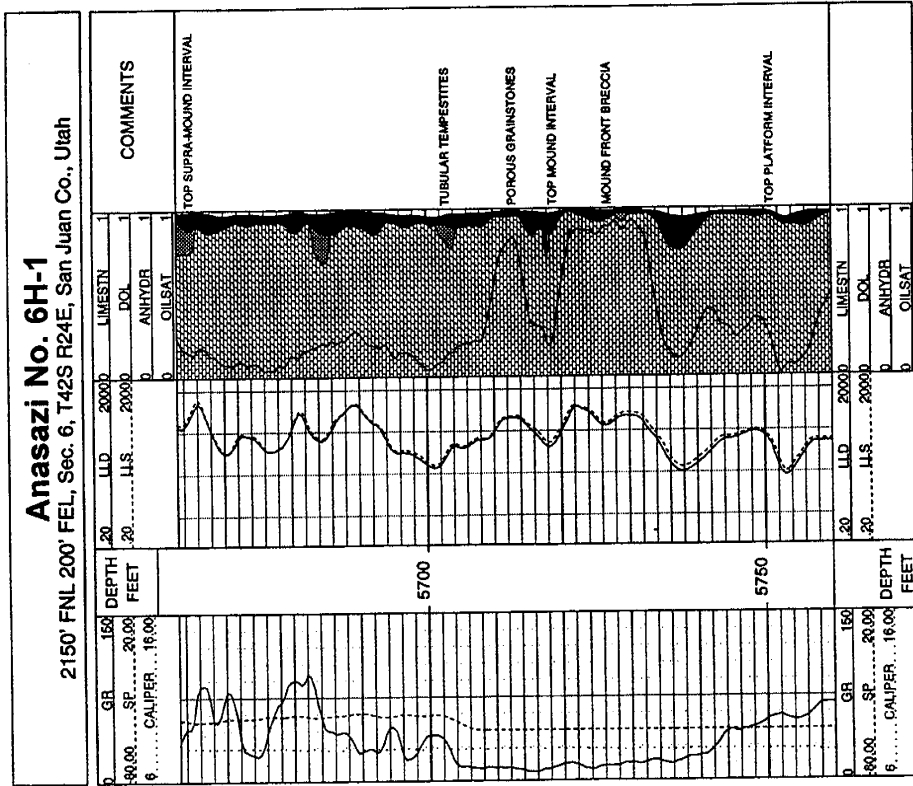


(B)

Figure 4.3. Computed geophysical well logs and lithology plots of the Desert Creek zone for the: (A) Anasazi No. 1, (B) Anasazi No. 5L-3, (C) Anasazi No. 6H-1, and (D) Sahgzie No. 1 wells, Anasazi field.



(D)

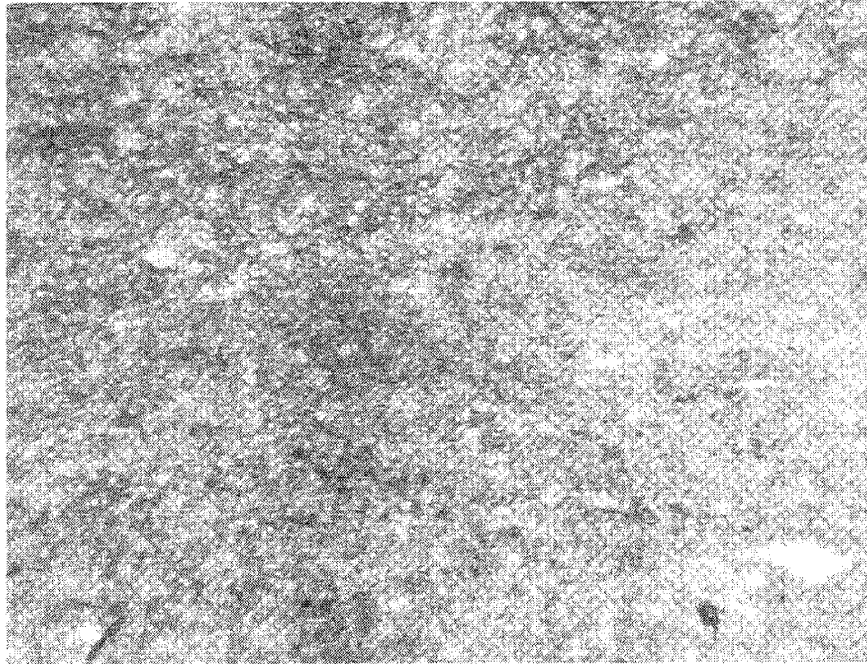


(C)

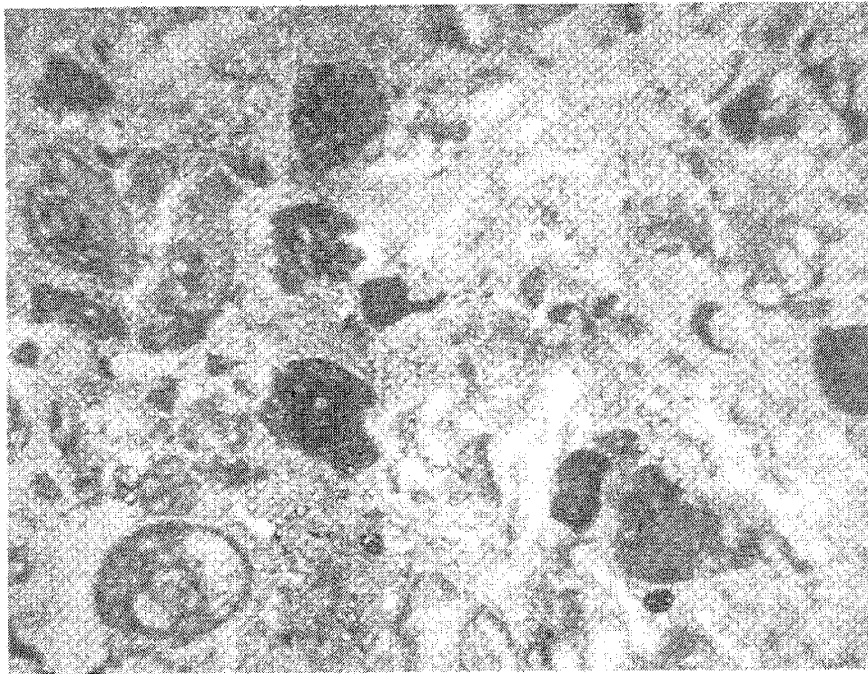
Figure 4.3. (continued).

Table 4.1. Average reservoir properties of architectural lithotypes, Anasazi field.

Lithotype	Average Bed Thickness (ft)	Average Porosity (%)	Average Permeability (md)	Volume Proportion
Tight Mudstone	3.7	2	0.25	0.24
Dolomitized Mudstone	5.5	9	1.51	0.06
Porous Mudstone	2.9	11	2.00	0.05
Tight Packstone/Wackestone	2.4	2	0.02	0.14
Porous Packstone/Wackestone	3.8	10	1.80	0.05
Tight Grainstone	2.2	2	0.15	0.07
Porous Grainstone	3.2	15	15.00	0.08
Tubular Tempestites in Mudstone/Wackestone/Packstone	6.7	9	8.00 (est)	0.07
Phylloid Algal Bafflestone	42.0	10	150.00	0.22
Mound-Flank Breccia	13.0	8	30.00 (est)	0.02

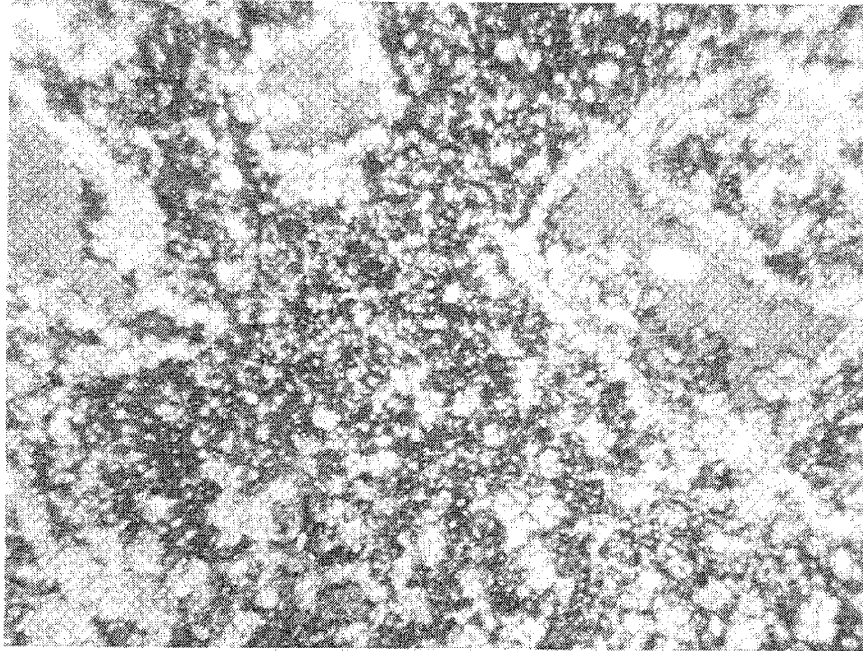


(A)

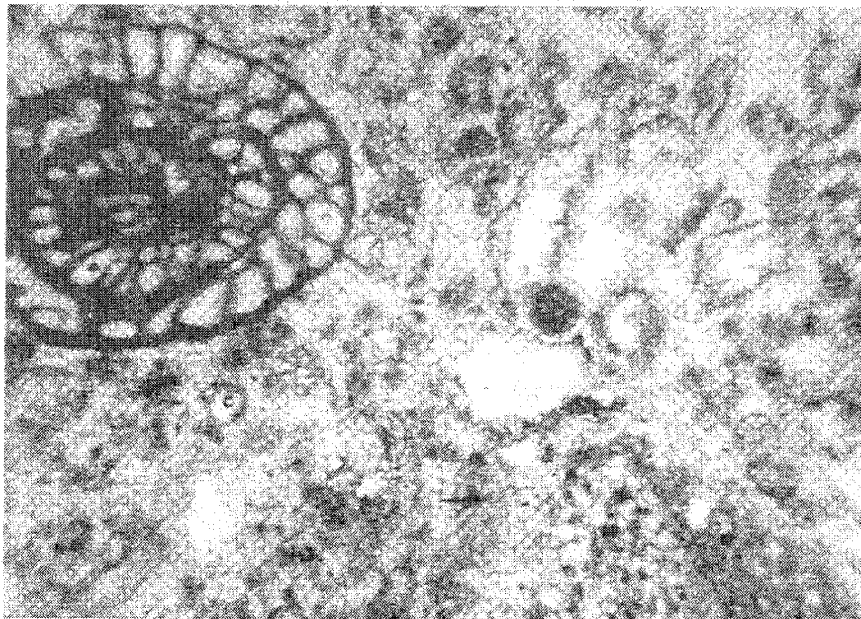


(B)

Figure 4.4. Photomicrographs of thin sections (plane light view) showing low-quality architectural lithotypes (24x). (A) Low-permeability mudstone from the Anasazi No. 1 well (sample depth = 5,622.6 feet [1,713.7 m]). White objects are recrystallized calcite. (B) Low-permeability grainstone from the Anasazi No. 5L-3 well (sample depth = 5,629.6 feet [1,715.8 m]). White areas are pore-filling calcite cement; dark objects are bioclastic fragments.

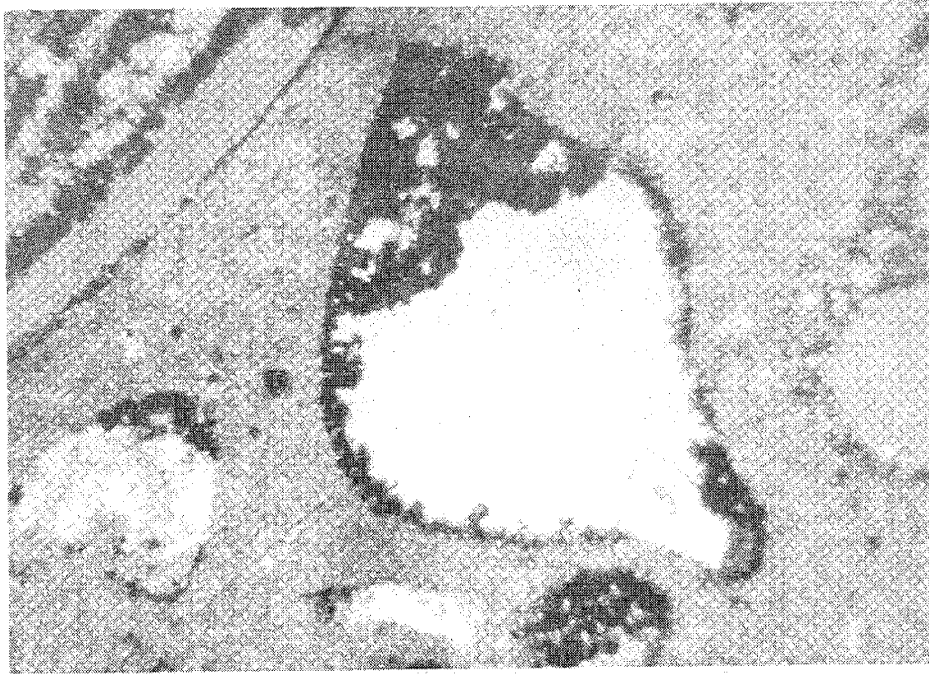


(A)



(B)

Figure 4.5. Photomicrographs of thin sections (plane light view) showing high-quality architectural lithotypes (24x). (A) Dolomitized mudstone, with enhanced porosity, from the Anasazi No. 6H-1 well (sample depth = 5,691.2 feet [1,734.6 m]). Gray objects are enhanced pores, recrystallized dolomite is white, and interstitial bitumen is black. (B) Grainstone, with enhanced porosity, from the Anasazi No. 5L-3 well (sample depth = 5,616.2 feet [1,711.7 m]). Pores are uniformly white to light gray; many are lined with cement; dark objects are bioclastic fragments.



(A)



(B)

Figure 4.6. Photomicrographs of thin sections (plane light view) showing moderate- to high-quality architectural lithotypes (24x). (A) Dolomitized packstone, with enhanced porosity, from the Anasazi No. 1 well (sample depth = 5,621 feet [1,713 m]). Large, uniform white and gray objects are enhanced pores; pinpoint white and gray areas are microcrystalline dolomite, and black areas are residual bitumen. (B) Tubular tempestitute (relict burrow) from the Anasazi No. 1 well (sample depth = 5,601 feet [1,707 m]). The burrow contains small and mid-size pores (white objects) surrounded by undisturbed, tight dolomitized mudstone.

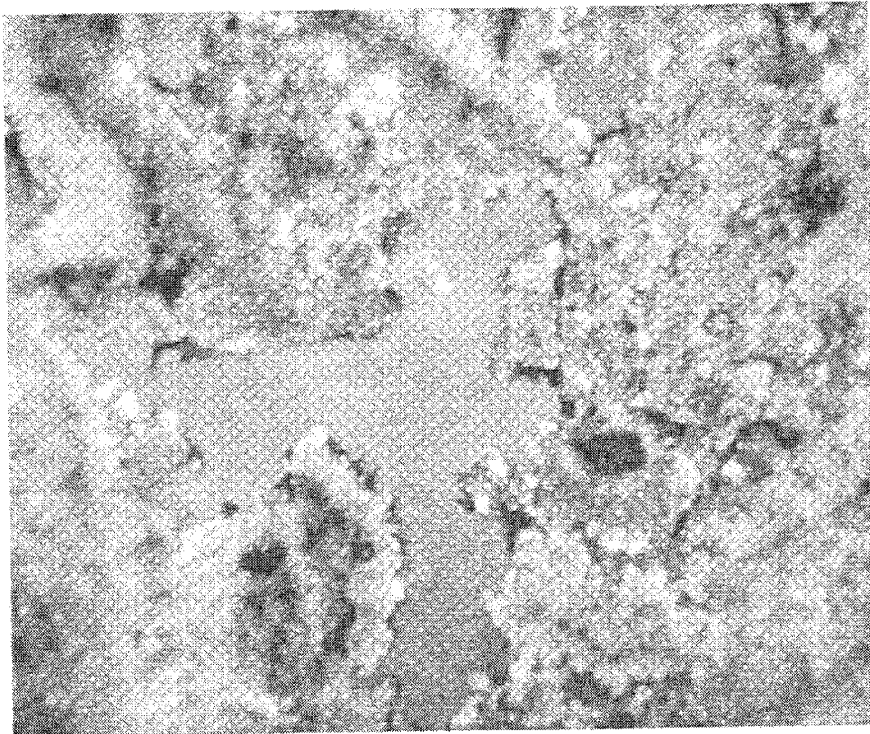


Figure 4.7. Photomicrograph of a thin section (plane light view) showing a phylloid algal bafflestone from the Anasazi No. 1 well (sample depth = 5,654.3 feet [1,723.3 m]) (24x). Large, irregularly-shaped, cement-lined pores (uniformly gray) are bounded by phylloid algal plates (dark elongate objects).

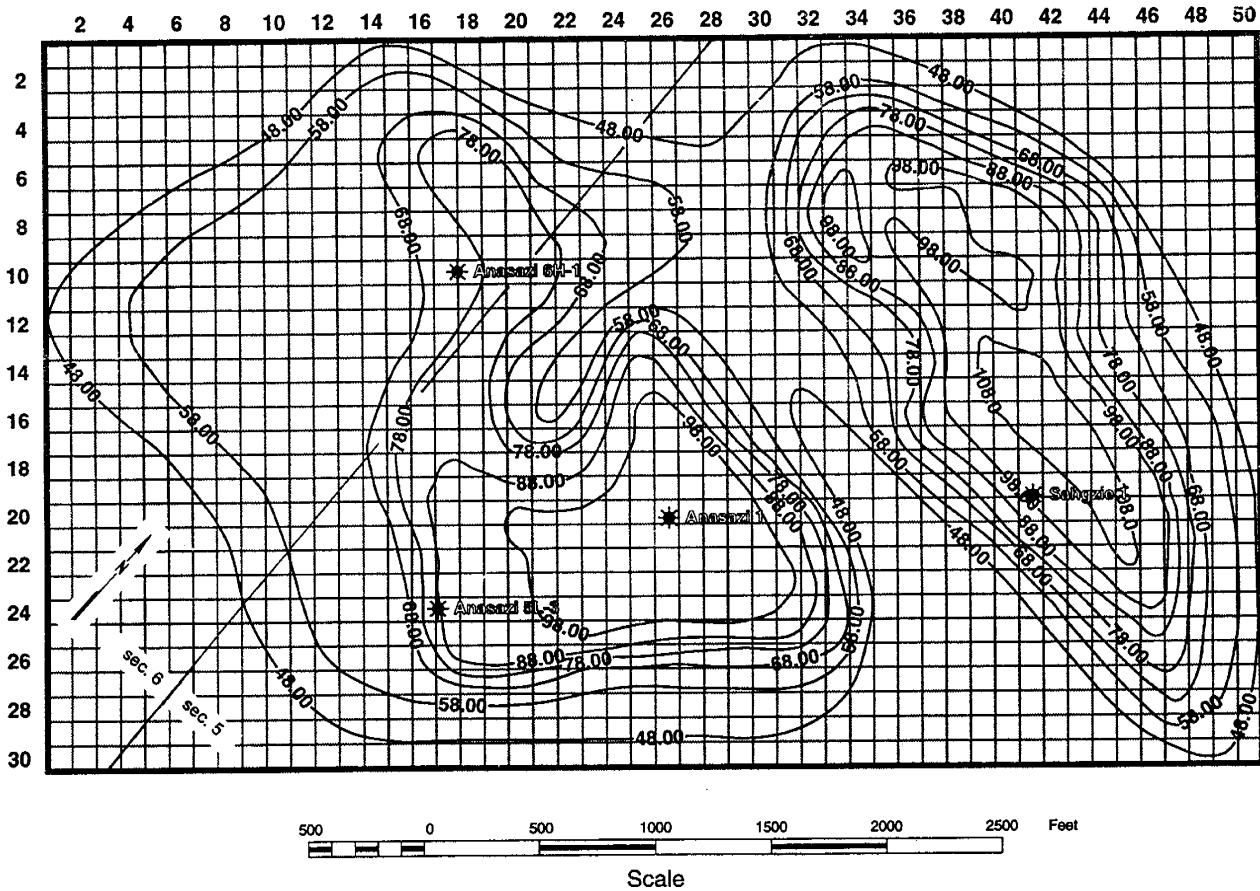


Figure 4.8. Anasazi reservoir gridded isolith map; contour interval = 10 feet, grid block = 105 square feet. Note that the geographic orientation of the map is rotated counterclockwise by 40° relative to figure 4.1.

4.4 Seismic Constraints

One of the most difficult problems normally encountered in reservoir characterization is the lack of adequate data on patterns of lateral variation in reservoir properties between wells. Lacking hard data from horizontal wells or detailed three-dimensional seismic records, the only recourse is to constrain the model using "soft" information from other sources. Fortunately, data from the six two-dimensional seismic lines over the Anasazi field (figure 4.1) are good quality and can be used to roughly characterize (constrain) lateral variations in average reservoir quality.

Based on two interpreted indices of reservoir quality from the common-depth-point stacked and migrated seismic cross sections, a single index (designated the "Reservoir Quality Index", or RQI), scaled from 0 to 10, was derived and mapped (figure 4.9). This map shows clearly that the best reservoir quality roughly coincides with areas of greatest mound buildup (figure 4.8). However, translation of RQI into equivalent quantitative expressions of standard reservoir properties is somewhat ambiguous. Acoustic properties of rocks are affected by such static reservoir properties

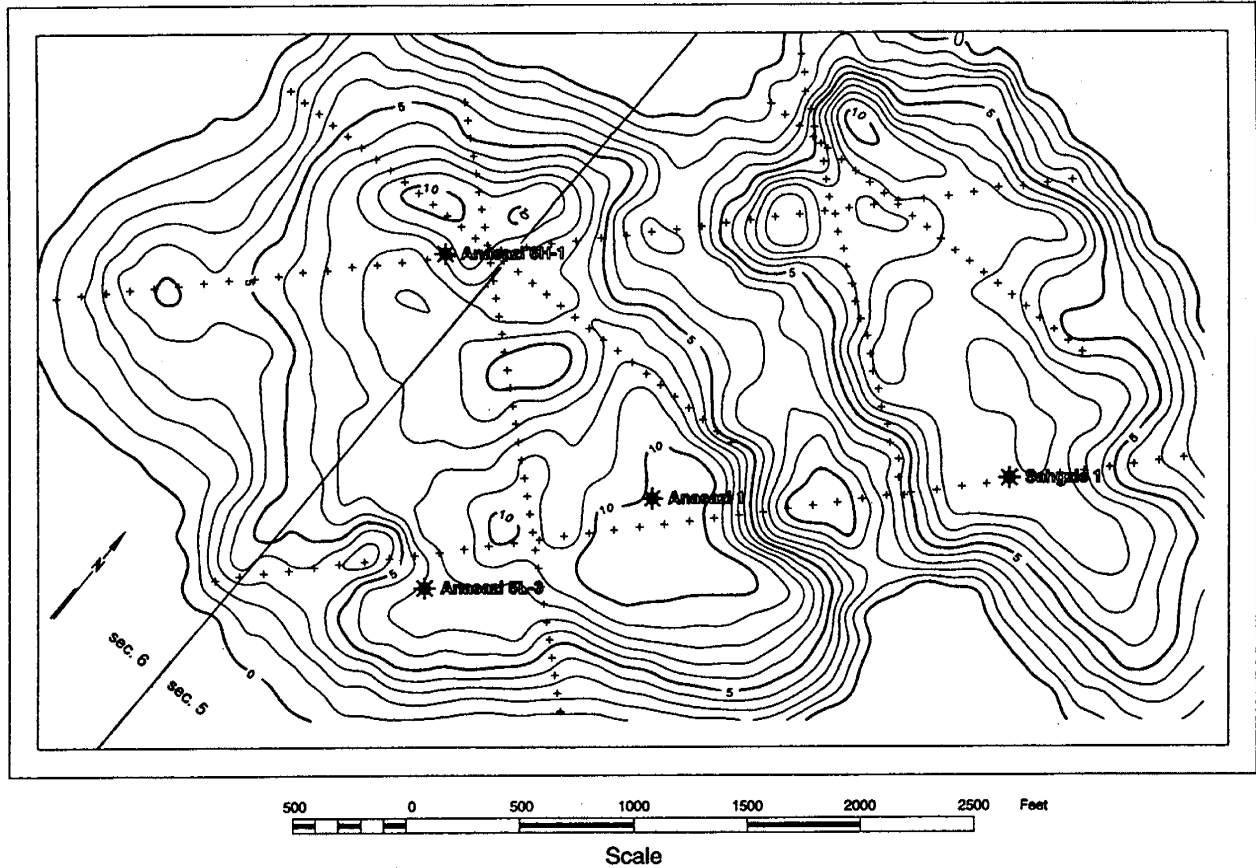


Figure 4.9. Reservoir quality index (RQI) map with seismic data points (+), Anasazi reservoir. Contour interval = 1.

as lithology, porosity, and thickness, but not (directly) by flow properties like permeability. Hence, since the original seismic interpretations were designed to complement the isochrons on which the reservoir thicknesses are based (figure 4.8), the RQI is likely to be primarily a function of porosity and lithology.

A plot of the RQI and average porosity derived from well logs in the four Anasazi wells (figure 4.10) shows that both lithology and porosity affect RQI. The anomalously low porosity relative to the high RQI in the Sahgzie No. 1 well is chiefly attributable to massive anhydrite plugging in the supra-mound dolomites (figure 4.3D). Because the distribution of anhydrite in the reservoir is unknown, the RQI-to-average porosity transfer function is defined as a separate linear function at each well (figure 4.10), thus fitting the hard data exactly. The common zero-intercept at an average porosity of 4 percent corresponds to the average porosity over all non-pay intervals among the four wells. At grid points between the wells, the slope coefficient is defined as an inverse-distance weighted average of the slopes at the four wells (figure 4.10). The resulting map of average reservoir porosity (figure 4.11) will be used as a constraining variable for lateral variation in the reservoir modeling.

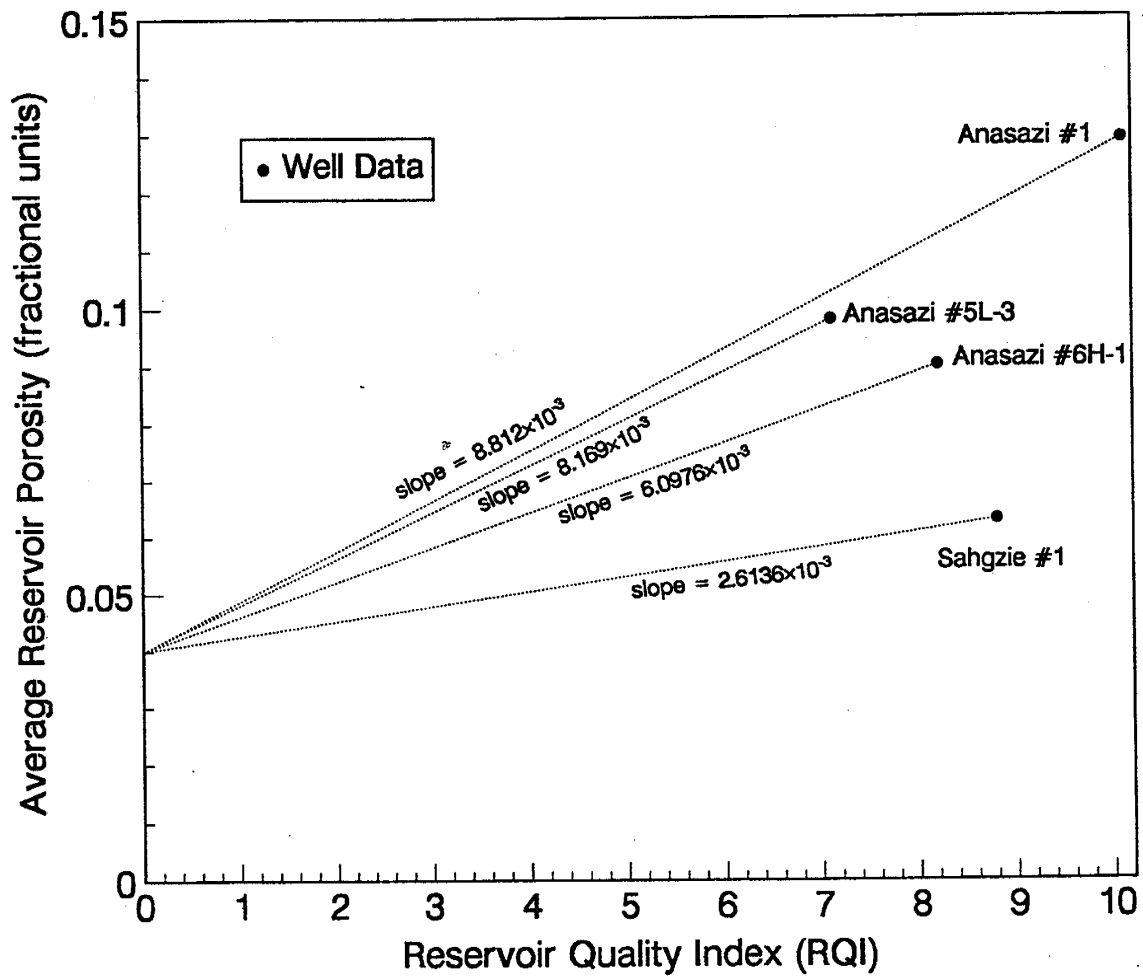


Figure 4.10. Estimation of average porosity from RQI, Anasazi reservoir.

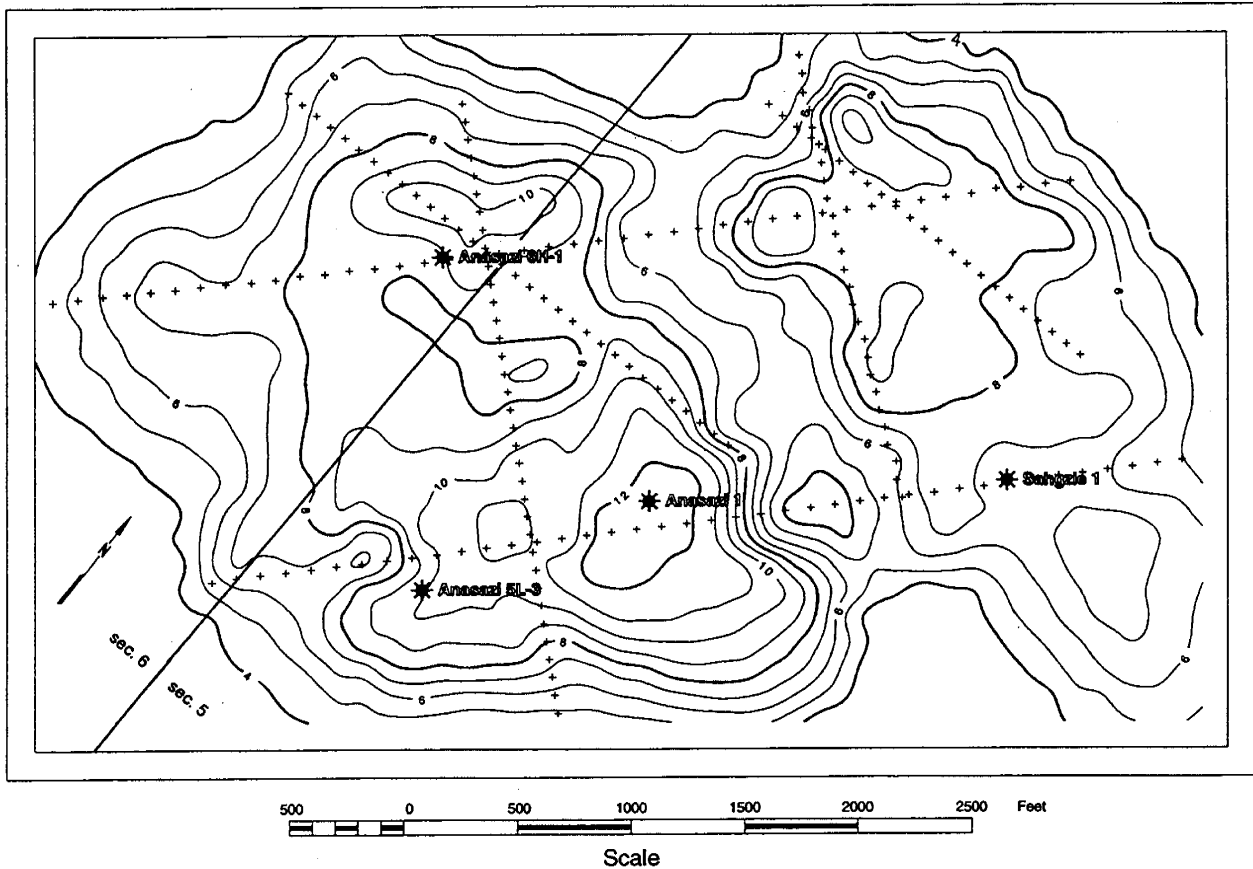


Figure 4.11. Map of average porosity derived from the RQI, Anasazi reservoir. Contour interval = 1 percent; seismic data points (+).

4.5 Reservoir Model Design

Although significant vertical and lateral variations in reservoir properties characterize the Anasazi reservoir, these variations can be partially resolved by representing the different lithotypes as distinct architectural components, within each of which the pattern of spatial variation distinctive of that lithotype can be treated individually. The overall modeling strategy is to first emplace the various lithotypes as separate "bodies" or "architectural objects" (a procedure termed "Boolean Emplacement"), then to rearrange individual grid blocks (under appropriate geological constraints) to improve conformance to the seismic-based average porosity constraint (see Section 4.4, Seismic Constraints), and finally to generate local patterns of vertical and lateral porosity variation within each lithotype using conventional geostatistical methods (Sequential Gaussian Simulation). Permeability will be generated from the modeled porosity using crossplot transfer functions developed from core data. At all stages of model development, the hard reservoir property data from the wells themselves is rigorously honored.

The data required to carry out the modeling procedures outlined above have been obtained from a number of different sources. Information on architectural lithotypes, their averages and

ranges of reservoir properties, stratigraphic distribution/succession, porosity/permeability relationships and layering/interface properties is based on logs and cores from the Anasazi wells. Geometric properties of the various architectural elements (for example packstone/wackestone patches, tidal-channel grainstones, and mound-flank breccias) were obtained from the outcrop investigations. The average porosity constraint on lateral spatial variation is based on seismic interpretation. Inferred patterns of vertical variation within each lithotype are based on well logs and cores; patterns of lateral variation have been developed from the outcrop studies and published information on Aneth field and its analogues (Best and others, 1995). These modeling procedures are currently being developed; implementation and generation of the initial reservoir models is anticipated during the first quarter of 1996.

4.6 References

Best, D.A., Wright, F.M., III, Sagar, Rajiv, and Weber, L.J., 1995, Contribution of outcrop data to improve understanding of field performance: rock exposures at Eight Foot Rapids tied to the Aneth field, *in* Stout, E.L., and Harris, P.M., editors, Hydrocarbon reservoir characterization - geologic framework and flow unit modeling: Society of Economic Paleontologists and Mineralogists Short Course No. 34, p. 31-50.

5. ENGINEERING RESERVOIR CHARACTERIZATION OF THE CARBONATE RESERVOIR IN THE DESERT CREEK ZONE

W.E. Culham
REGA Inc.

Two processes, with appropriate variations, are being evaluated for selection of the best (from a standpoint of oil recovery and economics) for implementing in a field pilot or demonstration project. Prior to evaluation of the two processes it will be necessary to model and history match the primary production phase of the Anasazi reservoir. Thus, the following general class of simulation studies will be performed:

1. primary depletion (history match),
2. waterflood, and
3. CO₂ flood.

A compositional simulation approach is being used to model all three processes. A compositional approach properly accounts for oil vaporization (high API gravity oils) during primary depletion and will provide the correct oil compositions to subsequently assess CO₂ flooding potential. A black oil approach could be used for the waterflood study, but again, potential compositional changes and their impact on resaturation of the oil with gas during fill up would be most rigorously accounted for in a compositional approach. Thus, compositional simulation was selected for all process evaluations.

The main tasks of the engineering portion of the work are:

1. review of existing field data including re-evaluation of well test data,
2. reservoir fluid and rock characterizations via an extensive laboratory program,
3. reservoir development (history match, process design/evaluation for waterflood and CO₂), and
4. economics.

Work has been completed on the first two items and some preliminary mechanistic two-dimensional reservoir simulation studies were completed using a simplified geologic model of the reservoir. These four work items are reviewed in the following sections.

5.1 Review of Existing Field Data and Re-evaluation of Well Test Data

5.1.1 Field Data Review

Basic field information reviewed for this study included historic production data for the Anasazi field, a review of special core tests (such as relative permeability data), and fluid characterization studies on associated Paradox basin reservoirs.

Historic production data for individual wells in the field were reformatted into data files for use during simulation work to provide a basis for comparing actual historic well/field performance versus simulated data to facilitate the history matching.

Review of relative permeability data (only one study involving cores from Runway and Anasazi was available) provided the basis for assessing the validity of existing data based on new comprehension wettability and relative permeability measurements (discussed later).

The review of the fluid properties studies provided the basis for identifying appropriate data sets to incorporate into equation of state tuning employing newly derived fluid property data. This review identified basic "black oil" pressure-volume-temperature (PVT) studies from seven different reservoirs (Anasazi, Mule, Blue Hogan, Brown Hogan, Heron North, Runway, and Jack fields [figure 1.1]) that were available for analysis. A review of compositions, bubble point pressures, and solution gas-oil ratios identified only the Jack field as being appropriate to integrate with existing Anasazi data and the newly generated fluid characterization information. As discussed below the data sets will be integrated with the newly generated data to "tune" an equation of state for use in the compositional simulation work.

5.1.2 Well Test Data Re-Evaluation

Well-test data can provide key insight into the nature of reservoir heterogeneities and also provide "large scale" quantitative data on actual reservoir properties such as storage and transmissibilities. Because of the complex geologic nature of Paradox basin target reservoirs, a re-evaluation of past transient well tests was done to determine if the test data was adequate to provide a quantitative assessment of the two key oil-producing facies (supra-mound and mound-core intervals [referred to in this and the next section as dolomite and limestone respectively]) from case-study reservoirs. Although a number of well tests have been conducted in all of the target reservoirs, only the initial well tests, which were conducted under liquid saturated conditions (above bubble point) were determined to provide quantitative reservoir properties information. A list of well tests re-evaluated in detail include:

Reservoir Well	Test Date
Brown Hogan No. 1A-2	April 1991
Blue Hogan No. 1J-1	February 1991
Mule No. 31-M	March 1992
Sahgzie No. 1	July 1991
Sahgzie No. 1	November 1989
Anasazi No. 1	January 1990
Anasazi No. 1	February 1990
Anasazi No. 1	January 1992
Anasazi No. 1	August 1993

To facilitate subsequent discussion, the following dual-property (porosity) well test parameters for the model type employed in the analysis are summarized below.

Dual-porosity model:

$$\text{Eq. 1} \quad \omega = \frac{(\phi c_t h)_f}{(\phi c_t h)_f + (\phi c_t h)_m}$$

$$\text{Eq. 2} \quad \lambda = \alpha r_w^2 \frac{k_m}{k_f}$$

$$\text{Eq. 3} \quad \omega_1 + \omega_2 = 1.0$$

$$\text{Eq. 4} \quad \alpha = 12/h^2 \text{ slab}$$

$$\text{Eq. 5} \quad \alpha = 15r_s^2 \text{ spherical}$$

$$\text{Eq. 6} \quad c_t = s_w c_w + s_o c_o + (1 - \phi) c_r$$

Fluid exchange between matrix and fracture:

- pseudo steady state $k_f > 100k_m$
 - one-dimensional transient
 - three-dimensional transient
- } $k_f > 10k_m$

Two-layer model:

$$\text{Eq. 7} \quad \omega = \frac{(\phi c_t h)_1}{(\phi c_t h)_1 + (\phi c_t h)_2}$$

$$\text{Eq. 8} \quad \lambda = \frac{2r_w^2 k_v}{[(kh)_1 + (kh)_2][h_1 + h_2]}$$

$$\text{Eq. 9} \quad \omega_1 + \omega_2 = 1.0$$

Variables used in the above equations are defined as:

- c_t = total compressibility
- c_o = oil compressibility
- c_w = water compressibility
- h = thickness
- h_i = $i = 1, 2$ layer thickness
- k = permeability
- k_v = vertical permeability
- k_i = $i = 1, 2$ layer permeability
- k_f = fracture system permeability
- k_m = matrix system permeability
- r_s = spherical radius of matrix fracture blocks
- r_w = well bore radius
- s_w = formation water saturation
- s_o = formation oil saturation
- α = interporosity flow parameter constant reflecting structural nature of fractured system
- ω = storativity ratio parameter
- λ = interporosity flow parameter
- ϕ = porosity (fraction)

The parameter " ω " is simply the ratio of storage ($\phi c h$) in one porosity unit to the total storage. The parameter " λ " provides a measure of interporosity flow or fluid communication as governed by the absolute permeability thickness product (or effective permeability thickness) of the porous and permeable units in the model.

The geologic review of the producing formation was used to establish basic guidelines in selecting the dual-property model. This model is different from the classical definition for dual-porosity and layered systems. The conventional definition for a dual-porosity/dual-permeability system is based on one dominant rock type or facies that exhibits a characteristic primary (or matrix) porosity and permeability. This single rock type is also fractured. Thus, a secondary (fracture) porosity and permeability system is present which is substantially different than the primary system. In the case of the Desert Creek zone, two dominant lithofacies are present (supra-mound dolomite and mound-core algal bafflestone [limestone]). These two lithofacies represent, in a generic sense, a dual-property system. Each rock type represents a single layer in a two-layer model; one layer represents the limestone and the other the dolomite, each with their own characteristic reservoir properties. In reality the limestone layer is comprised of a number of interconnected limestone units "sampled" by the well test and the dolomite layer represents the composite behavior of possibly several interconnected dolomite units. The observed well test response is governed by the interaction of the limestone facies with the dolomite facies. This type of response is consistent with data available in Bourdet (1985) which shows that behavior of multi-layer systems or heterogeneous systems characterized by high contrasts in rock properties among layers or units of the heterogeneous system can be modeled by using two elements (that is two layers). Multi-layer systems or heterogeneous systems with two dominant sets of properties behave like conventional two-layer systems with cross flow between layers (or units).

Unfortunately, of all the tests analyzed, only one provided enough detailed information to allow a meaningful "dual-porosity" interpretation. The purpose of all early well tests was to provide information on production performance and perhaps skin factors so insufficient data was gathered for quantitative dual-porosity interpretations. Pressure data in early well tests was measured infrequently and the duration of most tests was too short. The single test that could be quantitatively analyzed with a "dual-porosity" model was the Anasazi No. 1, January 1990 test.

Figures 5.1 to 5.3 present the match between measured data (+ symbol) and well test interpretation results (solid line) using a two-layer model with cross flow employing the parameters listed on each figure. A good match was obtained and indicates that the main limestone producing unit (mound-core interval) can be characterized as having a permeability of 194 md and the dolomite (supra-mound interval) a much lower permeability of 1.21 md. The storativity ratio " ω " indicates that roughly 3.5 percent of the storage of the combined system is contained in the limestone unit. This two-layer approach, with a similar range of properties, was employed in mechanistic simulation studies (discussed later in Section 6., Mechanistic Reservoir Simulation Studies) and supports this well test interpretation.

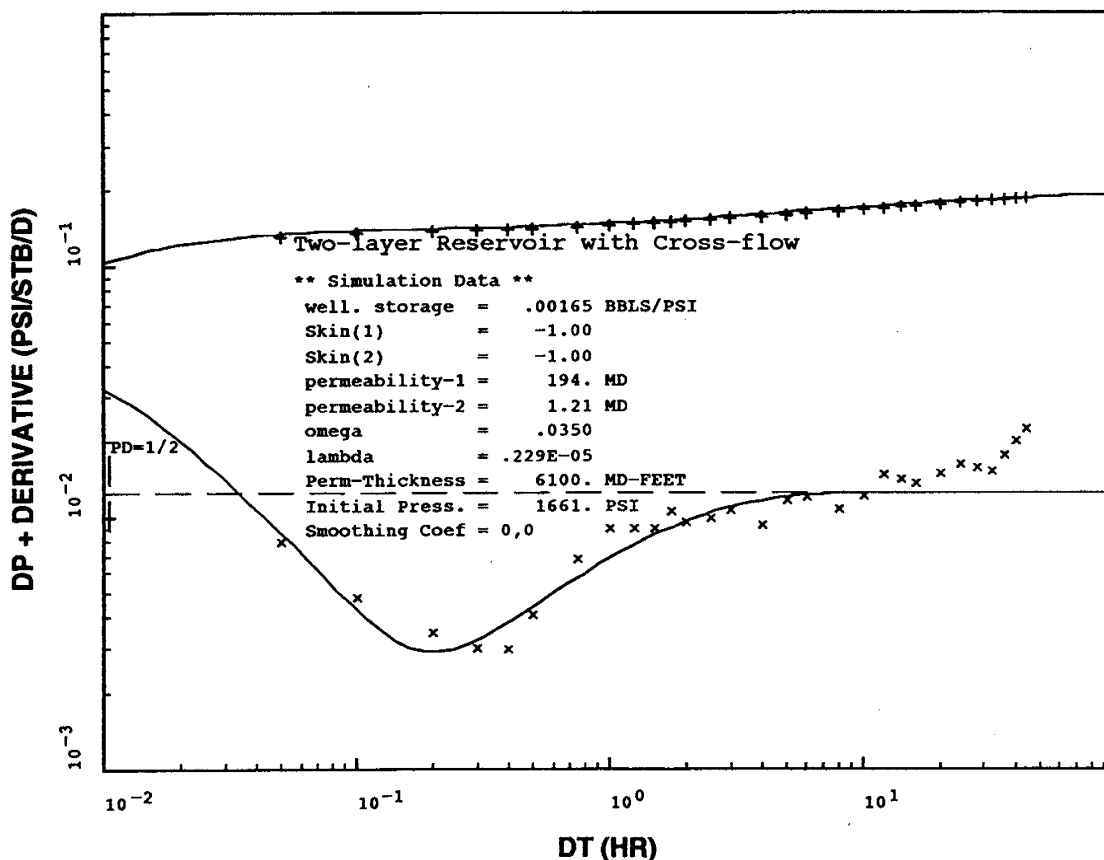


Figure 5.1. Anasazi No. 1 well test (1991) displaying pressure difference and pressure derivative match.

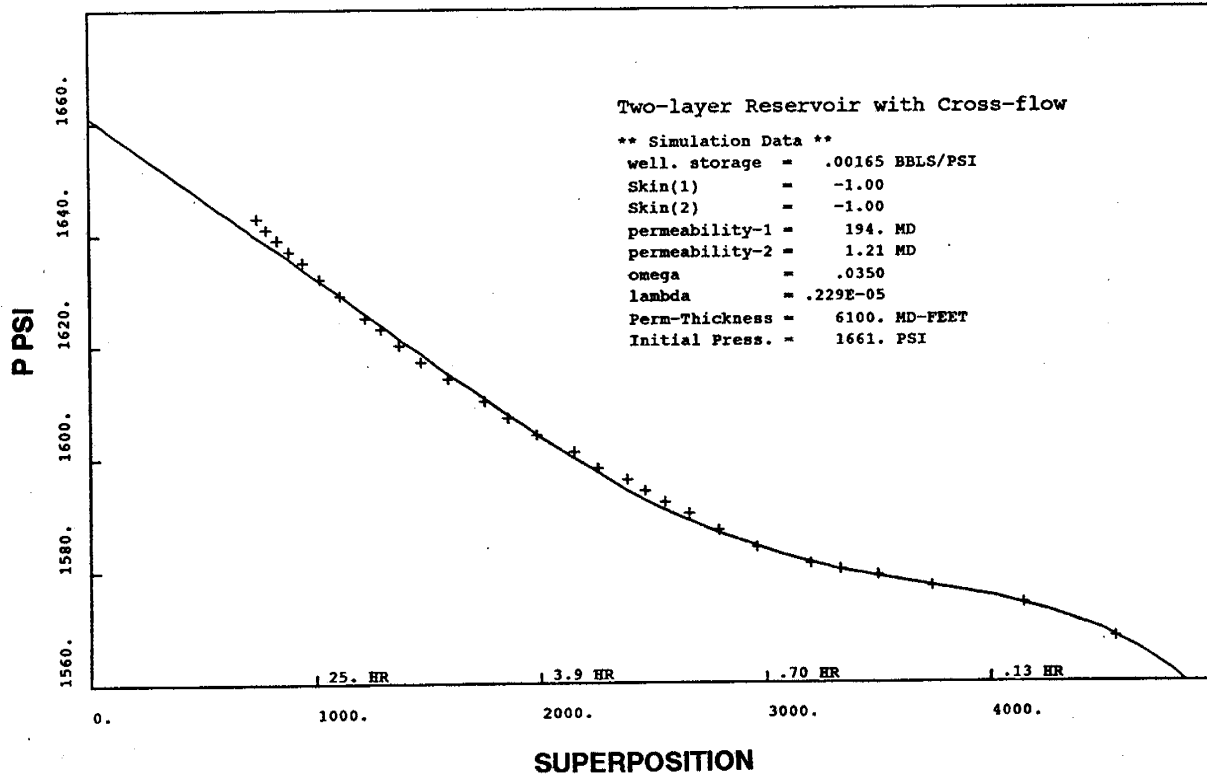


Figure 5.2. Anasazi No. 1 well test (1991) displaying superposition time vs. pressure match.

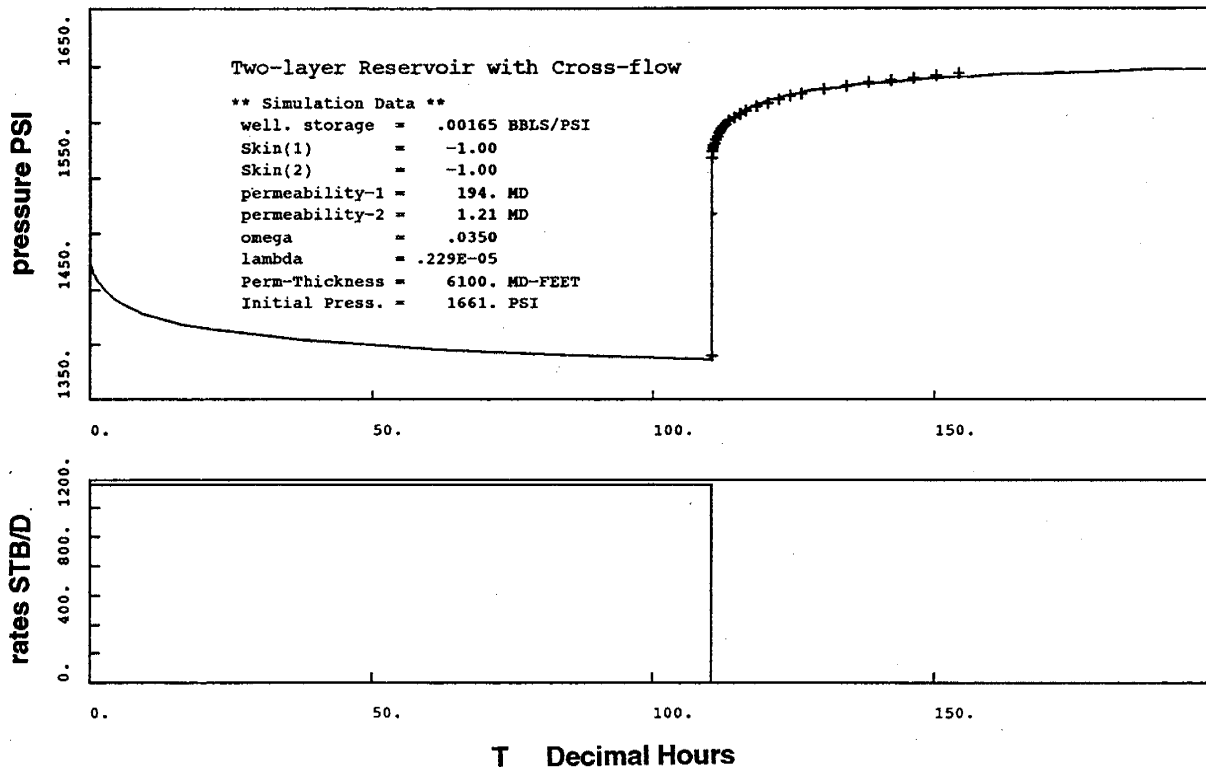


Figure 5.3. Anasazi No. 1 well test (1991) displaying pressure vs. time match.

5.2 Fluid Characterization

Two recovery processes are being evaluated to determine which has the greater recovery potential. The first is the waterflood, which can use fluid properties suitable for black oil reservoir studies. The second recovery process is CO₂ gas injection. Since CO₂ processes require compositional based data, more comprehensive fluid property data was needed. As discussed above, a compositional approach will be taken, even in the black oil cases. Existing black oil data may, however, be used to help in equation of state calibration activities. Review of existing PVT studies indicates an inadequate data set for compositional simulation and CO₂ process evaluation. Thus, the following laboratory work was proposed and carried out. Assessment of the CO₂ process will require calibration of an equation of state using the following laboratory work for tuning. The laboratory work includes:

1. extended (plus 30 carbon molecule [C30+]) compositional analysis on a recombined fluid sample,
2. a two-stage separator test, including a stock-tank condition, and
3. swelling tests employing four concentrations of CO₂ with measurements of two-phase relative volumes at eight pressures for each mixture. Saturated liquid density and viscosity measurements for each mixture. Swelling tests used four discrete additions of injection gas CO₂ which is added to the recombined reservoir oil.

A discussion and presentation of the results of the fluid composition work (extracted from D.B. Robinson Research Ltd. (1995) follows.

5.2.1 Sample Preparation and Compositional Analysis

The following Anasazi fluid samples were taken for study purposes:

- three separator oil cylinders (1 gal [3.8 L] each) labeled Anasazi 5L-3 field, cylinder nos. W4635, W8301, and W3A8302,
- three separator gas cylinders (one 500 cm³ and two 300 cm³) labeled Anasazi 5L-3 field, and
- three dead oil containers (1 gal [3.8 L] each) labeled as follows:
 - Anasazi 5L-3
 - Anasazi 6H-1 limestone perforation (5,723 to 5,730 feet [1,744-1,746 m])
 - Anasazi 6H-1 dolomite perforation (5,680 to 5,694 feet [1,731-1,735 m]).

Note that one of the three separator oil cylinders, namely W3A8302, was not properly filled during transferring; thereby, the corresponding fluid was not analyzed. Compositional analyses were conducted on separator oils, separator gases, and dead oils.

5.2.1.1 Separator Oils. The separator oils were initially equilibrated at 1,000 pounds per square inch gauge (psig [6,895 kpa]) and 73 °F (23 °C) (that is at single phase conditions). The separator conditions for these samples were reported to be 35 psig (241 kpa) and 85 °F (29 °C). Next, samples of the separator oils were analyzed for their C30+ composition by the flash procedure. Accordingly, an accurately measured volume of each fluid was isobarically (1,000 psig) displaced into a pycnometer where its density and mass were evaluated. The pycnometer was then connected to a gas-oil ratio (GOR) single-stage flash apparatus where the fluid was flashed to ambient pressure and temperature conditions. Subsequently, the evolved gas phase was circulated through the residual liquid for a period of time to achieve equilibrium between phases. Following circulation, the volume of equilibrium vapor and the mass of liquid remaining in the pycnometer were measured. The vapor phase was resolved to C5 by gas chromatography (GC) while the vapor C5+ fraction and the residual liquids were analyzed to C30+ also with the GC. From the measured composition and total mass of each phase, the composition of the original live fluid was calculated by a mass balance. The C30+ compositions of the two separator oils analyzed are listed in tables B.1 and B.2, Appendix B. Both separator oil samples are fairly representative of one another for they have similar compositions, densities, and GORs.

5.2.1.2 Separator Gases. Separator gases from the 300 cm³ cylinders (cylinder nos. 5EK088 and 6EK087) were analyzed for composition using GC analysis. The results are listed in tables B.3 and B.4, Appendix B. Both gases have essentially the same compositions within accepted GC precision.

5.2.1.3 Dead Oil. The dead oil samples received were heated in their respective containers to 120 °F (49 °C) and then agitated to homogenize them. Thereafter, a hot sample of each dead oil was dissolved in carbon disulfide and analyzed for composition using liquid GC analysis. The measured C30+ liquid compositions are presented in table B.5, Appendix B and plotted in figure 5.4. For ease of comparison, the corresponding results for the flashed separator oils are also included in this same table.

Before discussing these results, it is important to note that only the 5L-3 dead oil was flashed/collected directly from the separator. Both the 6H-1 dolomite and the 6H-1 limestone samples were collected during swab test operations and stored on site and thus, because of the nature of the containers, were subject to light end losses.

As can be seen from table B.5, the dead oils have relatively higher C30+ fractions than the corresponding dead oils flashed from the separator oils (cylinder nos. W4635 and W8301). More importantly, the 6H-1 limestone dead oil is observed to differ significantly in composition from the rest of the oil samples. The thermal histories, of the limestone and dolomite samples caused most of the light ends to evaporate.

5.2.2 Fluid Recombination and Swelling Tests

5.2.2.1 Fluid Recombination. Separator oil and gas samples (synthetic) were recombined at a separator GOR of 1,208 standard cubic feet per stock tank barrel (scf/STB [242 m³ of gas/m³ of oil]).

Details of the recombination are available in D.B. Robinson Research Ltd. (1995). The composition of the recombined sample is presented in table B.6, Appendix B.

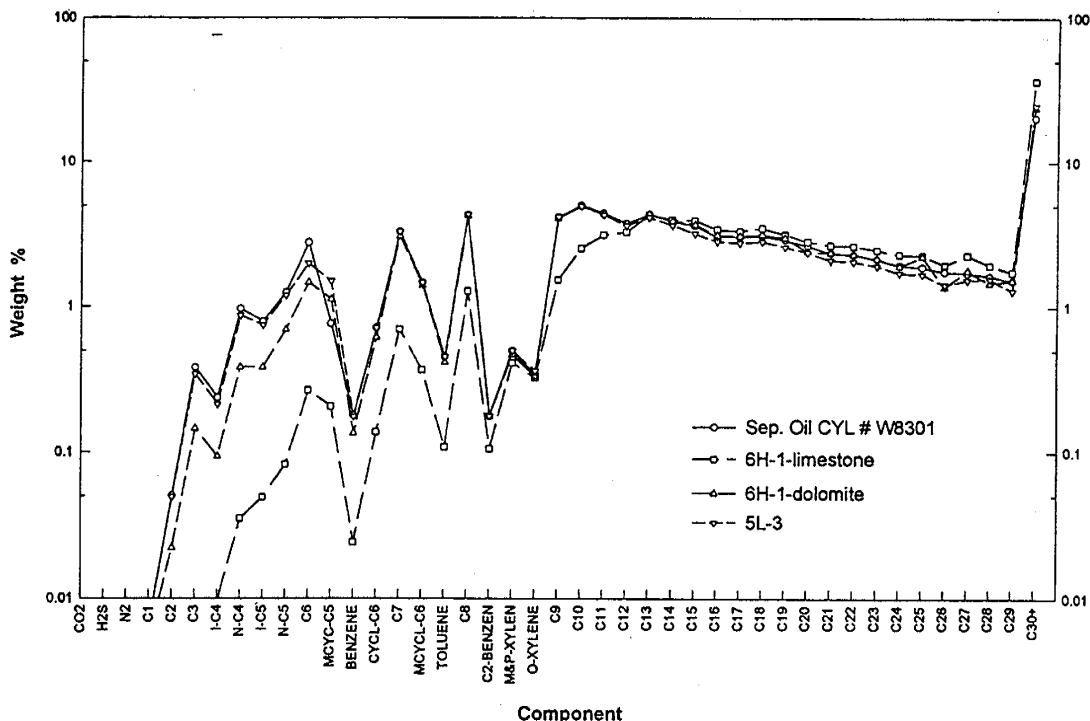


Figure 5.4. Comparison of the (C30+) weight-percent composition measured for the flashed separator oil (cylinder W8301) and dead oil samples (6H-1-limestone, 6H-1-dolomite, and 5L-3).

5.2.2.2 Swelling Tests. Preliminary simulation studies of the Anasazi field indicated that if the field was re-pressured the existing free gas phase would be forced into solution in the oil and the remaining liquid would exhibit a bubble point of approximately 2,050 pounds per square in absolute (psia). This was selected as a reasonable starting point, from a fluid compositional standpoint, for CO₂ swelling tests for future equation-of-state calibration work. Thus, the recombined fluid (table B.6) was used to prepare a fluid sample exhibiting a 2,050 psia (14,135 kpa) bubble point at a reservoir temperature of 130°F (54°C). Details of the sample preparation are contained in D.B. Robinson Research Ltd. (1995). The composition of this mixture is presented in table B.7, Appendix B.

Using the reservoir fluid with a bubble point of 2,050 psia (14,135 kpa), swelling tests employing 20, 40, 60, and 75 mole percent CO₂ were conducted. Laboratory measurements consisted of determining a number of pressure-volume (PV) data points for each mixture and also measuring the density and viscosity of each saturated liquid mixture. A sufficient number of PV measurements in the single phase and two phase region were made for each mixture to allow determination of the bubble point or dew point of each mixture. Results of these tests are presented in tables C.1 through C.10, Appendix C. A summary of the swelling tests are presented in table 5.1.

Table 5.1. Swelling test data for the Anasazi No. 5L-3 oil at 130°F (54°C).

CO ₂ Concentration (Mole%)	Saturation Pressure (psia)		V _{sat} (cm ³)	Bulk Density (g/cm ³)	Molar Volume (cm ³ /mol)	Swelling Factor** (cm ³ /cm ³)	μ (cP)
	Measured	Predicted*					
00.0	2,050†	2,050	59.61	0.664	129.12	1.000	0.464
20.0	2,294†	2,254	65.83	0.678	114.14	1.104	0.349
40.0	2,585†	2,586	72.45	0.697	99.63	1.215	0.270
60.0	3,176†	3,729	73.55	0.725	83.72	1.234	0.215
75.0	5,800‡		78.20	0.805	67.63	1.312	0.210

† Graphically

‡ Visually

* Predicted by Robinson's EQUI-90

**Swelling Factor = V_{sat} (of CO₂ + oil mixture)/V_{sat} (virgin oil)
where V_{sat} (virgin oil) = 59.61 cm³

5.2.3 Separator Tests

A two-stage separator test was conducted. The first stage involved flashing recombined fluid at 3,014 psia and 70°F (20,782 kpa and 21°C) to 35 psia and 85°F (241 kpa and 2°C). The second stage involved a flash to 0.0 psig and 60°F (16°C). Separator data are presented in tables 5.2 and 5.3; the gas compositional data are presented in table B.8, Appendix B.

Table 5.2. Separator test volumetric data.

Initial volume = 31.00 cm³ at 3,014 psia (20,782 kpa) and 70°F (21°C)
1st Stage Flash 35 psig (241 kpa) and 85°F (29°C)

	Volume (cm ³)	Density (g/cm ³)	MW (g/gmol)*
Vapor	1,248.16	0.0037	26.19
Liquid	19.72	0.7922	

Initial volume = 24.97 cm³ at 35 psia (241 kpa) and 85°F (29°C)
2nd Stage Flash 0 psig (0 kpa) and 60°F (16°C)

	Volume (cm ³)	Density (g/cm ³)	Gravity (API°)	MW (g/gmol)*
Vapor	98.16	0.0014		39.14
Liquid	24.76	0.8103	43.13	

*MW = molecular weight

Table 5.3. Separator test-produced GOR.

Stage	GOR (scf/STB)	
	per stage	cumulative
1st Stage Flash	1,197.4	1,197.4
2nd Stage Flash	20.4	1,217.8
Total	1,217.8	1,217.8

5.2.4 Summary

Detailed compositional analysis, separator tests, and swelling tests involving four concentrations of CO₂ were completed. Swelling factors exceeded 30 percent and oil viscosity was reduced by more than a factor of 2.0. This new fluid property data, in combination with existing basic black oil PVT data of the original reservoir fluid, provides the basis for calibrating or tuning an equation of state. The equation-of-state parameters will be used in the compositional reservoir simulation study to evaluate implementation of a CO₂ flood in typical Paradox basin reservoirs in the Desert Creek zone.

5.3 Rock Characterization

One of the key data sets required for reservoir recovery process evaluation via simulation is relative permeability data. Although an extensive core inventory exists for the Paradox basin reservoirs in the Desert Creek zone, all cores are in an unpreserved state. With the drilling of the Anasazi No. 6H-1 well in 1995, an opportunity existed to obtain a fresh core and preserve the core. Preserved cores can be used to conduct wettability and relative permeability measurements employing various core preparation procedures. Analysis of the resulting data from these measurements can provide guidelines for core preparation in future relative permeability work and provide a valid data set for future reservoir simulation studies. Representative samples from the preserved Anasazi No. 6H-1 core were taken (see section 3.3.2, Anasazi No. 6H-1 Well, Anasazi Field), based on CAT scans of the core, and used for a suite of capillary pressure, wettability, and relative permeability measurements.

Since a representative Desert Creek limestone interval was not present in the Anasazi No. 6H-1 well, the tests were performed on samples from the dolomite interval. Once the proper core preparation procedures were identified, unpreserved core material from another Anasazi well could be used for future limestone relative permeability measurements (Anasazi No. 1 well was selected and these tests are ongoing). In addition to the above discussed tests, samples from the Anasazi No. 6H-1 (dolomite) and Anasazi No. 1 (limestone) wells were used for rock compressibility measurements. Because an important part of the production life of the Paradox basin reservoirs in the Desert Creek zone involved liquid expansion and no compressibility data existed, it was important to obtain representative data to use in reservoir performance modeling.

All these tests (except limestone relative permeability) have been completed and results are summarized in the following sections, using extracted material from Westport Technology Center International (1995) and TerraTek, Inc. (1995) reports.

5.3.1 Relative Permeability Measurements

5.3.1.1 Fluid Measurements. The brine used in these experiments was a synthetic formation brine. The water analysis was for a sample collected on July 28, 1995 from the Sahgzie No. 1 well separator. The sample was filtered through a 0.45 micron filter (see table 5.4) after mixing. The original brine was a saturated solution at ambient temperatures and was diluted to 3/4 strength to prevent salt precipitation during the temperature cycling the samples were subjected to in the course of the testing.

Table 5.4. Brine composition.

Brine	Wt %
Sodium Chloride (NaCl)	9.10
Calcium Chloride (CaCl ₂ · 2H ₂ O)	6.00
Magnesium Chloride (MgCl ₂ · 6H ₂ O)	2.00
Potassium Chloride (KCl)	0.23

The crude oil was obtained from the surface separator for Anasazi No. 5L-3 well in August 1995 and used after filtering through a 0.45 micron filter at 73°F (23°C). Fluid properties were measured from 73°F to 135°F (23-57°C) since fluid saturations had to be measured at ambient conditions and the experiments conducted at 130°F (54°C). Data is provided for the oil properties in table 5.5. The surface and interfacial tension measurements were made using a ring pull tensiometer and thus are nonequilibrium measurements.

Table 5.5. Fluid properties.

Fluid	Temp (°F)	Density (g/cm ³)	Viscosity (cP)	Interfacial Tension (dynes/cm)	Surface Tension (dynes/cm)
Brine	75.000	1.1930	1.975	17.200	
Brine	130.000	1.1791	1.005	15.600	
Crude Oil	75.000	0.8229	4.730		26.800
Crude Oil	130.000	0.8014	2.580		25.500

5.3.1.2 Experimental Procedures. Collected data was analyzed using techniques by Hirasaki and others (1990). The capillary pressure data was analyzed using a constrained Hassler-Brunner

modeling technique. The relative permeability experiment was an unsteady state displacement in which only the displaced phase permeability can be analyzed. The data was corrected for capillary hold up, invading phase mobility, and speed ramp up effects then fitted to a bimodal Corey model to account for mobility shock production.

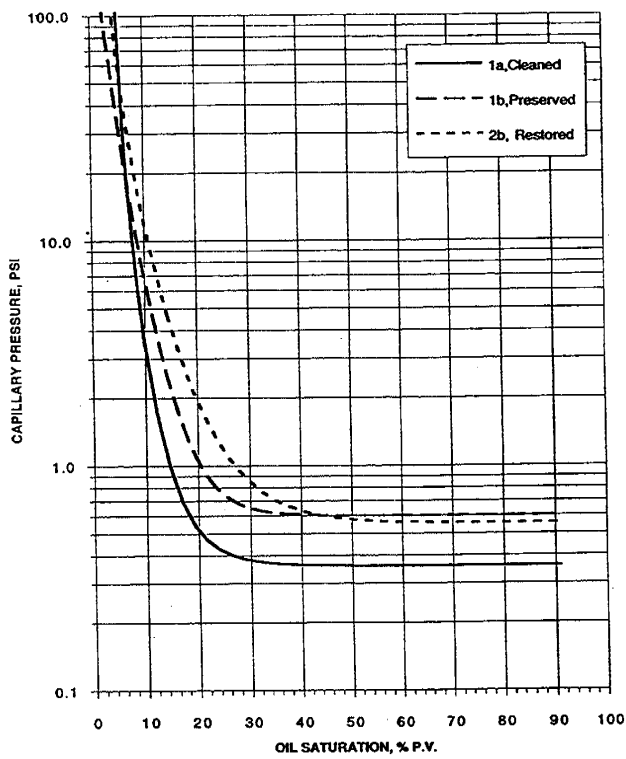
5.3.1.3 Resaturation and K_{ew} Measurements. Because of the saturated condition of the reservoir brine, all samples were flushed with the lower salinity brine in an attempt to remove any precipitated salts from the materials. Samples 1a, 1b, 2, and 4a had "as received" flowing permeabilities measured using this brine. Core 2 was then cleaned using a sequential solvent flow cleaning procedure and cut into samples 2a and 2b. Core 1a was then flow cleaned using the same equivalent solvent cleaning technique. Cores 1a and 2b were then brine saturated under 500 psi (3,448 kpa) back pressure and effective water permeability (K_{ew}) values measured at 100 percent brine saturation.

5.3.1.4 Initial Oil/Brine Drainage Experiment and Aging. An initial oil/brine drainage capillary pressure experiment was conducted on cores 1b and 2b to establish a high initial oil saturation for the aging process. Aging was accomplished for 14 days at 130°F (54°C). Near the end of the aging process an oil/brine drainage capillary pressure experiment was conducted on core 1a to establish a high initial oil saturation without the aging of the other cores.

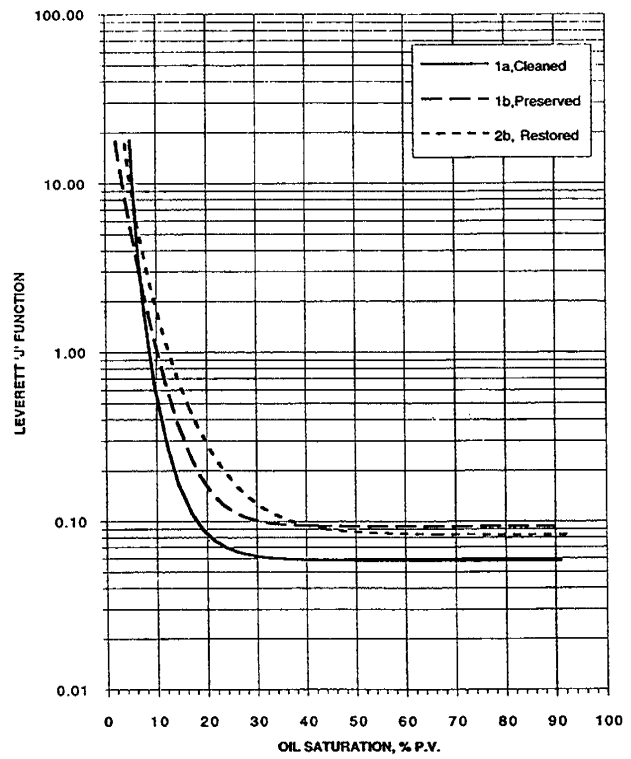
5.3.1.5 Brine/Oil Imbibition Capillary Pressure Test. Initial flowing oil permeabilities were measured and then an imbibition capillary pressure experiment was conducted for use in wettability determination. A comparison of the data is given in figure 5.5. The curve shapes indicate an oil wetting condition since the oil saturation continues to decrease with increased capillary pressure until a value below 5 percent remaining oil is achieved near 100 psi (690 kpa). Comparisons of the core entry values using the Leverett "J" function seen in figure 5.5B indicate a slightly stronger oil wetting condition in the preserved and restored cores over the cleaned but unrestored core.

5.3.1.6 K_{ew} Measurements and Oil/Brine Secondary Drainage Test. The samples were mounted in flow cells with an overburden pressure of 1,000 psi (6,895 kpa) and heated to 130°F (54°C). Brine was then introduced and a fluid pressure of 500 psi (3,448 kpa) maintained while the K_{ew} at residual oil saturation (S_{or}) measurements were taken. The samples were cooled while maintaining the 500 psi (3,448 kpa) fluid pressure. The samples were then placed in the centrifuge drainage cells. The cells were heated to 130°F (54°C) and a multi-speed experiment was conducted to determine the secondary drainage capillary pressure curves presented in figure 5.6. The Leverett "J" function curves indicate stronger water wetting in core 1a with the preserved core 1b having the least water wetting condition.

5.3.1.7 Brine/Oil Imbibition Relative Permeability Test. Initial flowing oil permeabilities were measured and then an imbibition capillary pressure experiment was conducted for use in wettability determination. A comparison of the data is given in figure 5.7. The initial permeabilities were fixed to the measured initial flowing permeabilities and the data was history matched to produce the curves. The final oil saturation to which the curves are plotted is the final average saturation in the cores. This explains why the saturations are not as low as the capillary pressure final saturations which are the saturations calculated at the inflow end of the core.



(A)



(B)

Figure 5.5. Brine - oil primary imbibition capillary pressure curves from elevated temperature, automated centrifuge data for Anasazi No. 6H-1 well. (A) capillary pressure, psi, and (B) capillary pressure curve, Leverett's J Function.

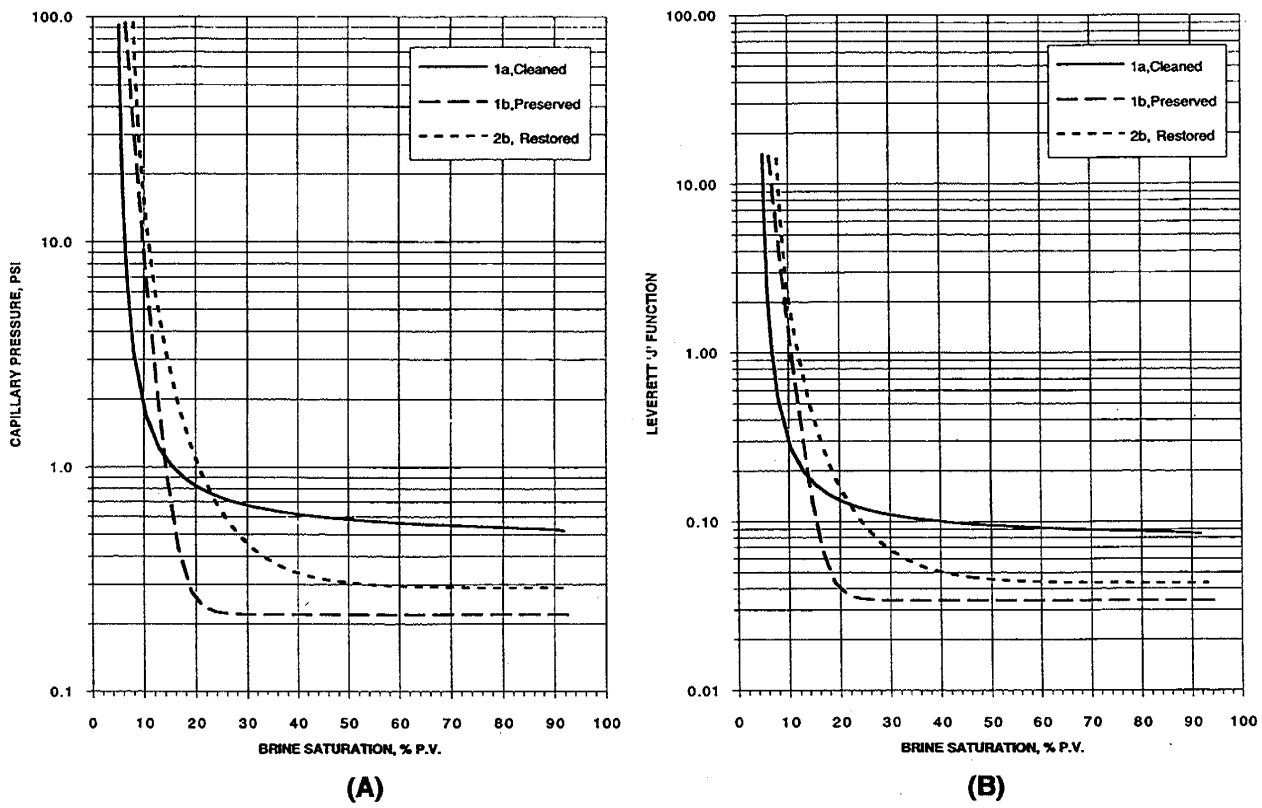


Figure 5.6. Oil - brine secondary drainage capillary pressure curves from elevated temperature, automated centrifuge data for Anasazi No. 6H-1 well. (A) capillary pressure, psi, and (B) capillary pressure curve, Leverett's J Function.

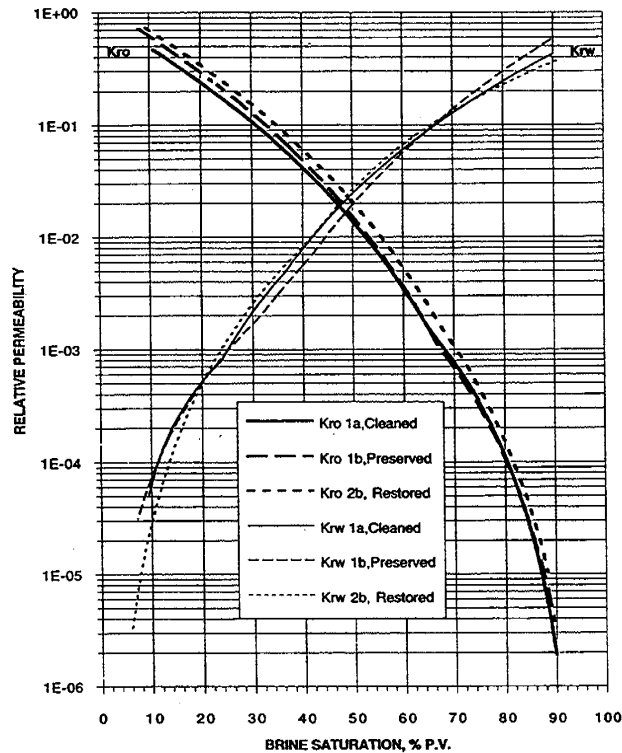


Figure 5.7. Oil - brine relative permeability curves from elevated temperature, automated centrifuge data for Anasazi No. 6H-1 well.

5.3.1.8 Oil/Brine Drainage Relative Permeability Test. Initial flowing brine permeabilities were measured and then a drainage capillary pressure experiment was conducted for use in wettability determination (figure 5.8). A comparison of the data is given in figure 5.7. The initial permeabilities were fixed to the measured flowing permeabilities and the data was history matched to produce the curves. The final oil saturations to which the curves are plotted is the final average saturation in the cores. This explains why the saturations are not as low as the capillary pressure final saturations which are the saturations calculated at the inflow end of the core.

5.3.1.9 Gas/Oil Capillary Pressure and Relative Permeability Experiment. A gas/oil drainage capillary pressure experiment was conducted. The data presented in figure 5.9 indicate the expected oil wetting in the presence of gas. The S_{or} value between 0.8 and 2.5 percent is reflective of the lack of trapping sites in the core material. The slightly higher capillary entry pressure, when compared to the oil/brine system, may be indicative of the non-equilibrium tension measurements used. The samples were mounted in flow cells with an overburden pressure of 1,000 psi (6,895 kpa) and heated to 130°F (54°C). Oil was then introduced and a fluid pressure of 500 psi (3,448 kpa) maintained during resaturation and the effective oil permeability at irreducible water saturation (K_{eo} at S_{wr}) measurements taken. The samples were cooled while maintaining the 500 psi (3,448 kpa) fluid

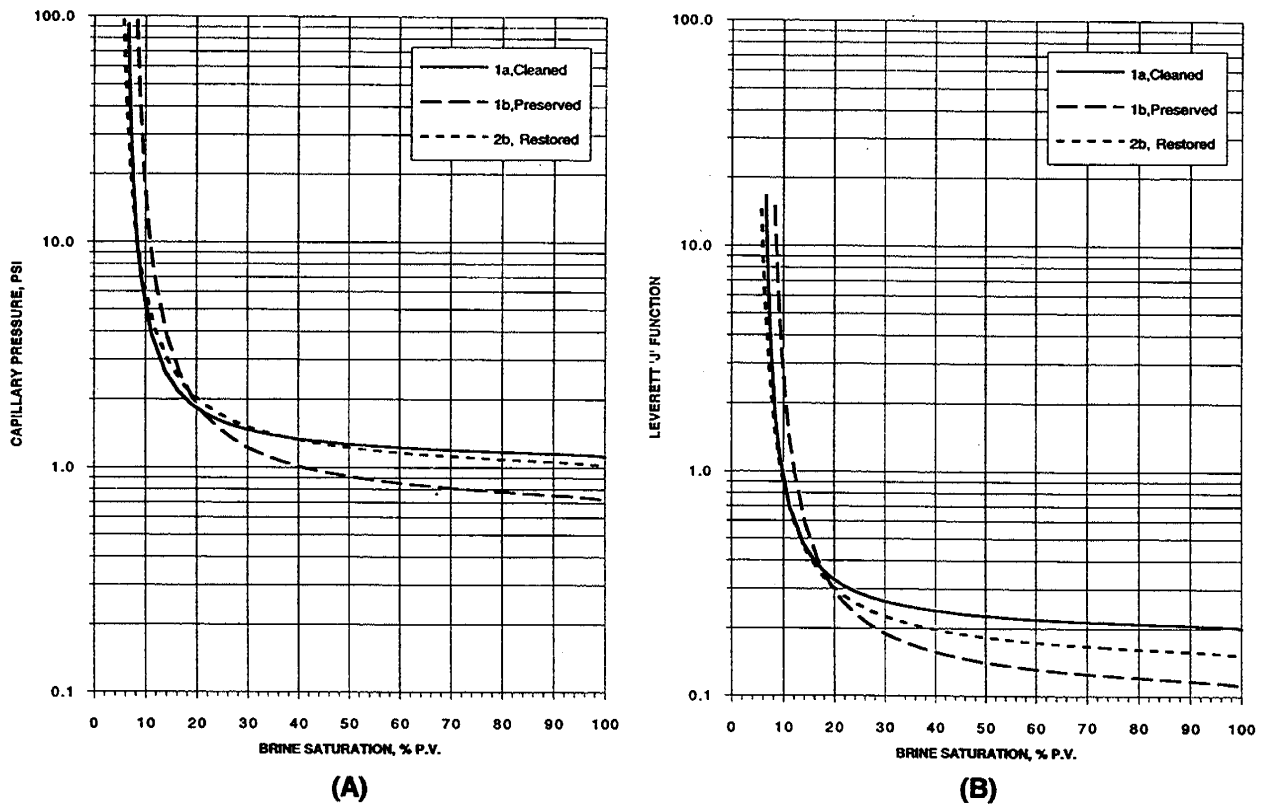


Figure 5.8. Oil - brine primary drainage capillary pressure curve from elevated temperature, automated centrifuge data for Anasazi No. 6H-1 well. (A) capillary pressure, psi, and (B) capillary pressure curve, Leverett's J Function.

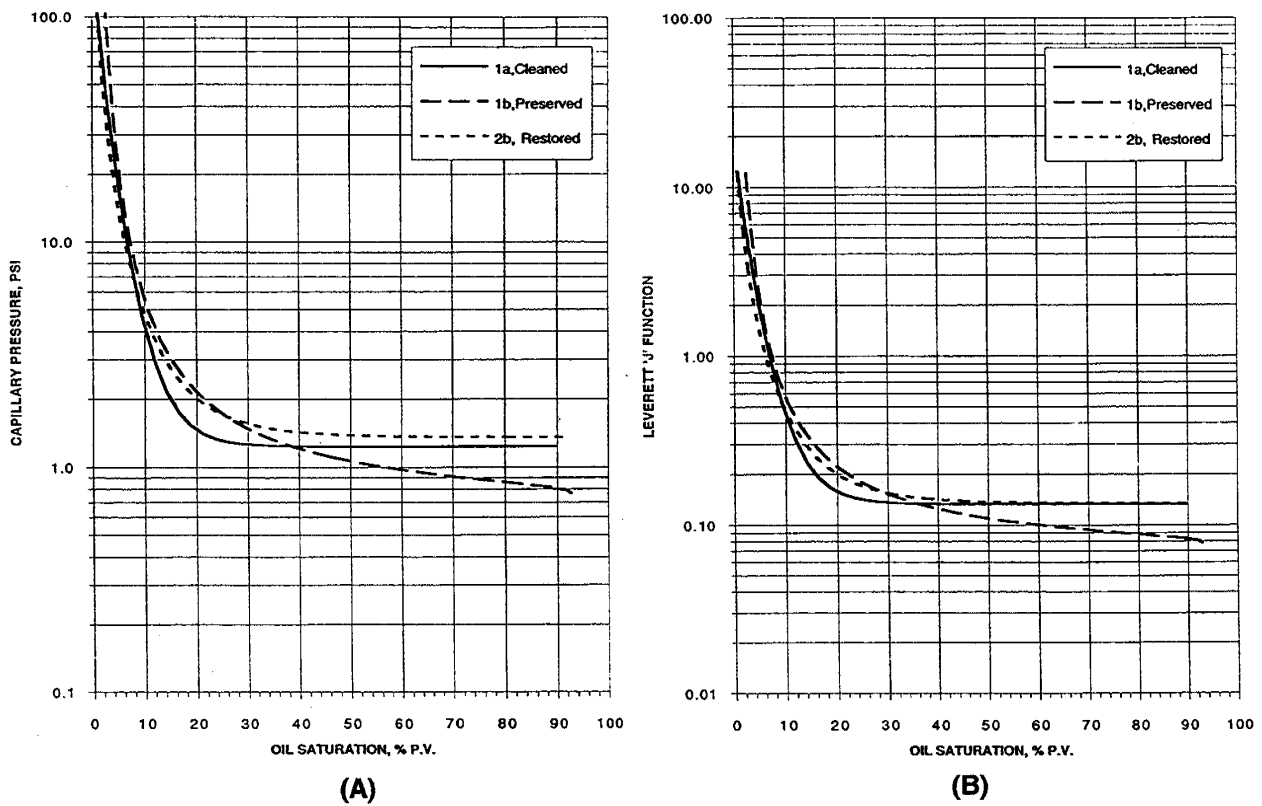


Figure 5.9. Gas - oil drainage capillary pressure curve from elevated temperature, automated centrifuge data for Anasazi No. 6H-1 well. (A) capillary pressure, psi, and (B) capillary pressure curve, Leverett's J Function.

pressure. The samples were then placed in the centrifuge drainage cells. The cells were heated to 130°F (54°C) and a single speed experiment was conducted to determine the gas/oil drainage relative permeability curves to oil presented in figure 5.10. The curves agree quite well to values of about 5×10^{-4} at which point the cleaned core begins to deviate due at least in part to the inability of the bimodal model to fit the production data. At the conclusion of the experiment gas permeability at S_{or} and S_{wr} was measured and is presented in table 5.6.

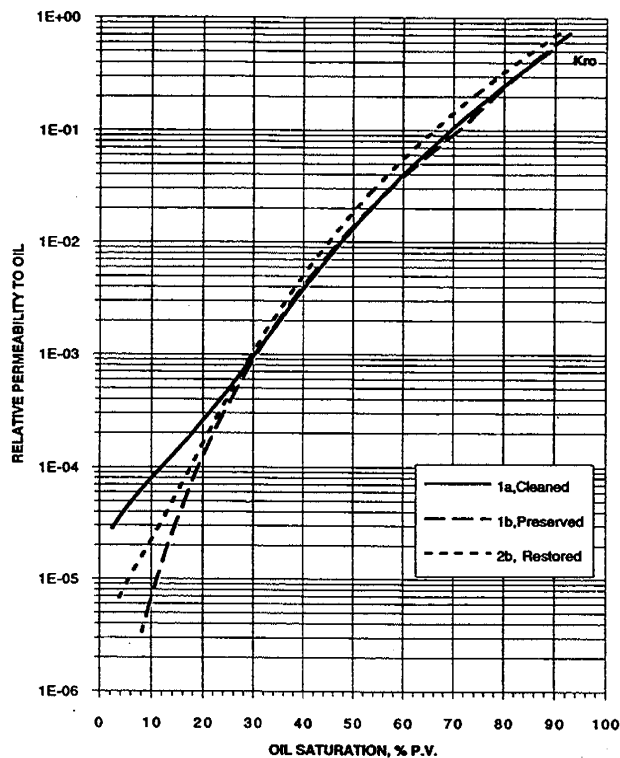


Figure 5.10. Gas - oil relative permeability curves from elevated temperature, automated centrifuge data for Anasazi No. 6H-1 well.

Table 5.6. Permeability and porosity data summary for the Anasazi No. 6H-1.

Test No.	Core 1a	Core 1b	Core 2	Core 2a	Core 2b	Core 4a
Depth (ft)	5691.210	5691.210	5691.460	5691.460	5691.460	5691.800
Initial Core Properties at 500 psi NCS						
Length (cm)	4.097	4.252	9.073	4.470	4.257	4.262
Average Area (cm ²)	11.158	11.159	11.187	11.194	11.194	11.153
Bulk Volume (cc)	45.716	47.447	101.502	50.044	47.652	47.534
Gas Pore Volume (cc)	8.221	8.273	17.715	8.070	9.054	7.454
Grain Volume (cc)	37.495	39.174	83.787	41.974	38.598	40.080
Gas Porosity (% Bulk volume)	17.982	17.436	17.453	16.125	19.000	15.681
Grain Density (gm/cc)	2.849	2.840	2.826	2.821	2.825	2.771
Gas Permeability (md)	30.000	26.400	15.100	13.600	26.700	3.800
Oil Permeability No. 1 (md)	12.950	20.710			18.420	
Core Properties at 2,000 psi NCS						
Length (cm)	4.097	4.252	9.073	4.470	4.257	4.262
Average Area (cm ²)	11.125	11.106	11.148	11.150	11.160	11.111
Bulk Volume (cc)	45.578	47.224	101.149	49.847	47.509	47.355
Gas Pore Volume (cc)	8.083	8.050	17.362	7.873	8.911	7.275
Gas Porosity (% Bulk volume)	17.735	17.046	17.165	15.794	18.756	15.362
Gas Permeability (md)	26.500	23.100	13.200	12.300	24.400	2.900
Brine Permeability (as received) (md)	10.400	8.300	4.300			1.000
Brine Permeability (at cleaning) (md)	20.200				13.800	
Centrifuge Values*						
Initial Residual Water Saturation (S _{wri}) (in S _w % Pore volume)	8.990	10.240			7.950	
K _{eo} @ S _{wri} (md)	12.950	20.710			18.420	
Residual Oil Saturation (S _{or}) (in S _o % Pore volume)	6.010	5.480			6.860	
Water Saturation @ S _{or} (S _w @S _{or}) (in S _w % Pore volume)	93.990	94.520			93.140	
K _{ew} @ S _{or} (md)	16.400	16.800			10.900	
Residual Water Saturation (S _{wri}) (in S _o % Pore volume)	10.790	7.910			9.300	
K _{eo} @ S _{wri} (md)	9.400	18.900			14.5	

Table 5.6. (continued)

Test No.	Core 1a	Core 1b	Core 2	Core 2a	Core 2b	Core 4a
Centrifuge Values* (continued)						
Residual Oil Saturation S_{or} (in S_o % Pore volume)	10.100	10.400			11.700	
Water Saturation @ S_{or} (S_w @ S_{or}) (in S_w % Pore volume)	89.990	89.600			90.720	
K_{ew} @ S_{or} (md)	12.700	15.100			9.860	
Final Residual Water Saturation (S_{wrf}) (in S_w % Pore volume)	9.490	7.180			5.920	
K_{eo} @ S_{wrf} (md)	15.220	19.180			19.370	
Residual Oil Saturation (S_{or}) (in S_o % Pore volume)	2.410	8.220			3.220	
K_{eg} ** @ S_{or} (md)	25.700	25.900			22.300	
Final Brine 100% saturated (md)	23.700	13.400			14.200	

*Centrifuge cores
 1a - cleaned
 1b - preserved
 2b - restored

**Effective gas permeability

5.3.1.10 Final Saturation Determination via Dean-Stark. A Dean-Stark extraction was performed on the core material to determine the final oil and brine saturations and to check the weight-determined values used in the study. The material was then cleaned using a sequential-solvent-flow cleaning procedure using: (1) a 3 percent potassium chloride brine to remove the precipitated salts from the extraction and (2) toluene and methanol flushes to properly clean the material.

5.3.1.11 Gas Property Measurements. Gas permeability and porosity measurements were made on the cleaned core material at 500 and 2,000 psi (3,448 and 13,790 kpa) net confining stress. The data are presented in table 5.6.

5.3.1.12 Saturation and K_w . The dry cores were weighed, evacuated, and degassed brine was introduced. The core holders were then pressurized to 2,000 psi (13,790 kpa) and held for 16 hours at 73°F (23°C). The cores were removed from the cells and weighed. They were then placed in flow permeability cells with an overburden pressure of 1,000 psi (6,895 kpa) and a fluid pressure of 500 psi (3,448 kpa). Flow was established and when stabilized the absolute permeability of the water-saturated rock (K_w) measurement was made (see table 5.6).

5.3.1.13 Primary Drainage Capillary Pressure Measurements. After the flowing permeability measurements, the samples were mounted in the centrifuge drainage cells, surrounded with crude oil, and heated to 130°F (54°C). Thirteen centrifuge speed steps were used to define the capillary pressure curves. Each speed was maintained for eight hours before moving on to the next speed. The final average saturations were then extrapolated to infinite time using the production data and a Corey exponent of 2.5 for the extrapolation. The resultant average saturation curve was then converted to the capillary pressure curve at the inflow end of the core using a constrained Hassler-Brunner fit. The samples were cooled to 73°F (23°C) and weighed for saturation determinations. The resulting curves are seen in figure 5.8 and indicate a stronger water wetting nature than the secondary drainage curves seen in figure 5.6. This is evident from the higher Leverett "J" function entry pressure for the primary drainage curves. There appears to be a slight lowering in the entry pressure of the restored-state core and an even lower value for the preserved core. This effect could be due to a surface oil adsorption which is time dependent and which requires stronger solvent cleaning than was accomplished using toluene and methanol.

5.3.1.14 U.S. Bureau of Mines and Amott Wettability Indices. Both the U.S. Bureau of Mines (USBM) and Amott wettability indices were determined from the primary waterflood and secondary oil flood capillary pressure experiments. The USBM index is the ratio of the areas under the two capillary pressure curves. The areas were calculated to a common pressure of 90 psi (620 kpa). The results ranged in values from -0.33 to -0.49. These values are commonly classified as mixed wet values with a slightly stronger oil than water wetting. The Amott results were the ratio of the production during the first speed step of the centrifuge divided by the total production during the experiment. This value is an upper limit for the "spontaneous" imbibition value since a slight amount of pressure was actually applied to the cores to produce the initial fluid. The values indicate no spontaneous water production and 6 to 25 percent spontaneous oil production. This spontaneous oil production was at an applied pressure of 0.6 psi (4.1 kpa) while the water production values occurred at about 0.2 psi (1.4 kpa) due to the difference in holder and sample configuration during

the two experiments. If a spontaneous value for the oil production is calculated by extrapolating the curves to 0.2 psi (1.4 kpa) the values all become zero as in the water production case. This would be consistent with the USBM results of mixed wettability. The higher entry pressure for the oil curves when compared to the water entry pressures on the preserved and restored cores supports this favorable oil wetting as well.

5.3.1.15 Bond Number versus S_{or}/S_{oi} . Figure 5.11 shows the relationship between the residual oil saturation to initial oil saturation (S_{or}/S_{oi}) values and the Bond Number for the waterflood capillary pressure experiments. The vertical lines are an artifact of the capillary entry pressure for the experiments. The remainder of the curves from about 10^{-7} to 10^{-5} on figure 5.11 show a film drainage mechanism common to thinning of oil films with increased pressure. The low residuals between 2 to 6 percent reflect the lack of trapping mentioned earlier.

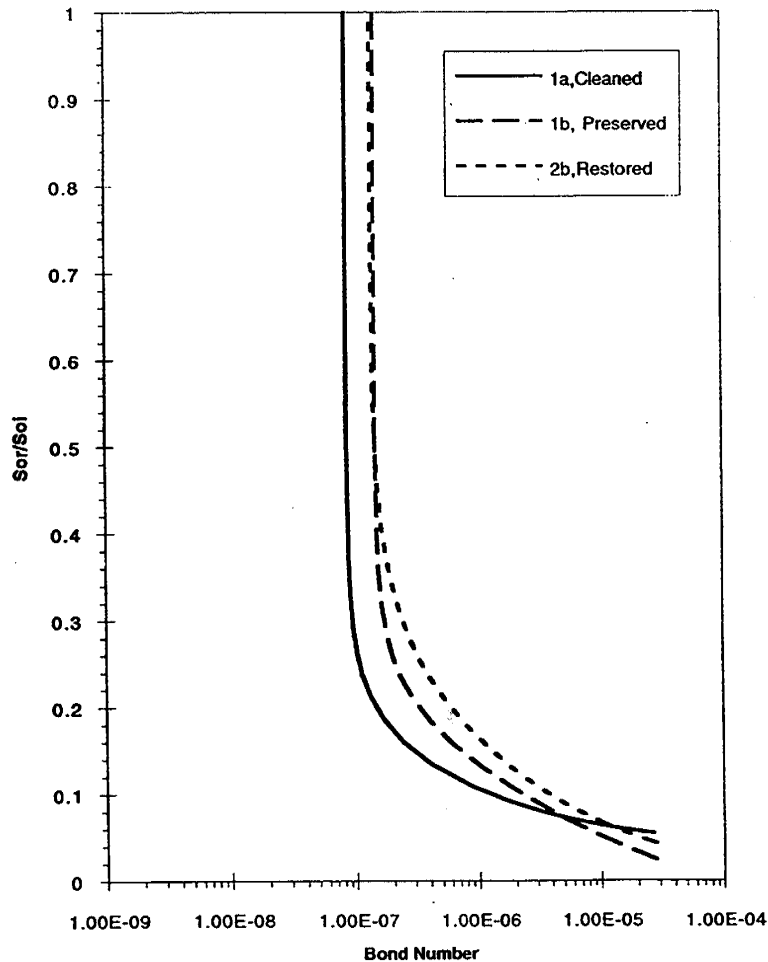


Figure 5.11. Bond number vs. S_{or}/S_{oi} curves from elevated temperature, automated centrifuge data for Anasazi No. 6H-1 well.

5.3.1.16 Summary. Centrifuge tests were performed on three core plugs to provide oil-brine and gas-oil capillary pressure and oil-brine and gas-oil relative permeability curves. The samples were

prepared in three ways; core 1a was cleaned but not aged, core 1b was preserved, and core 2b was cleaned and aged to restore wettability. The tests were performed at 130°F (54°C) with a confining pressure of about 200 psi (1,379 kpa) provided by shrinkable teflon jackets.

The data indicate a mixed wetting condition typical of carbonate systems with a slightly stronger oil wetting tendency in the preserved core and a nearly neutral wetting for the cleaned and unrestored core with the restored core falling between the others. The dominant feature of the cores is the lack of trapping sites, yielding very low residuals in both the oil and brine phases. This feature overwhelms the slight differences in the wetting states of the core preparation techniques and yields capillary pressure and relative permeability curves that compare quite well.

5.3.2 Rock Compressibility Measurements

Compressibility testing was conducted on two carbonate samples obtained from the Anasazi Nos. 1 and 6H-1 wells. The core material consisted of one sample of unpreserved limestone exhibiting vugular porosity from the Anasazi No. 1 well and one unpreserved microporous dolomite sample from the Anasazi No. 6H-1 well.

Compressibility of a porous medium is defined as the relative volume change due to a unit change in applied stress. Three types of compressibilities were determined for both carbonate samples: (1) bulk compressibility (C_b), (2) the solid (grain) compressibility (C_g), and (3) the pore volume compressibility (C_p). The bulk compressibility represents the relative changes in bulk volume of the medium; the grain compressibility represents the relative volumetric change of the solid portion of the medium; and the pore volume compressibility represents the relative change in pore volume. The sample depth, pre-test bulk density, effective grain density, and effective porosity for both samples are presented in table 5.7. In addition to the compressibility determinations, each specimen was loaded under triaxial conditions for determination of quasi-static elastic moduli and Poisson's ratio. The results of this work are summarized in tables 5.8 through 5.11.

Table 5.7. Pre-test sample conditions and physical properties for selected samples from the Anasazi Nos. 1 and 6H-1 wells.

Sample Depth (ft)	Rock Type	Length (in)	Diameter (in)	Pre-Test Density (gm/cm ³)			Porosity* (%)	Permeability to Gas (md)
				Saturated Bulk	Dry Bulk	Grain		
5,648.5 - 5,648.9	Limestone (Anasazi No. 1 Well)	3.724	1.998	2.390	2.244	2.698	16.83	51.45
5,692.0 - 5,692.4	Dolomite (Anasazi No. 6H-1 Well)	3.881	1.997	2.588	2.487	2.814	11.62	0.65

* Effective grain density and porosity determined - reflects only interconnected pore space

Simulated *in-situ* conditions were used for the compressibility and triaxial compression tests. The testing scenario was based on an approximate average horizontal stress gradient of 0.65 pounds per square inch per foot (psi/ft [15 kpa/m]), a reservoir pore pressure of 2,000 psi (13,790 kpa), and a vertical stress gradient of 1 psi/ft (23 kpa/m) (overburden stress). The target *in-situ* pressures for this test program are shown in table 5.8.

Table 5.8. Target pressures for simulated *in-situ* conditions.

Rock Type	Depth (ft)	Target Confining Pressure (psi)	Target Pore Pressure (psi)	Target Stress Difference (psi)	Axial Stress (psi)
Limestone	5,648.5-9	3,670	2,000	1,980	5,650
Dolomite	4,592.0-.4	3,700	2,000	1,990	5,690

TerraTek, Inc. (1995) presented details on sample preparation and testing conditions. Table 5.9 presents the compressibility and Biot's coefficient under hydrostatic stress conditions. Table 5.10 presents the quasi-static mechanical properties determined from the triaxial compression segment of the compressibility tests. Table 5.11 presents the compressibilities determined under uniaxial strain conditions. Both the bulk compressibility (defined under uniaxial strain boundary conditions as the axial compaction coefficient [C_{bp}^u]) and pore volume compressibilities (C_{pp}^u) are provided in table 5.11. The pore pressure range from which the compressibilities were calculated are also included in table 5.11.

Table 5.9. Compressibilities determined from hydrostatic compression for samples from the Anasazi Nos. 1 and 6H-1 wells.

Sample Depth (ft)	Rock Type	Stress Range (psi)	Grain Compressibility (10^{-6} psi ⁻¹)	Bulk Compressibility (10^{-6} psi ⁻¹)	Pore Volume Compressibility (10^{-6} psi ⁻¹)	Biot's Constant α
5,648.5 - 5,648.9	Limestone (Anasazi No. 1 Well)	60 to 320		21.593	12.830	0.998
		525 to 1,956	5.1203			
		2,243 to 2,807		4.0396	2.4002	0.987
		3,083 to 3,636		1.7226	1.0235	0.970
5,692.0 - 5,692.4	Dolomite (Anasazi No. 6H-1 Well)	75 to 315		1.6797	1.4468	0.994
		547 to 1,805	1.0400			
		2,368 to 2,910		1.7074	1.4706	0.994
		3,050 to 3,690		1.2950	1.1154	0.992

Table 5.10. Quasi-static mechanical properties determined from triaxial compression for samples from the Anasazi Nos. 1 and 6H-1 wells.

Sample Depth (ft)	Rock Type	Axial Stress Difference Range for Properties Calculations (psi)		Triaxial Compression Moduli (10^6 psi)		
				Young's	Bulk	Shear
5,648.5-.9	Limestone	610 to 1,390	0.20	2.37	1.30	0.99
5,692.0-.4	Dolomite	605 to 1,390	0.15	3.21	1.51	1.40

Table 5.11. Parameters determined during uniaxial strain/pore pressure drawdown segment.

Sample Depth (ft)	Rock Type	Pore Pressure Stress Range (psi)	Compaction Coefficient ($C_b^u \cdot 10^{-7}$ / psi)	Pore Volume Compressibility ($C_p^u \cdot 10^{-6}$ / psi)
5,648.5-.9	Limestone	1,935 to 300	3.9263	2.3329
5,692.0-.4	Dolomite	1,915 to 275	3.6977	3.1849

5.4 References

- Bourdet, D, 1985, Pressure behavior of layered reservoirs with crossflow: Society of Petroleum Engineers Technical Paper 13628, California Regional Meeting, Bakersfield, CA, p. 405-416.
- D.B. Robinson Research Ltd., 1995, Laboratory PVT program for Harken Energy reservoir fluid phase 1: Unpublished report for REGA Inc., D.B. Robinson Research Ltd. file 205136, 44 p.
- Hirasaki, G.J., Rohan, J.A., and Dubey, S.T., 1990, Wettability evaluation during restored-state core analysis: Society of Petroleum Engineers Technical Paper 20506, 65th Annual Technical Conference and Exhibition, Production Operations and Engineering Volume, p. 361-375.
- TerraTek, Inc., 1995, Compressibility of carbonate from the Anasazi No. 1 and No. 6H-1 wells: Unpublished report for REGA Inc., no. TR96-23, 20 p.
- Westport Technology Center International, 1995, Harken Energy special core analysis - Anasazi 6H: Unpublished report for Harken Energy Corporation, no. WTCI95-201, 76 p.

6. MECHANISTIC RESERVOIR SIMULATION STUDIES

W.E. Culham
REGA Inc.

6.1 Introduction

To provide some initial insight into the basic production mechanism of the Anasazi reservoir some simple one- and two-dimensional compositional simulation studies were conducted prior to developing final reservoir description models and the final three-dimensional simulation study. In addition to gaining insight into possible production mechanisms, the simulation studies were used to estimate a fluid bubble-point pressure that might be realized if the reservoir was re-pressured after producing the current volumes of oil and gas. This bubble-point data was used for preparing fluid samples for CO₂ swelling tests discussed in the previous section.

6.2 Model Description

The bulk volume of the reservoir required to roughly match observed pressure-production conditions was established with a series of one-dimensional simulation runs that adjusted reservoir bulk volume until a reasonable match of observed production data (GOR) was obtained. This volume was used to guide the overall volume of the two-dimensional model (2,500 feet X 2,500 feet X 100 feet [762 m X 762 m X 30 m] - Anasazi reservoir units only).

The geologic model was a simplistic two-unit model consisting of a dolomite unit and a limestone unit. The homogeneous units were assigned an average thickness of 70 feet (21 m) and 30 feet (9 m) for the dolomite and limestone units respectively. Several simulation runs were used to arrive at an overall vertical to horizontal permeability (k_v/k_h) ratio of 0.02. This gave the best GOR match of ratios investigated. The dolomite unit was assigned a uniform lateral permeability of 10.0 md and a vertical permeability of 0.2 md using the $k_v/k_h = 0.02$. The limestone unit, at the base of the Desert Creek zone, was assigned a uniform lateral permeability of 200 md and a vertical permeability of 4.0 md. The average uniform porosities assigned to the dolomite and limestone units were 10.4 percent and 9.0 percent respectively. An initial oil saturation of 0.85 and an initial irreducible water saturation of 0.15 was used. The initial pressure was set to 2,260 psia (15,583 kpa). The numerical grid for the model consisted of 200 x-direction blocks, one y-direction block, and 20 z-direction blocks. The dolomite and limestone geologic units were assigned 10 layers (made up of 200 x-direction blocks, one y-direction block, and 10 z-direction blocks).

6.3 Fluid Properties and Production Data

An equation of state was calibrated using black oil PVT data from the Anasazi reservoir and the Jack reservoir fluid properties study was used to provide C7+ characterization. A nine pseudo component representation of the fluid was developed which provided a good match of volumetric fluid property data available from the Anasazi reservoir fluid study. The calibrated equation of state was used in the compositional simulation to conduct the simple mechanistic reservoir studies.

As discussed earlier, the actual well by well, and thus field production data, was organized in data files formatted for comparison with simulation production results. The actual historic monthly production data was used as input to the simulation during the history match phase.

6.4 Stimulation Study Procedure

The simplistic two-dimensional models and compositional simulation were used to history match the production performance of the Anasazi reservoir through March 1995. The main parameters investigated were the overall vertical to lateral permeability ratio and the degree of communication between the dolomite and limestone units. A qualitative match rather than a detailed match was used for assessing the results.

6.5 Study Results

The first notable result was that to provide a reasonable match of reservoir response, particularly during the liquid expansion phase of production, an initial oil-in-place value of 8.2 million stock tank barrels (MMSTB [1.3 million m³]) was needed. This compares to an approximate volumetric value of 5.3 MMSTB (0.8 million m³). The oil in place needed to support the correct modeling of primary depletion thus exceeds volumetric data by over 3.0 MMSTB (0.5 million m³). Future full three-dimensional studies will be used to identify the reason for this difference.

Simulation results for the $k_v/k_h = 0.02$ case results for the Anasazi reservoir are presented in figures 6.1 and 6.2. Figure 6.1A presents field oil production for the Anasazi reservoir versus time. This data was used as input to the model via single well monthly oil rate specifications. Figures 6.1B and 6.1C present the simulation production and the observed field gas production rate and the GOR (predicted values represented by solid lines and historic data by + symbols). The match between predicted and observed data is considered reasonable, given the simplicity of the two-dimensional geologic model, for understanding basic reservoir production mechanisms. The initial constant GOR period, representing the liquid expansion portions of the depletion, is well matched. The rate of GOR increase and ultimately leveling off is reflecting fluid migration between the dolomite/limestone intervals and gas segregation via gravity facies. The gas segregation after 1,461 days of production clearly shows in figure 6.2. This figure shows higher gas saturation buildups at the top of the dolomite (layer 1) and top of the limestone (layer 11).

Figure 6.1D illustrates the average reservoir pressure decline to the current expected value of 400 to 500 psi (2,758-3,448 kpa). Figures 6.1E and 6.1F present oil production and oil in place from and in the two geologic units respectively. Figure 6.1E shows that over 90 percent of the production comes from the limestone interval. However, figure 6.1F illustrates that despite the major portion of production being from the limestone interval there is not a corresponding decrease in the oil in place in the limestone interval. This behavior clearly supports the gravity drainage of oil from the upper dolomite interval into the lower limestone interval from which the producing wells major share of production arises (figure 6.1E). This qualitative assessment prompted further analysis and since the simulator provides data that summarizes the flow of oil between the dolomite and limestone intervals, it was possible to determine the ratio of this flow to the limestone production. Figure 6.3 shows the various fluid rates (in bbls of oil per month [BOPM]) used in the analysis, where q_d and q_l are dolomite and limestone production respectively at the well, and q_v is

vertical flow from the dolomite interval (supra-mound) to the limestone interval (mound core). Table 6.1 provides specific data on the relation of gravity-drained oil into the limestone interval versus actual limestone interval production.

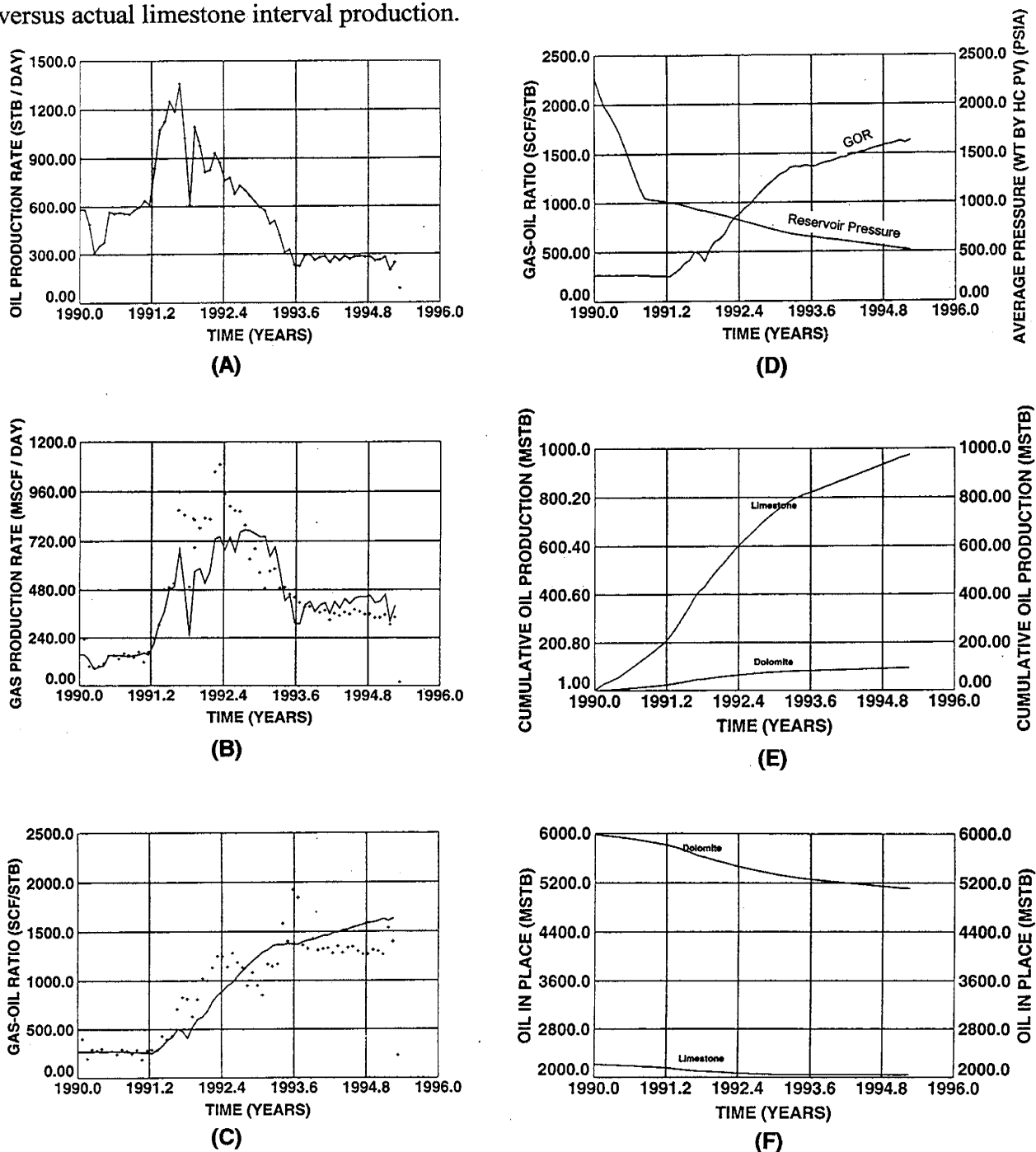


Figure 6.1. Results of two-dimensional reservoir simulation of the Anasazi field (k_v/k_h ratio = 0.02). (A) historic oil production rate vs. time, (B) predicted (solid line) and actual (+ symbol) gas production data vs. time, (C) predicted (solid line) and actual (+ symbol) GORs vs. time, (D) predicted GOR and reservoir pressure vs. time, (E) predicted limestone and dolomite oil production vs. time, and (F) predicted limestone and dolomite oil-in-place variation with time.

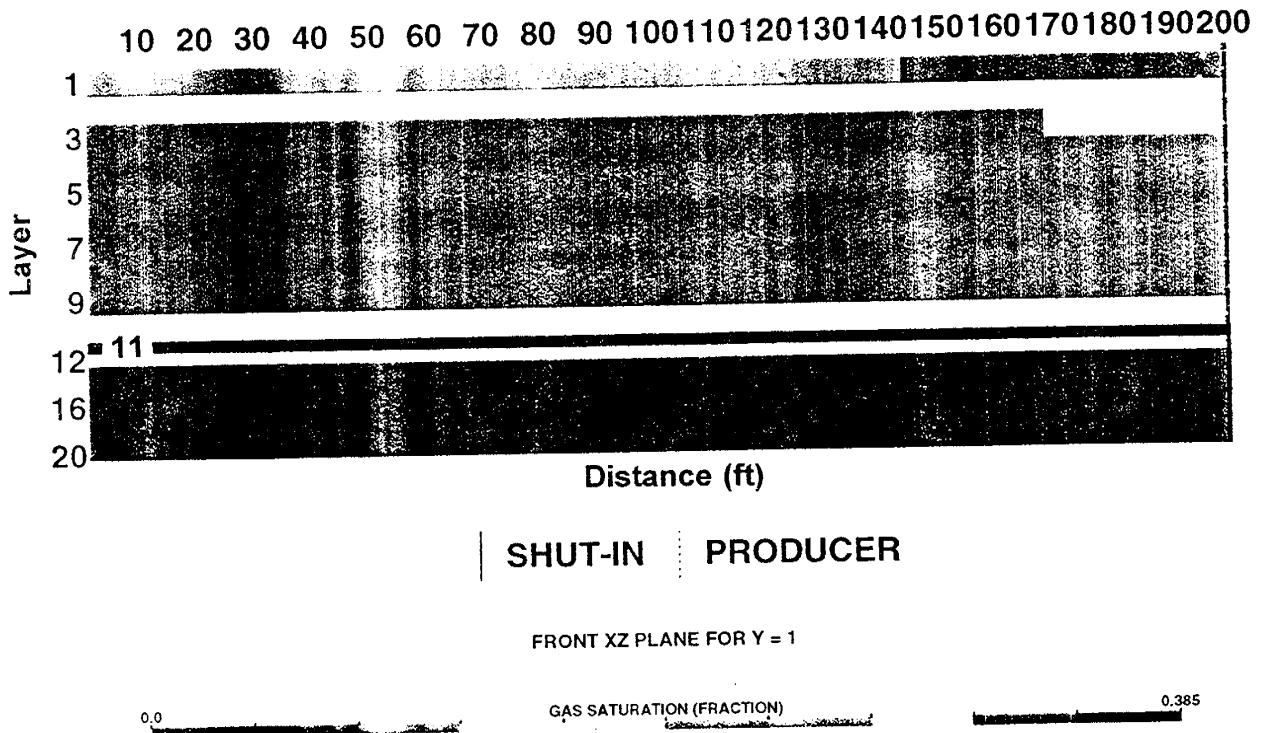


Figure 6.2. Two-dimensional reservoir simulation of the Anasazi field showing gas saturation for XZ plane after 1,461 days of production on January 1, 1994.

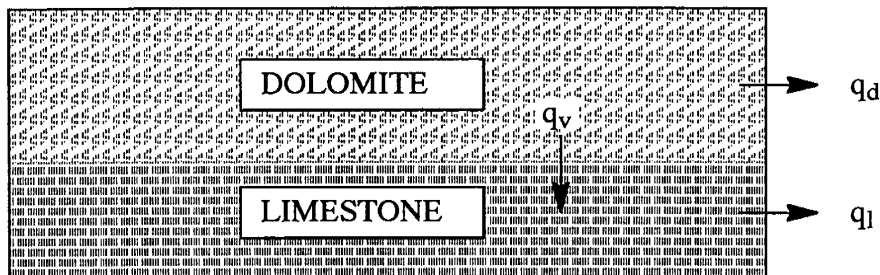


Figure 6.3. Schematic reservoir simulator model of the Anasazi reservoir. Arrows indicate fluid-flow directions.

Table 6.1. Analysis of gravity drainage behavior.

Month Ending	Fluid Rates			
	q_d : BOPM	q_l : BOPM	q_v : BOPM	q_v / q_l
1/31/90	1,889.70	16,121.30	11,069.10	0.687
6/30/90	1,787.00	15,222.90	10,553.60	0.693
1/31/91	2,101.50	17,642.00	12,515.90	0.709
6/30/91	3,826.00	33,645.90	24,458.20	0.727
1/31/92	2,196.00	23,041.20	19,755.10	0.857
6/30/92	1,910.30	21,461.60	17,970.10	0.837
1/31/93	1,333.20	16,462.20	14,003.10	0.851
6/30/93	683.70	9,127.00	9,310.00	1.020
1/31/94	585.60	8,250.40	8,089.40	0.981
6/30/94	515.90	7,555.30	7,323.70	0.969
1/31/95	529.00	8,153.00	7,241.10	0.888

These data, specifically q_v/q_l , show that after June 1993, the production rate from the limestone interval approximately equals the volume of oil draining from the dolomite interval into the limestone interval. This type of production behavior is clearly evident in figure 6.1A. After the relatively rapid production rate decline the production rate becomes constant at about 300 BOPD. This corresponds to the time identified in table 6.1 when q_v approximately equals q_l , and is interpreted as representing the slower gravity drainage replenishment of the limestone interval. The impact of production from the dolomite interval, q_d , is minimal since it represents a small fraction of the total production. Additional simulation runs project a 22 percent recovery factor under primary depletion (through the year 2020).

6.6 Future Work

Upon completion of the last set of relative permeability work for the limestone interval and calibration of the equation of state, the final field simulation study will begin. The reservoir model (see section 4., Geological Characterization of the Carbonate Reservoir in the Desert Creek Zone) will be used and three-dimensional simulation will start with a history match of past field performance. This will be followed with reservoir performance predictions to assess waterflooding and CO₂ injection processes during 1996.

7. TECHNOLOGY TRANSFER

Thomas C. Chidsey, Jr.
Utah Geological Survey

The UGS is the Principal Investigator and prime contractor for three government-industry cooperative petroleum-research projects including the Paradox basin project. These projects are designed to improve recovery, development, and exploration of the nation's oil and gas resources through use of better, more efficient technologies. The projects involve detailed geologic and engineering characterization of several complex heterogeneous reservoirs. The Class II Paradox basin and the Class I Bluebell field (Uinta Basin) projects will include practical oil-field demonstrations of selected technologies. The third project involves geological characterization and reservoir simulation of the Ferron Sandstone on the west flank of the San Rafael uplift as a surface analogue of a fluvial-dominated deltaic reservoir. The U.S. Department of Energy (DOE) and multidisciplinary teams from petroleum companies, petroleum service companies, universities, and State agencies are co-funding the three projects.

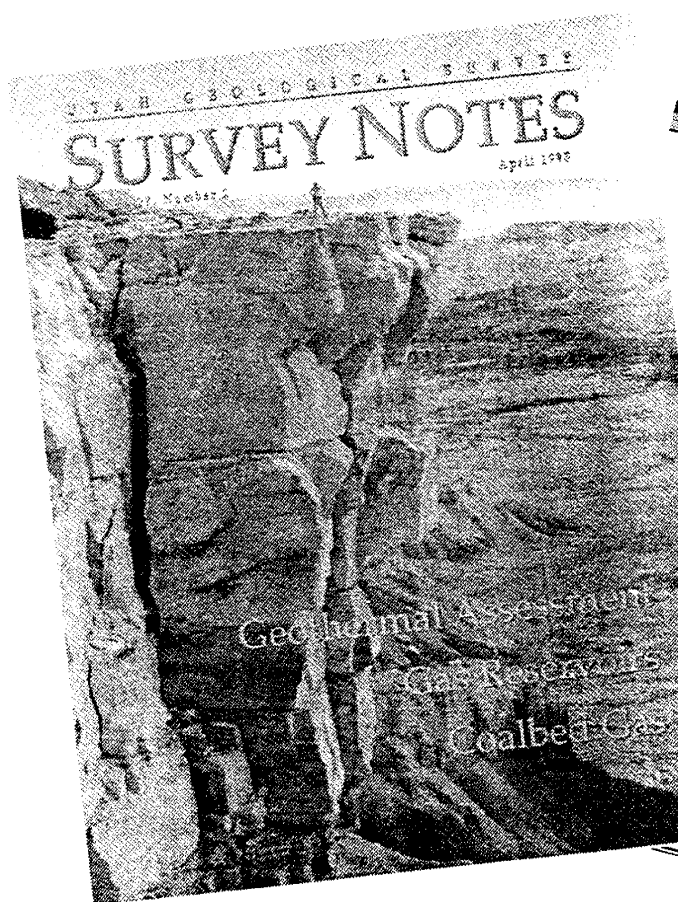
The UGS will release all products of the Paradox basin project in a series of formal publications. These will include all the data as well as the results and interpretations. Syntheses and highlights will be submitted to referred journals as appropriate, such as the *American Association of Petroleum Geologists (AAPG) Bulletin* and *Journal of Petroleum Technology*, and to trade publications such as the *Oil and Gas Journal*, as well as the UGS *Petroleum News* and *Survey Notes* (figure 7.1).

Project materials, plans, and objectives were displayed at the UGS booth during the 1994 and 1995 annual national conventions of the AAPG in Denver, Colorado and Houston, Texas; the 1995 AAPG Rocky Mountain Section meeting in Reno, Nevada; and at the 1995 regional convention of the Society of Petroleum Engineers in Denver, Colorado. Three to four UGS scientists staffed the display booth at these events. Abstracts were submitted for technical presentations at future AAPG national and regional meetings. Project displays will be included as part of the UGS booth at these meetings throughout the duration of the project.

The UGS has established a home page on the Internet. The address is <http://utstdpwww.state.ut.us/~ugs/>. The site includes (among other things) a page under the heading *Utah's Petroleum Resources*, describing the UGS/DOE cooperative studies (Paradox basin, Bluebell field, and Ferron Sandstone) and *Petroleum News*.

7.1 Utah Geological Survey *Petroleum News* and *Survey Notes*

The purpose of the UGS *Petroleum News* newsletter is to keep petroleum companies, researchers, and other parties involved in exploring and developing Utah energy resources, informed of the progress on various energy-related UGS projects. The UGS *Petroleum News* contains articles on: (1) DOE-funded and other UGS petroleum project activities, progress, and results, (2) current drilling activity in Utah including coalbed methane, (3) new acquisitions of well cuttings, core, and crude oil at the UGS Sample Library, and (4) new UGS petroleum publications. The purpose of *Survey Notes* is to provide nontechnical information on contemporary geologic topics, issues, events, and ongoing UGS projects to Utah's geologic community, educators, state and local officials and



UGS
Petroleum News

Purpose
The purpose of the Petroleum News newsletter is to help petroleum companies, researchers, and other parties involved in exploring and producing Utah's energy resources. It is published on various energy-related projects of the UGS.

Location
It is located at 2363 Midway, Salt Lake City, Utah 84143. Phone: 467-7970, 467-4670. Fax: 467-5060. Website: www.ugssurvey.gov

Project
The Ferron Sandstone project geologists completed an extremely fruitful first year and are eager to begin a second field season. This classic lithofacies typically found in a fluvial-deltaic reservoir, and, of course, to assist oilmen in discovering additional sources of the coveted "black gold."

Goals of the project
The project work in the first and second years (1993-94) involves regional stratigraphic analysis and local area case studies. Development of reservoir models and field-scale evaluation of exploration strategies will be completed during the third year. The Ferron project is a geologist's dream according to project manager, Tom Chidsey of the Utah Geological Survey. During their field clothes, over 30 geologists, technicians, and student assistants spent 11-hour days throughout last summer and fall measuring, lifting, sampling, and sealing the imposing cliffs of the Ferron Sandstone in Emery County, Utah. The winter and spring months were spent digitizing, compiling, and interpreting data and planning the next phase of field research.

Each group of geologists performed specific tasks. Several team members obliquely photographed 80 miles of Ferron Sandstone outcrop within the study area. These photos were then digitized, transferred to compact discs, reprocessed, and assembled into photomosaics. Another field team plotted lithofacies and measured sections, marked vertical and horizontal scales, and placed other data on the photomosaics as part of both the regional and case-study analyses. Other geologic teams collected, compiled, interpreted, and

Figure 1. Location map of the Ferron Sandstone study area (cross-hatched) showing case-study sites (outlined by heavy dashed lines).

Figure 7.1. UGS Survey Notes and Petroleum News provide project updates, publication notices, and announcements of presentations to both industry and lay public.

other decision makers, and the public. *Survey Notes* is published three times yearly and *Petroleum News* is published semi-annually. Single copies are distributed free of charge and reproduction (with recognition of source) is encouraged. The UGS maintains a database which includes those companies or individuals specifically interested in the Paradox basin project (90 as of February 1996) or other DOE-sponsored projects.

7.2 Workshops, Presentations, and the 1996 Paradox Basin Symposium

The UGS, Harken Southwest Corporation, and the DOE sponsored a core workshop to examine several cores from the Paradox basin to determine oil reservoir characteristics of several types of algal mounds and other carbonate buildups that comprise the five project fields targeted for detailed study. The workshop was held during the AAPG Annual Convention in Denver, Colorado, June 1994. Thirty-two participants attended the free workshop. This workshop was the first of several planned in the future as part of the technology transfer activities for the project.

The core workshop was a "hands-on" introduction to the relation between production and reservoir characteristics of carbonate buildups in the Paradox Formation (figure 7.2). Representative cores from five types of oil-producing buildups were discussed and examined. Planned activities for this DOE project were described during the workshop. Participants were encouraged to ask questions and discuss all aspects of the project, and make suggestions or recommendations concerning the project. The UGS plans to publish the workshop course notes in the near future.

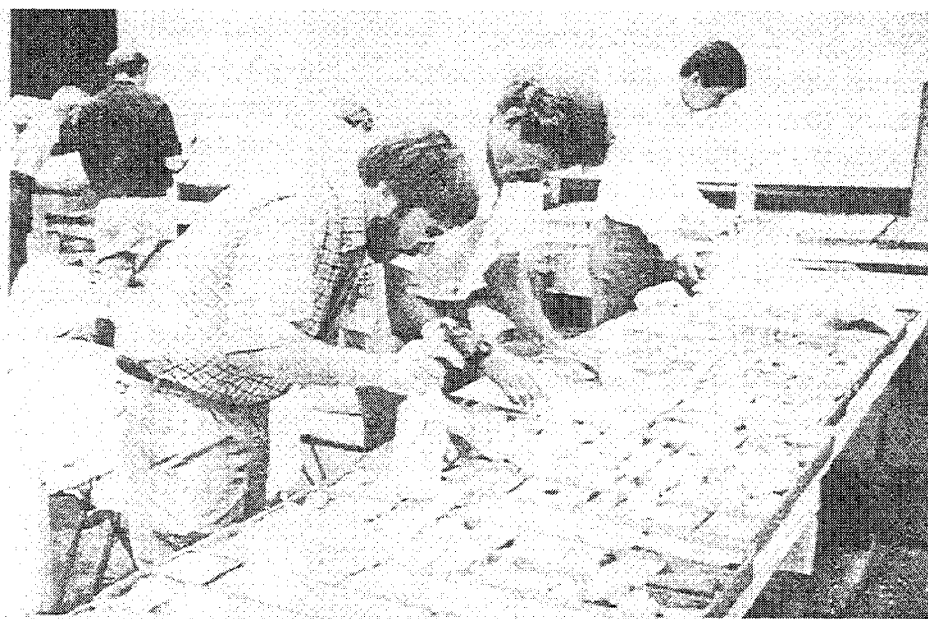


Figure 7.2. Participants at the UGS-sponsored core workshop, during the 1994 AAPG Annual Convention in Denver, Colorado, examine cores representing various types of oil-producing reservoirs from the Paradox basin project fields.

A presentation entitled "Composition of Seismically Identified Upper Pennsylvanian Mounds Surrounding Greater Aneth Field: Implications for Increased Oil Production Utilizing Secondary and Tertiary Recovery" was given by David E. Eby at the Fort Worth Geological Society's monthly meeting, Fort Worth, Texas, November 13, 1995. The Paradox Formation reservoir types, reservoir controls, and project objectives were discussed.

Future technology transfer includes a *Geology and Resources of the Paradox Basin* symposium and field trip scheduled for September 17-21, 1996 in Durango, Colorado. Sponsoring organizations are the Bureau of Indian Affairs, Utah Geological Survey, Colorado Geological Survey, U.S. Geological Survey, Utah Geological Association, Four Corners Geological Society, Fort Lewis College, and Ute Mountain Ute Indian Tribe. The two-day symposium will be preceded by a three-day field trip. The symposium will include poster and oral technical sessions, keynote addresses, and a UGS workshop presenting the results of the geological and reservoir characterization (phase I [budget period 1]) of the Class II Paradox basin project. The UGS will conduct visits to outcrop reservoir analogues along the San Juan River and tours of production facilities at Mule field during the field trip. A special guidebook will be published as part of the symposium and will include papers derived from the UGS project.

7.3 Addressing Regulatory Issues

The UGS Director and Energy Section Chief were invited to meet with county commissioners from every oil producing county in the State, representatives from the State Tax Commission, and Utah Association of Counties to address regulatory issues affecting future oil production and activities. State tax incentives for enhanced oil-recovery (EOR), particularly CO₂ floods, and horizontal-drilling projects were discussed. The UGS explained technical aspects of such projects using the DOE-sponsored Bluebell, Monument Butte (both Class I), and Paradox basin (Class II) as examples of the economic potential of EOR and horizontal drilling.

UGS personnel also met with the Utah Department of Natural Resources Executive Director and representatives of the Utah Office of Energy and Resource Planning. That meeting helped establish the Department's position on a state legislative bill that provides tax incentives for EOR and horizontal-drilling projects.

The UGS is preparing a white paper in cooperation with the Utah Office of Energy and Resource Planning outlining a state strategic initiative to increase oil production in Utah. The strategy will focus on expanding government/industry partnerships similar to those established in the Paradox basin and Bluebell projects, and modifying tax philosophies and regulatory processes to take into account varying reservoir conditions.

APPENDIX A

**PARADOX BASIN PROJECT FIELD SUMMARIES
NAVAJO NATION
SAN JUAN COUNTY, UTAH**

RUNWAY
T. 40 S., R. 25 E., of the Salt Lake Base Line
San Juan County, Utah

General Field Data

Regional Setting: Southwestern shelf, Paradox basin
Producing Formation(s): Pennsylvanian, Desmoinesian-Desert Creek and Ismay zones of the Paradox Formation
Type of Trap: Stratigraphic, carbonate buildup (bryozoan-dominated mound and phylloid algal intervals)
Exploration Method Leading to Discovery: Geophysical seismic surveys, subsurface geology
Other Significant Shows: Lower Ismay zone of the Paradox Formation
Oldest Stratigraphic Horizon Penetrated: Pennsylvanian - Hermosa Group
Surface Formation(s): Jurassic - Morrison Formation
Spacing: state-wide, 40 acres
Productive Area: 193 acres
Completion Practice: Selective perforation and acidize (treatment size varies)
Logging Practice: Dual laterolog-microspherically focused log (DLL-MSFL) with gamma ray (GR), microlog, compensated neutron log-formation compensated density log (CNL-FDC) litho-density with GR, borehole-compensated (BHC-) sonic with GR, rotary sidewall core (SWC), mudlog
Number of Producing Wells: 3
Number of Abandoned Producers: 0
Number of Dry Holes: 0
Number of Shut-in Wells: 0
Number of Disposal Wells: 0
Number of Secondary Recovery Injection Wells: 0
Market for Production: Oil to Gary-Williams Energy Corporation, Denver, Colorado and Giant Refining Company, Scottsdale, Arizona; gas to El Paso Natural Gas Company, El Paso, Texas
Method of Transportation: Oil is trucked to Tex-New Mexico pipeline at Montezuma Creek, Utah; gas transported via pipeline to Aneth Gas Plant which connects to Western Gas Resources pipeline at Montezuma Creek
Major Operators: Harken Southwest Corporation

Discovery Well

Name: Runway No. 10-G-1
Location: SW1/4NE1/4 section 10, T. 40 S., R. 25 E., of the Salt Lake Base Line
Date of Completion: June 24, 1990
Initial Potential: Desert Creek and Upper Ismay zones commingled - initial potential flow (IPF) 825 BOPD and 895 MCFGPD on a 24/64-inch choke (ck), flowing tubing pressure (FTP) 640 psi

Initial Pressure: 2,162 psig (Desert Creek)

Perforations: Upper Ismay - 5,896-5,906 feet (w/ 2 shots/foot [shots/ft]); Desert Creek - 6,042-68 feet (w/ 2 shots/ft), 6,086-6,104 feet (w/ 4 shots/ft)

Treatment: 5,896-5,906 feet acidized w/ 2,000 gallons (gals) 28 percent MSR-100, 250 gals 28 percent MSR-100+, and 4,000 gals 28 percent gelled acid; 6,042-68 feet acidized w/ 3,600 gals 28 percent MSR-100, 6,086-6,104 feet acidized w/ 5,200 gals 28 percent MSR-100

Casing: 8 5/8 inch @ 516 feet, 5 1/2 inch @ 6,201 feet

Total Depth: 6,213 feet, Paradox Formation, Akah salt zone

Elevation: 5,219 feet - graded elevation (GR); 5,233 feet - kelly bushing (KB)

Reservoir Data

Producing Formation: Paradox Formation, Desert Creek zone

Lithology: Bryozoan-dominated mound - bindstone and framestone rarely dolomitized; phylloid algal mound - porous algal bafflestone, some grainstone and dolomitized zones. Both carbonate buildups are interbedded with low permeable wackestone and mudstone.

Type of Drive: Gas expansion

Net Pay Thickness: 50 feet

Geometry of Reservoir Rock: Lenticular, west to east-northeast trending lobate mound, 0.9 miles long and 0.5 miles wide

Porosity: 6.0-20.3 percent, average 11.9 percent (from geophysical logs and cores)

Permeability: 0.1-63.8 md, average 17.3 md (from core analysis)

Water Saturation: 10-63.4 percent, average 15 percent (from geophysical logs and cores)

Rw and/or Salinity: Resistivity = 0.07 ohm-m @ 67°F; pH = 6.0; total dissolved solids = 199,709 ppm, 42,900 ppm Na, 31,700 ppm Ca, 729 ppm Mg, 124,000 ppm Cl, 366 ppm HCO₃, 14 ppm SO₄ (from produced water from tank battery [commingled Desert Creek and Ismay])

Bottom-Hole Temperature (BHT): 126°F @ 6,203 feet (from geophysical logs)

Initial Gas-Oil Ratio: 967 scf/STB

Initial Field Pressure: 2,162 psig

Present Field Pressure: 200-300 psi

Oil and/or Gas Characteristics: Oil: 40.5° API gravity, viscosity 0.314 centipoise (cP) @ initial reservoir conditions, sulfur 0.0 percent by weight, dark green color; gas: British thermal units/foot³ (BTU/ft³) - 1,356.5, specific gravity - 0.779, carbon dioxide - 0.6 percent, nitrogen - 1.1 percent, oxygen - 0.0 percent, methane - 71.5 percent, ethane - 15.4 percent, propane - 7.3 percent, i-butane - 0.7 percent, n-butane - 0.4 percent, i-pentane 0.4 percent, n-pentane - 0.4 percent, hexanes - 0.6 percent, heptanes+ - 0.0 percent, hydrogen sulfide - N/A.

Gas, Oil, and Water Contact: Unknown

Estimated Primary Recovery: 720,000 BO, 2.83 BCFG

Type of Secondary Recovery: None present, may initiate waterflood or CO₂ flood

Estimated Secondary Recovery: Unknown

Estimated Ultimate Recovery: Unknown

Reservoir Data

Producing Formation: Paradox Formation, Ismay zone

Lithology: Limestone and sucrosic dolomite

Type of Drive: Gas expansion

Net Pay Thickness: 22 feet

Geometry of Reservoir Rock: Lenticular, southwest to northeast trending lobate mound, 0.9 miles long and 0.4 miles wide

Porosity: 9.0-14.9 percent, average 11.7 percent (from geophysical logs and cores)

Permeability: 1.4-6.4 md, average 2.7 md (from core analysis)

Water Saturation: 16-33 percent, average 23.6 percent (from geophysical logs and cores)

Rw and/or Salinity: Resistivity = 0.07 ohm-m @ 67°F; pH = 6.0; total dissolved solids = 199,709 ppm, 42,900 ppm Na, 31,700 ppm Ca, 729 ppm Mg, 124,000 ppm Cl, 366 ppm HCO₃, 14 ppm SO₄ (from produced water from tank battery [commingled Desert Creek and Ismay])

Bottom-Hole Temperature: 126°F @ 6,203 feet (from geophysical logs)

Gas-Oil Ratio: 1,085:1

Initial Field Pressure: 2,162 psig

Present Field Pressure: 200-300 psi

Oil and/or Gas Characteristics: Oil: 43.2° API gravity, sulfur 0.0 percent by weight, color dark green; gas: BTU/ft³ - 1,804.5, specific gravity - 1.319, carbon dioxide - 0.1 percent, nitrogen - 17.8 percent, oxygen - 0.0 percent, methane - 14.5 percent, ethane - 20.7 percent, propane - 31.3 percent, i-butane - 3.2 percent, n-butane - 5.0 percent, i-pentane 1.9 percent, n-pentane - 2.1 percent, hexanes - 3.5 percent, hydrogen sulfide - 0.0 percent.

Gas, Oil, and Water Contact: Unknown

Estimated Primary Recovery: 80,000 BO, 0.16 BCFG

Type of Secondary Recovery: None present, may initiate waterflood or CO₂ flood

Estimated Secondary Recovery: Unknown

Estimated Ultimate Recovery: Unknown

Cumulative Production (Desert Creek and Ismay zones commingled): 750,772 BO, 2,268,636 thousand cubic feet of gas (MCFG), and 3,036 bbls of water (BW) as of January 1, 1996 (Utah Division of Oil, Gas and Mining, 1996)

HERON NORTH
T. 41 S., R. 25 E., of the Salt Lake Base Line
San Juan County, Utah

General Field Data

Regional Setting: Southwestern shelf, Paradox basin

Producing Formation(s): Pennsylvanian, Desmoinesian-Desert Creek zone of the Paradox Formation

Type of Trap: Stratigraphic, carbonate buildup (bioclastic calcarenite mound)

Exploration Method Leading to Discovery: Geophysical seismic surveys, subsurface geology

Other Significant Shows: Ismay zone of the Paradox Formation

Oldest Stratigraphic Horizon Penetrated: Pennsylvanian - Hermosa Group

Surface Formation(s): Jurassic - Morrison Formation

Spacing: state-wide, 40 acres

Productive Area: 110 acres

Completion Practice: Selective perforation and acidize (treatment size varies)

Logging Practice: DLL-MSFL with GR, CNL-FDC litho-density with GR, BHC-sonic with GR, mudlog

Number of Producing Wells: 1

Number of Abandoned Producers: 0

Number of Dry Holes: 0

Number of Shut-in Wells: 0

Number of Disposal Wells: 0

Number of Secondary Recovery Injection Wells: 0

Market for Production: Oil to Gary-Williams Energy Corporation, Denver, Colorado and Giant Refining Company, Scottsdale, Arizona; gas to El Paso Natural Gas Company, El Paso, Texas

Method of Transportation: Oil is trucked to Tex-New Mexico pipeline at Montezuma Creek, Utah; gas transported via pipeline to Aneth Gas Plant which connects to Western Gas Resources pipeline at Montezuma Creek

Major Operators: Harken Southwest Corporation

Discovery Well

Name: North Heron No. 35-C

Location: NE1/4NW1/4 section 35, T. 41 S., R. 25 E., of the Salt Lake Base Line

Date of Completion: October 26, 1991

Initial Potential: Desert Creek zone - IPF 605 BOPD and 230 MCFGPD on a 24/64-inch ck, FTP 260 psig

Initial Pressure: 1,934 psig

Perforations: 5,584-5,606 feet (w/ 4 shots/ft)

Treatment: 5,584-5,606 feet acidized w/ 4,400 gals 28 percent MSR-100

Casing: 8 5/8 inch @ 522 feet, 5 1/2 inch @ 5,752 feet

Total Depth: 5,752 feet, Paradox Formation, Akah salt zone
Elevation: 4,747 feet - GR; 4,760 feet - KB

Reservoir Data

Producing Formation: Paradox Formation, Desert Creek zone

Lithology: Porous, dolomitized calcarenite (packstone to grainstone to rudstone) above tight, anhydrite- and salt-plugged algal bafflestone. The calcarenite and bafflestone intervals are separated by low permeable, dolomitized wackestone and mudstone

Type of Drive: Gas expansion

Net Pay Thickness: 60 feet

Geometry of Reservoir Rock: Lenticular, northwest to southeast trending linear mound/beach complex, 0.75 miles long and 0.5 miles wide

Porosity: 7.8-20.9 percent, average 15 percent (from geophysical logs and cores)

Permeability: 1.2-70.1 md, average 17.7 md (from core analysis)

Water Saturation: 19.3-66.6 percent, average 15 percent (from core analysis)

Rw and/or Salinity: 0.035 ohm-m @ BHT

Bottom-Hole Temperature: 126°F @ 5,752 feet (from geophysical logs)

Initial Gas-Oil Ratio: 644 scf/STB

Initial Field Pressure: 1,934 psig

Present Field Pressure: 200-300 psi

Oil and/or Gas Characteristics: Oil: 44.0° API gravity, viscosity 0.475 cP @ initial reservoir conditions, sulfur 0.0 percent by weight, color dark green; gas: BTU/ft³ - 1,321, specific gravity - 0.8335, carbon dioxide - 4.3 percent, nitrogen - 1.1 percent, oxygen - N/A, methane - 64.6 percent, hydrogen sulfide - N/A.

Gas, Oil, and Water Contact: Unknown

Cumulative Production: 200,759 BO, 305,669 MCFG, and 23,578 BW as of January 1, 1996 (Utah Division of Oil, Gas and Mining, 1996)

Estimated Primary Recovery: 990,000 BO, 2.65 BCFG

Type of Secondary Recovery: None present, may initiate waterflood or CO₂ flood

Estimated Secondary Recovery: Unknown

Estimated Ultimate Recovery: Unknown

MULE
T. 41 S., R. 24 E., of the Salt Lake Base Line
San Juan County, Utah

General Field Data

Regional Setting: Southwestern shelf, Paradox basin
Producing Formation(s): Pennsylvanian, Desmoinesian-Desert Creek zone of the Paradox Formation
Type of Trap: Stratigraphic, carbonate buildup (phylloid algal mound)
Exploration Method Leading to Discovery: Geophysical seismic surveys, subsurface geology
Other Significant Shows: Ismay zone of the Paradox Formation
Oldest Stratigraphic Horizon Penetrated: Pennsylvanian - Hermosa Group
Surface Formation(s): Jurassic - Morrison Formation
Spacing: 80 acres
Productive Area: 48 acres
Completion Practice: Selective perforation and acidize (treatment size varies)
Logging Practice: DLL with GR, CNL-FDC litho-density with GR, BHC-sonic-GR, formation microscanner (FMS), microlog, mudlog
Number of Producing Wells: 1
Number of Abandoned Producers: 0
Number of Dry Holes: 0
Number of Shut-in Wells: 1
Number of Disposal Wells: 0
Number of Secondary Recovery Injection Wells: 0
Market for Production: Oil to Gary-Williams Energy Corporation, Denver, Colorado and Giant Refining Company, Scottsdale, Arizona; gas to El Paso Natural Gas Company, El Paso, Texas
Method of Transportation: Oil is trucked to Tex-New Mexico pipeline at Montezuma Creek, Utah; gas transported via pipeline to Aneth Gas Plant which connects to Western Gas Resources pipeline at Montezuma Creek
Major Operators: Harken Southwest Corporation

Discovery Well

Name: Mule No. 31-K-1 (N)
Location: SW1/4SW1/4 section 31, T. 41 S., R. 24 E., of the Salt Lake Base Line
Date of Completion: October 13, 1991
Initial Potential: Desert Creek zone - approximately 10 bbls of oil per hour (based on several swab tests) w/ water cut increasing on each test
Initial Pressure: rapid draw down
Perforations: 6,003-08 feet, 6,010-29 feet (w/ 4 shots/ft)
Treatment: 6,003-08 feet acidized w/ 4,800 gals 28 percent gelled MSR-100; 6,010-29 feet acidized w/8,000 gals 28 percent gelled MSR-100

Casing: 8 5/8 inch @ 520 feet, 5 1/2 inch @ 6,162 feet
Total Depth: 6,162 feet, Paradox Formation, Akah salt zone
Elevation: 4,940 feet - GR; 4,952 feet - KB

Reservoir Data

Producing Formation: Paradox Formation, Desert Creek zone
Lithology: Porous algal bafflestone and crinoidal packstone with dolomitized zones interbedded with low permeable wackestone, mudstone, and dolomite
Type of Drive: Gas expansion
Net Pay Thickness: 47 feet
Geometry of Reservoir Rock: Lenticular, northeast to east trending linear mound/mound flank deposit, 0.5 miles long and 900 feet wide
Porosity: 7.5-24.2 percent, average 13 percent (from geophysical logs and core analysis)
Permeability: 0.1-234 md; average for mound core interval (30 percent of the reservoir) approximately \approx 190 md, average for the supra-mound interval (70 percent of the reservoir) \approx 2 md (from core analysis)
Water Saturation: 12-50.4 percent, average 15 percent (from core analysis)
Rw and/or Salinity: 0.035 ohm-m @ BHT
Bottom-Hole Temperature: 128° F @ 5,804 feet (from geophysical logs)
Initial Gas-Oil Ratio: 478 scf/STB
Initial Field Pressure: 2,050 psi
Present Field Pressure: 200-300 psi
Oil and/or Gas Characteristics: 44.0° API gravity, sulfur 0.0 percent by weight, color dark green; gas: BTU/ft³ - 1,539, specific gravity - 0.8890, carbon dioxide - 0.04 percent, nitrogen - 1.5 percent, oxygen - 0.0 percent, methane - 61.8 percent, hydrogen sulfide - 0.0 percent.
Gas, Oil, and Water Contact: Unknown
Cumulative Production: 343,180 BO, 203,116 MCFG, and 17,930 BW as of January 1, 1996 (Utah Division of Oil, Gas and Mining, 1996)
Estimated Primary Recovery: 430,603 BO, 0.288 BCFG
Type of Secondary Recovery: None present, may initiate waterflood or CO₂ flood
Estimated Secondary Recovery: Unknown
Estimated Ultimate Recovery: Unknown

BLUE HOGAN
T. 42 S., R. 23 E., of the Salt Lake Base Line
San Juan County, Utah

General Field Data

Regional Setting: Southwestern shelf, Paradox basin
Producing Formation(s): Pennsylvanian, Desmoinesian-Desert Creek zone of the Paradox Formation
Type of Trap: Stratigraphic, carbonate buildup (phylloid algal mound)
Exploration Method Leading to Discovery: Geophysical seismic surveys, subsurface geology
Other Significant Shows: None
Oldest Stratigraphic Horizon Penetrated: Pennsylvanian - Hermosa Group
Surface Formation(s): Jurassic - Morrison Formation
Spacing: 80 acres
Productive Area: 89 acres
Completion Practice: Selective perforation and acidize (treatment size varies)
Logging Practice: DLL-MSFL with GR, microlog, CNL-FDC litho-density with GR, BHC-sonic with GR, mudlog
Number of Producing Wells: 1
Number of Abandoned Producers: 0
Number of Dry Holes: 0
Number of Shut-in Wells: 0
Number of Disposal Wells: 0
Number of Secondary Recovery Injection Wells: 0
Market for Production: Oil to Gary-Williams Energy Corporation, Denver, Colorado and Giant Refining Company, Scottsdale, Arizona; gas to El Paso Natural Gas Company, El Paso, Texas
Method of Transportation: Oil is trucked to Tex-New Mexico pipeline at Montezuma Creek, Utah; gas transported via pipeline to Aneth Gas Plant which connects to Western Gas Resources pipeline at Montezuma Creek
Major Operators: Harken Southwest Corporation

Discovery Well

Name: Blue Hogan No. 1-J-1
Location: NE1/4NW1/4SE1/4 section 1, T. 42 S., R. 23 E., of the Salt Lake Base Line
Date of Completion: February 6, 1991
Initial Potential: Desert Creek zone - IPF 1,167 BOPD, 722 MCFGPD, and 5 bbls of water per day (BWPD) on a 30/64-inch ck, FTP 265 psi
Initial Pressure: 1,800 psi
Perforations: 5,400-46 feet, 5,454-77 feet, 5,488-5,522 feet, 5,530-42 feet, 5,554-62 feet(w/ 4 shots/ft)

Treatment: 5,400-46 feet acidized w/ 13,800 gals 28 percent MSR-100; 5,454-77 feet acidized w/ 6,900 gals 28 percent MSR-100; 5,488-5,522 feet acidized w/ 10,200 gals 28 percent MSR-100; 5,530-42 feet acidized w/ 3,600 gals 28 percent MSR-100; 5,554-62 feet acidized w/ 2,400 gals 28 percent MSR-100

Casing: 8 5/8 inch @ 492 feet, 5 1/2 inch @ 5,611 feet

Total Depth: 5,613 feet, Paradox Formation, Akah salt zone

Elevation: 4,995 feet - GR; 5,009 feet - KB

Reservoir Data

Producing Formation: Paradox Formation, Desert Creek zone

Lithology: Porous algal bafflestone and dolomitized zones interbedded with low permeable wackestone and mudstone

Type of Drive: Gas expansion

Net Pay Thickness: 82 feet

Geometry of Reservoir Rock: Lenticular, northwest to southeast trending linear mound, 0.5 miles long and 1,000 feet wide

Porosity: 6-16.5 percent, average 9.1 percent (from geophysical logs and cores)

Permeability: 0.1-425 md; average for mound core interval (30 percent of the reservoir) approximately \approx 190 md, average for the supra-mound interval (70 percent of the reservoir) \approx 2 md (from core analysis)

Water Saturation: 17-56 percent, average 15 percent (from geophysical logs and cores)

Rw and/or Salinity: 0.035 ohm-m @ BHT

Bottom-Hole Temperature: 128°F @ 5,613 feet (from geophysical logs)

Initial Gas-Oil Ratio: 487 scf/STB

Initial Field Pressure: 1,800 psi

Present Field Pressure: 200-300 psi

Oil and/or Gas Characteristics: 40.6° API gravity, viscosity 0.811 cP @ initial reservoir conditions, sulfur 0.0 percent by weight, color dark green; gas: BTU/ft³ - 1,497, specific gravity - 0.8992, carbon dioxide - 0.1 percent, nitrogen - 2.4 percent, oxygen - 0.0 percent, methane - 60.6 percent, hydrogen sulfide - 0.0 percent.

Gas, Oil, and Water Contact: Unknown

Cumulative Production: 282,718 BO, 256,006 MCFG, and 1,699 BW as of January 1, 1996 (Utah Division of Oil, Gas and Mining, 1996)

Estimated Primary Recovery: 645,000 BO, 0.968 BCFG

Type of Secondary Recovery: None present, may initiate waterflood or CO₂ flood

Estimated Secondary Recovery: Unknown

Estimated Ultimate Recovery: Unknown

ANASAZI
T. 42 S., R. 24 E., of the Salt Lake Base Line
San Juan County, Utah

General Field Data

Regional Setting: Southwestern shelf, Paradox basin
Producing Formation(s): Pennsylvanian, Desmoinesian-Desert Creek zone of the Paradox Formation
Type of Trap: Stratigraphic, carbonate buildup (phylloid algal mound)
Exploration Method Leading to Discovery: Geophysical seismic surveys, subsurface geology
Other Significant Shows: Ismay zone of the Paradox Formation
Oldest Stratigraphic Horizon Penetrated: Pennsylvanian - Hermosa Group
Surface Formation(s): Jurassic - Morrison Formation
Spacing: 80 acres
Productive Area: 165 acres
Completion Practice: Selective perforation and acidize (treatment size varies)
Logging Practice: DLL-MSFL with GR and spontaneous potential (SP), microlog, CNL-FDC litho-density with GR, BHC-sonic with GR, rotary SWC, mudlog
Number of Producing Wells: 4
Number of Abandoned Producers: 0
Number of Dry Holes: 0
Number of Shut-in Wells: 0
Number of Disposal Wells: 0
Number of Secondary Recovery Injection Wells: 0
Market for Production: Oil to Gary-Williams Energy Corporation, Denver, Colorado and Giant Refining Company, Scottsdale, Arizona; gas to El Paso Natural Gas Company, El Paso, Texas
Method of Transportation: Oil is trucked to Tex-New Mexico pipeline at Montezuma Creek, Utah; gas transported via pipeline to Aneth Gas Plant which connects to Western Gas Resources pipeline at Montezuma Creek
Major Operators: Harken Southwest Corporation

Discovery Well

Name: Anasazi No. 1
Location: SE1/4SW1/4NW1/4 section 5, T. 42 S., R. 24 E., of the Salt Lake Base Line
Date of Completion: January 23, 1990
Initial Potential: Desert Creek zone - IPF 1,705 BOPD and 833 MCFGPD on a 48/64-inch ck, FTP 170 psi
Initial Pressure: 1,945 psi
Perforations: 5,574-5,630 feet, 5,646-70 feet (w/ 2 shots/ft)
Treatment: 5,574-5,630 feet acidized w/ 22,400 gals 28 percent MSR-100, 5,646-70 feet acidized w/ 4,800 gals 28 percent MSR-100

Casing: 8 5/8 inch @ 504 feet, 5 1/2 inch @ 5,780 feet
Total Depth: 5,780 feet, Paradox Formation, Akah salt zone
Elevation: 4,778 feet - GR; 4,790 feet - KB

Reservoir Data

Producing Formation: Paradox Formation, Desert Creek zone
Lithology: Porous algal bafflestone, some grainstone and dolomitized zones interbedded with low permeable wackestone and mudstone
Type of Drive: Gas expansion
Net Pay Thickness: 46 feet (average from four wells)
Geometry of Reservoir Rock: Lenticular, west to northeast trending lobate mound, 0.9 miles long and 2,000- to 3,000-feet wide
Porosity: 6.8-24.5 percent, average 14.1 percent (from geophysical logs and cores)
Permeability: 0.1-2,180 md; average for mound core interval (30 percent of the reservoir) approximately \approx 190 md, average for the supra-mound interval (70 percent of the reservoir) \approx 2 md (from core analysis)
Water Saturation: 10-57 percent, average 15 percent (from geophysical logs and cores)
Rw and/or Salinity: 0.035 ohm-m @ bottom-hole temperature (BHT)
Bottom-Hole Temperature: 138°F @ 5,777 feet (from geophysical logs)
Initial Gas-Oil Ratio: 364 scf/STB
Initial Field Pressure: 1,945 psi
Present Field Pressure: 200-300 psi
Oil and/or Gas Characteristics: Oil: 41° API gravity, viscosity 0.951 cP @ initial reservoir conditions, sulfur 0.0 percent by weight, color dark green; Gas: BTU/ft³ - 1,400.3, specific gravity - 0.8080, carbon dioxide - 2.3 percent, nitrogen - 0.4 percent, oxygen - 0.0 percent, methane - 20.2 percent, hydrogen sulfide - 0.0 percent.
Gas, Oil, and Water Contact: None
Cumulative Production: 1,650,133 BO, 1,281,713 MCFG, and 25,274 BW as of January 1, 1996 (Utah Division of Oil, Gas and Mining, 1996)
Estimated Primary Recovery: 2,069,392 BO, 1.89 BCFG
Type of Secondary Recovery: None present, may initiate waterflood or CO₂ flood
Estimated Secondary Recovery: Unknown
Estimated Ultimate Recovery: Unknown

REFERENCES

Utah Division of Oil, Gas and Mining, 1996, Oil and gas production report, December 1995: non-paginated.

APPENDIX B

**COMPOSITIONAL ANALYSES OF OIL AND GAS
ANASAZI FIELD
NAVAJO NATION
SAN JUAN COUNTY, UTAH**

Table B.1. Composition of Anasazi No. 5-L separator oil cylinder No. W8301 at 73°F (23°C) and 1,014 psia (6,992 kpa).

Component	Molecular Weight (g/mole)	Gas Mole %	Liquid Wt %	Overall Wt %	Mole %	Group Mole %
CO ₂	44.010	0.000	0.000	0.000	0.000	0.000
H ₂ S	34.080	0.000	0.000	0.000	0.000	0.000
N ₂	28.013	0.000	0.000	0.000	0.000	0.000
C1	16.043	12.818	0.000	0.061	0.673	0.673
C2	30.070	24.311	0.050	0.266	1.568	1.568
C3	44.097	30.424	0.382	0.775	3.112	3.112
I-C4	58.124	5.552	0.236	0.329	1.001	1.001
N-C4	58.124	14.474	0.966	1.203	3.665	3.665
I-C5	72.151	3.652	0.791	0.859	2.108	2.108
N-C5	72.151	4.214	1.253	1.327	3.257	3.257
C6	86.200	2.301	2.760	2.782	5.718	9.272
MCYCL-C5	84.160	0.431	0.767	0.768	1.616	
Benzene	78.110	0.109	0.177	0.177	0.402	
CYCL-C6	84.160	0.282	0.715	0.712	1.536	
C7	100.200	0.692	3.268	3.246	5.738	
MCYCL-C6	98.190	0.231	1.460	1.447	2.611	23.077
Toluene	92.140	0.062	0.453	0.449	0.863	
C8	114.230	0.275	4.270	4.223	6.549	
C2-Benzene	106.170	0.012	0.176	0.174	0.290	
M&P-XYLENE	106.170	0.019	0.497	0.491	0.819	
O-XYLENE	106.170	0.007	0.343	0.339	0.565	
C9	128.300	0.083	4.137	4.086	5.641	
C10	134.000	0.033	4.996	4.932	6.519	23.772
C11	147.000	0.009	4.406	4.348	5.240	
C12	161.000	0.003	3.751	3.702	4.073	
C13	175.000	0.002	4.336	4.279	4.331	
C14	190.000	0.001	3.868	3.817	3.559	

Table B.1. (continued)

Component	Molecular Weight (g/mole)	Gas Mole %	Liquid Wt %	Overall Wt %	Mole %	Group Mole %
C15	206.000	0.001	3.615	3.567	3.068	11.783
C16	222.000	0.001	3.052	3.012	2.403	
C17	237.000	0.000	3.039	2.999	2.242	
C18	251.000	0.000	3.086	3.045	2.149	
C19	263.000	0.000	2.891	2.853	1.922	
C20+11.783	275.000	0.000	2.643	2.608	1.680	10.622
C21	291.000	0.000	2.346	2.315	1.409	
C22	305.000	0.000	2.295	2.265	1.315	
C23	318.000	0.000	2.134	2.106	1.173	
C24	331.000	0.000	1.947	1.921	1.028	
C25	345.000	0.000	1.888	1.863	0.957	
C26	359.000	0.000	1.755	1.732	0.855	
C27	374.000	0.000	1.725	1.702	0.806	
C28	388.000	0.000	1.639	1.617	0.738	
C29	402.000	0.000	1.519	1.499	0.661	
C30+10.622	580.000	0.000	20.371	20.104	6.140	6.140
<p>The sample had a density of 0.809 g/cc and a gas-oil ratio (GOR) of 34.4 scf/STB. The average molecular weight of the (1) gas phase = 44.274 g/mole, (2) liquid phase = 184.503 g/mole, and (3) gas and liquid phase combine = 177.137 g/mole.</p>						

Table B.2. Composition of Anasazi No. 5-L separator oil cylinder No. W4635 at 73°F (23°C) and 1,014 psia (6,992 kpa).

Component	Molecular Weight (g/mole)	Gas Mole %	Liquid Wt %	Overall Wt %	Mole %	Group Mole %
CO ₂	44.010	0.000	0.000	0.000	0.000	0.000
H ₂ S	34.080	0.000	0.000	0.000	0.000	0.000
N ₂	28.013	0.000	0.000	0.000	0.000	0.000
C1	16.043	12.873	0.000	0.062	0.683	0.683
C2	30.070	24.310	0.053	0.272	1.597	1.597
C3	44.097	30.619	0.392	0.793	3.171	3.171
I-C4	58.124	5.583	0.239	0.334	1.011	1.011
N-C4	58.124	14.542	0.975	1.217	3.689	3.689
I-C5	72.151	3.602	0.793	0.861	2.102	2.102
N-C5	72.151	4.093	1.256	1.328	3.244	3.244
C6	86.200	2.238	2.767	2.788	5.700	9.243
MCYCL-C5	84.160	0.417	0.768	0.768	1.609	
Benzene	78.110	0.106	0.178	0.178	0.402	
CYCL-C6	84.160	0.272	0.717	0.714	1.532	
C7	100.200	0.659	3.284	3.26	5.734	23.114
MCYCL-C6	98.190	0.217	1.466	1.453	2.608	
Toluene	92.140	0.060	0.456	0.452	0.864	
C8	114.230	0.253	4.306	4.257	6.568	
C2-Benzene	106.170	0.011	0.176	0.174	0.289	
M&P-XYLENE	106.170	0.018	0.500	0.494	0.82	
O-XYLENE	106.170	0.004	0.360	0.355	0.59	23.721
C9	128.300	0.073	4.160	4.107	5.642	
C10	134.000	0.029	5.006	4.941	6.498	
C11	147.000	0.009	4.447	4.388	5.261	
C12	161.000	0.004	3.732	3.683	4.031	
C13	175.000	0.003	4.373	4.315	4.345	
C14	190.000	0.001	3.919	3.867	3.587	

Table B.2. (continued)

Component	Molecular Weight (g/mole)	Gas Mole %	Liquid Wt %	Overall Wt %	Mole %	Group Mole %
C15	206.000	0.000	3.610	3.562	3.047	11.822
C16	222.000	0.000	3.104	3.063	2.431	
C17	237.000	0.000	3.089	3.048	2.266	
C18	251.000	0.000	3.111	3.070	2.155	
C19	263.000	0.000	2.907	2.868	1.922	
C20	275.000	0.000	2.647	2.612	1.674	10.686
C21	291.000	0.000	2.362	2.331	1.411	
C22	305.000	0.000	2.319	2.288	1.322	
C23	318.000	0.000	2.152	2.123	1.177	
C24	331.000	0.000	1.950	1.924	1.024	
C25	345.000	0.000	1.929	1.903	0.972	
C26	359.000	0.000	1.783	1.759	0.864	
C27	374.000	0.000	1.844	1.819	0.857	
C28	388.000	0.000	1.693	1.670	0.759	
C29	402.000	0.000	1.447	1.427	0.625	
C30+	580.000	0.000	19.372	19.470	5.916	5.916

The sample had a density of 0.809 g/cc and a gas-oil ratio (GOR) of 34.3 scf/STB. The average molecular weight of the (1) gas phase = 44.130 g/mole, (2) liquid phase = 183.634 g/mole, and (3) gas and liquid phase combine = 176.229 g/mole.

Table B.3. Composition of Anasazi No. 5-L separator gas cylinder No. 5EK088.

Component	Molecular Weight (g/mole)	Recombine Gas Analyses (wt%)	Convert Recombined Gas Composition to Mole % Basis		Group Mole %
			w/Molecular Weight	Mole %	
CO ₂	44.010	0.103	0.002	0.062	0.062
H ₂ S	34.080	0.000	0.000	0.000	0.000
N ₂	28.013	10.570	0.038	1.002	1.002
C1	16.043	35.181	2.193	58.211	58.211
C2	30.070	23.285	0.774	20.555	20.555
C3	44.097	19.624	0.445	11.813	11.813
I-C4	58.124	3.485	0.060	1.592	1.592
N-C4	58.124	8.472	0.146	3.869	3.869
I-C5	72.151	2.158	0.030	0.794	0.794
N-C5	72.151	2.524	0.035	0.928	0.928
C6	86.200	1.797	0.021	0.553	0.759
MCYCL-C5	84.160	0.337	0.004	0.106	
Benzene	78.110	0.083	0.001	0.028	
CYCL-C6	84.160	0.225	0.003	0.071	
C7	100.200	0.717	0.007	0.190	0.395
MCYCL-C6	98.190	0.232	0.002	0.063	
Toluene	92.140	0.063	0.001	0.018	
C8	114.230	0.359	0.003	0.083	
C2-Benzene	106.170	0.015	0.000	0.004	
M&P-XYLENE	106.170	0.025	0.000	0.006	
O-XYLENE	106.170	0.012	0.000	0.003	
C9	128.300	0.133	0.001	0.028	0.020
C10	134.000	0.066	0.000	0.013	
C11	147.000	0.024	0.000	0.004	
C12	161.000	0.009	0.000	0.001	
C13	175.000	0.004	0.000	0.001	
C14	190.000	0.001	0.000	0.000	
C15	206.000	0.001	0.000	0.000	
C16	222.000	0.001	0.000	0.000	
C17	237.000	0.002	0.000	0.000	
C18	251.000	0.002	0.000	0.000	
C19	263.000	0.005	0.000	0.000	

Average molecular weight of the gas in the sample = 26.54 g/mole.

Table B.4. Composition of Anasazi No. 5-L separator gas cylinder No. 6EK087.

Component	Molecular Weight (g/mole)	Recombine Gas Analyses (wt%)	Convert Recombined Gas Composition to Mole % Basis		Group Mole %
			w/Molecular Weight	Mole %	
CO ₂	44.010	0.109	0.002	0.065	0.065
H ₂ S	34.080	0.000	0.000	0.000	0.000
N ₂	28.013	1.053	0.038	0.997	0.997
C1	16.043	35.166	2.192	58.149	58.149
C2	30.070	23.461	0.780	20.698	20.698
C3	44.097	19.518	0.443	11.742	11.742
I-C4	58.124	3.560	0.061	1.625	1.625
N-C4	58.124	8.474	0.146	3.867	3.867
I-C5	72.151	2.149	0.030	0.790	0.790
N-C5	72.151	2.506	0.035	0.921	0.921
C6	86.200	1.767	0.020	0.544	0.744
MCYCL-C5	84.160	0.329	0.004	0.104	
Benzene	78.110	0.081	0.001	0.027	
CYCL-C6	84.160	0.220	0.003	0.069	
C7	100.200	0.696	0.007	0.184	0.382
MCYCL-C6	98.190	0.224	0.002	0.061	
Toluene	92.140	0.060	0.001	0.017	
C8	114.230	0.346	0.003	0.080	
C2-Benzene	106.170	0.015	0.000	0.004	
M&P-XYLENE	106.170	0.026	0.000	0.007	
O-XYLENE	106.170	0.010	0.000	0.002	
C9	128.300	0.128	0.001	0.027	0.018
C10	134.000	0.062	0.000	0.012	
C11	147.000	0.022	0.000	0.004	
C12	161.000	0.008	0.000	0.001	
C13	175.000	0.004	0.000	0.001	
C14	190.000	0.002	0.000	0.000	
C15	206.000	0.001	0.000	0.000	
C16	222.000	0.001	0.000	0.000	
C17	237.000	0.001	0.000	0.000	
C18	251.00	0.000	0.000	0.000	
C19	263.000	0.002	0.000	0.000	

Average molecular weight of the gas in the sample = 26.54 g/mole.

Table B.5. Dead oil liquid composition of the Anasazi flashed separator oils and dead oils.

Component	Molecular Weight (g/mole)	Cylinder No. W4635 (wt %)	Cylinder No. W8301 (wt %)	Anasazi No. 6H-1 (Limestone) (wt %)	Anasazi No. 6H-1 (Dolomite) (wt %)	Anasazi No. 5L-3 (wt %)
CO ₂	44.010	0.000	0.000	0.000	0.000	0.000
H ₂ S	34.080	0.000	0.000	0.000	0.000	0.000
N ₂	28.013	0.000	0.000	0.000	0.000	0.000
C1	16.043	0.000	0.000	0.000	0.000	0.000
C2	30.070	0.053	0.050	0.001	0.022	0.049
C3	44.097	0.392	0.382	0.009	0.145	0.343
I-C4	58.124	0.239	0.236	0.009	0.093	0.212
N-C4	58.124	0.975	0.966	0.035	0.383	0.870
I-C5	72.151	0.793	0.791	0.049	0.383	0.745
N-C5	72.151	1.256	1.253	0.082	0.694	1.196
C6	86.200	2.757	2.760	0.265	1.473	1.979
MCYCL-C5	84.160	0.768	0.767	0.206	1.127	1.504
Benzene	78.110	0.178	0.177	0.024	0.134	0.175
CYCL-C6	84.160	0.717	0.715	0.137	0.614	0.714
C7	100.200	3.284	3.268	0.701	3.060	3.293
MCYCL-C6	98.190	1.466	1.460	0.366	1.406	1.472
Toluene	92.140	0.456	0.453	0.108	0.413	0.454
C8	114.230	4.306	4.270	1.286	4.206	4.335
C2-Benzene	106.170	0.176	0.176	0.105	0.176	0.177
M&P-XYLENE	106.170	0.500	0.497	0.413	0.472	0.500
O-XYLENE	106.170	0.360	0.343	0.323	0.331	0.362
C9	128.300	4.160	4.137	1.538	4.066	4.154
C10	134.000	5.006	4.996	2.529	4.881	4.913
C11	147.000	4.447	4.406	3.128	4.376	4.286
C12	161.000	3.732	3.751	3.284	4.737	3.635
C13	175.000	4.373	4.336	4.301	4.347	4.138
C14	190.000	3.919	3.868	3.994	3.924	3.652
C15	206.000	3.610	3.615	3.943	3.701	3.208
C16	222.000	3.104	3.052	3.427	3.124	2.830
C17	237.000	3.089	3.039	3.336	3.082	2.763
C18	251.000	3.111	3.086	3.494	3.152	2.823

Table B.5. (continued)

Component	Molecular Weight (g/mole)	Cylinder No. W4635 (wt %)	Cylinder No. W8301 (wt %)	Anasazi No. 6H-1 (Limestone) (wt%)	Anasazi No. 6H-1 (Dolomite) (wt %)	Anasazi No. 5L-3 (wt %)
C19	263.000	2.907	2.891	3.160	2.987	2.596
C20	275.000	2.647	2.643	2.825	2.401	2.375
C21	291.000	2.362	2.346	2.660	2.360	2.101
C22	305.000	2.319	2.295	2.635	2.295	2.058
C23	318.000	2.152	2.134	2.468	2.155	1.922
C24	331.000	1.950	1.947	2.304	1.917	1.729
C25	345.000	1.929	1.888	2.277	2.229	1.692
C26	359.000	1.783	1.755	1.954	1.378	1.437
C27	374.000	1.844	1.725	2.275	1.782	1.549
C28	388.000	1.693	1.639	1.944	1.473	1.573
C29	402.000	1.446	1.519	1.740	1.521	1.300
C30+	580.000	19.732	20.371	36.664	23.980	24.885
Total average molecular weight (g/mole) of the oil samples		186.634	184.503	272.062	200.546	189.014

Table B.6. Composition of Anasazi No. 5-L recombined separator oil at 70°F (21°C) and 3,014 psia (20,782 kpa).

Component	Molecular Weight (g/mole)	Gas Mole %	Liquid Wt %	Overall Wt %	Mole %	Group Mole %
CO ₂	44.010	0.078	0.000	0.031	0.055	0.055
H ₂ S	34.080	0.000	0.000	0.000	0.000	0.000
N ₂	28.013	1.003	0.000	0.255	0.702	0.702
C1	16.043	55.141	0.011	8.052	38.647	38.647
C2	30.070	19.748	0.076	5.456	13.971	13.941
C3	44.097	12.165	0.274	5.080	8.872	8.872
I-C4	58.124	1.902	0.143	1.111	1.472	1.472
N-C4	58.124	4.792	0.565	2.951	3.909	3.909
I-C5	72.151	1.241	0.481	1.170	1.249	1.249
N-C5	72.151	1.561	0.829	1.637	1.748	1.748
C6	86.200	1.123	2.404	2.659	2.375	3.562
MCYCL-C5	84.160	0.194	0.601	0.594	0.543	
Benzene	78.110	0.051	0.142	0.142	0.140	
CYCL-C6	84.160	0.135	0.605	0.551	0.504	
C7	100.200	0.397	3.247	2.765	2.125	8.257
MCYCL-C6	98.190	0.128	1.390	1.143	0.896	
Toluene	92.140	0.037	0.442	0.358	0.299	
C8	114.230	0.170	4.465	3.480	2.346	
C2-Benzene	106.170	0.008	0.165	0.130	0.094	
M&P-XYLENE	106.170	0.013	0.521	0.398	0.289	
O-XYLENE	106.170	0.005	0.383	0.288	0.209	
C9	128.300	0.056	4.412	3.330	1.999	8.092
C10	134.000	0.027	5.293	3.950	2.270	
C11	147.000	0.011	4.617	3.432	1.798	
C12	161.000	0.005	3.851	2.857	1.367	
C13	175.000	0.003	4.500	3.335	1.467	
C14	190.000	0.002	3.965	2.937	1.191	
C15	206.000	0.002	3.644	2.700	1.009	3.959
C16	222.000	0.001	3.175	2.352	0.816	
C17	237.000	0.001	3.139	2.324	0.755	
C18	251.000	0.000	3.218	2.382	0.731	
C19	263.000	0.000	2.991	2.214	0.648	

Table B.6. (continued)

Component	Molecular Weight (g/mole)	Gas Mole %	Liquid Wt %	Overall Wt %	Mole %	Group Mole %
C20	275.000	0.000	2.651	1.962	0.549	3.509
C21	291.000	0.000	2.413	1.786	0.473	
C22	305.000	0.000	2.351	1.740	0.439	
C23	318.000	0.000	2.205	1.632	0.395	
C24	331.000	0.000	1.971	1.459	0.339	
C25	345.000	0.000	1.938	1.434	0.320	
C26	359.000	0.000	1.687	1.248	0.268	
C27	374.000	0.000	1.842	1.363	0.281	
C28	388.000	0.000	1.552	1.149	0.228	
C29	402.000	0.000	1.533	1.134	0.217	
C30+	580.000	0.000	20.309	15.029	1.995	1.995

The sample had a density of 0.681 g/cc. The average molecular weight of the (1) gas phase = 28.591 g/mole, (2) liquid phase = 190.065 g/mole, and (3) gas and liquid phase combined = 77.005 g/mole.

Table B.7. Composition of Anasazi No. 5-L recombined oil flashed to 2,050 psia (14,135 kpa) at 130°F (54°C).

Component	Molecular Weight (g/mole)	Gas Mole %	Liquid Wt %	Overall Wt %	Mole %	Group Mole %
CO ₂	44.010	0.000	0.000	0.000	0.000	0.000
H ₂ S	34.080	0.000	0.000	0.000	0.000	0.000
N ₂	28.013	0.928	0.000	0.191	0.586	0.586
C1	16.043	53.274	0.000	6.291	33.617	33.617
C2	30.070	22.122	0.087	4.965	14.157	14.157
C3	44.097	14.215	0.328	4.875	9.477	9.477
I-C4	58.124	2.023	0.232	1.050	1.549	1.549
N-C4	58.124	4.668	1.005	2.796	4.125	4.125
I-C5	72.151	0.872	0.832	1.125	1.336	1.336
N-C5	72.151	0.960	1.346	1.580	1.878	1.878
C6	86.200	0.488	3.043	2.730	2.715	4.078
MCYCL-C5	84.160	0.079	0.709	0.613	0.624	
Benzene	78.110	0.021	0.165	0.143	0.157	
CYCL-C6	84.160	0.052	0.677	0.571	0.582	
C7	100.200	0.141	3.451	2.849	2.437	9.413
MCYCL-C6	98.190	0.001	1.435	1.142	0.997	
Toluene	92.140	0.012	0.449	0.365	0.340	
C8	114.230	0.092	4.416	3.589	2.694	
C2-Benzene	106.170	0.003	0.177	0.143	0.115	
M&P-XYLENE	106.170	0.005	0.502	0.403	0.325	
O-XYLENE	106.170	0.002	0.555	0.443	0.358	9.275
C9	128.300	0.020	4.015	3.212	2.146	
C10	134.000	0.013	5.055	4.033	2.581	
C11	147.000	0.005	4.405	3.509	2.046	
C12	161.000	0.001	3.759	2.991	1.593	
C13	175.000	0.000	4.351	3.461	1.696	
C14	190.000	0.000	3.789	3.014	1.360	4.507
C15	206.000	0.000	3.520	2.800	1.165	
C16	222.000	0.000	3.003	2.389	0.923	
C17	237.000	0.000	2.963	2.357	0.853	
C18	251.000	0.000	3.029	2.409	0.823	
C19	263.000	0.000	2.867	2.280	0.743	

Table B.7. (continued)

Component	Molecular Weight (g/mole)	Gas Mole %	Liquid Wt %	Overall Wt %	Mole %	Group Mole %
C20	275.000	0.000	2.307	1.835	0.572	3.996
C21	291.000	0.000	2.290	1.821	0.537	
C22	305.000	0.000	2.240	1.781	0.501	
C23	318.000	0.000	2.094	1.665	0.449	
C24	331.000	0.000	1.879	1.494	0.387	
C25	345.000	0.000	1.964	1.562	0.388	
C26	359.000	0.000	1.616	1.285	0.307	
C27	374.000	0.000	1.805	1.436	0.329	
C28	388.000	0.000	1.626	1.293	0.286	
C29	402.000	0.000	1.419	1.129	0.241	
C30+	580.000	0.000	20.596	16.380	2.006	2.006

The sample had a density of 0.664 g/cc and a GOR of 1,037 scf/STB. The average molecular weight of the (1) gas phase = 27.811 g/mole, (2) liquid phase = 184.796 g/mole, and (3) gas and liquid phase combined = 85.734 g/mole.

Table B.8. Vapor compositional data for the two separator tests.

Component	Molecular Weight (g/mole)	35 psig & 85°F 1st Stage (mole %)	0 psig & 60°F 2nd Stage (mole %)
CO ₂	44.010	0.000	3.983
H ₂ S	34.080	0.000	0.000
N ₂	28.013	1.224	0.435
C1	16.043	58.890	25.500
C2	30.070	20.432	29.578
C3	44.097	11.588	23.915
I-C4	58.124	1.547	3.447
N-C4	58.124	3.664	7.940
I-C5	72.151	0.757	1.588
N-C5	72.151	0.883	1.796
C6	86.200	0.505	0.965
MCYCL-C5	84.160	0.083	0.149
Benzene	78.110	0.022	0.047
CYCL-C6	84.160	0.056	0.098
C7	100.200	0.160	0.263
MCYCL-C6	98.190	0.048	0.081
Toluene	92.140	0.014	0.026
C8	114.230	0.059	0.118
C2-Benzene	106.170	0.005	0.006
M&P-XYLENE	106.170	0.004	0.007
O-XYLENE	106.170	0.001	0.001
C9	128.300	0.014	0.030
C10	134.000	0.005	0.009
C11	147.000	0.002	0.008
C12	161.000	0.002	0.003
C13	175.000	0.002	0.002
C14	190.000	0.001	0.002
C15	206.000	0.002	0.001
C16	222.000	0.000	0.001
C17	237.000	0.001	0.001
C18	251.000	0.000	0.000
C19	263.000	0.000	0.001

The molecular weight of the 1st stage sample was 26.19 g/mole and the density was 0.0037 g/cc. The molecular weight of the 2nd stage sample was 36.14 g/mole and the density was 0.0014 g/cc.

Note: The component molecular weights listed in these tables and used to convert the measured weight fractions into mole fractions represent average values which account for n-paraffins as well as undefined carbon numbers (such as cyclo-paraffins or naphthenes) contained in the oil. These values were selected based on extensive experience with previously analyzed crude oils by D.B. Robinson Research Ltd.

APPENDIX C

**SWELLING TEST DATA
ANASAZI FIELD
NAVAJO NATION
SAN JUAN COUNTY, UTAH**

Table C.1. Swelling test CO₂ concentration data.

Test No.	CO ₂ Concentration (Mole %)
1	0
2	20
3	40
4	60
5	75

Table C.2. Relative volumes of the liquid and vapor phases as a function of pressure at 130°F (54°C) (CO₂ concentration = 20 mole percent).

Pressure (psig)	Total Volume (cm ³)	*Relative Volume (cm ³ /cm ³)	Phase Volume (cm ³)		Observations
			Liquid	Vapor	
3,986	64.09	0.974	64.09	0.00	single phase
3,486	64.61	0.981	64.61	0.00	single phase
2,987	65.07	0.988	65.07	0.00	single phase
2,487	65.64	0.997	65.64	0.00	single phase
2,227	66.55	1.011	66.55	0.00	single phase
2,177	67.11	1.019	64.31	2.80	two phase
2,127	67.83	1.030	63.89	3.94	two phase
1,986	70.07	1.064	62.32	7.75	two phase

*Defined as the ratio of the total volume to the saturation volume

Table C.3. Properties of the saturated fluid with 20 mole percent CO₂ at 130°F (54°C).

Saturation Pressure (psia)	2,294.000
Saturation Volume (cm ³)	65.830
Bulk Density (g/cm ³)	0.678*
Swelling Factor	1.104**
Viscosity (cP)	0.349*

*Measured at 50 psi (345 kpa) above actual bubble point pressure

**Defined as the ratio of the saturation volume of CO₂/oil mixture to that of the virgin oil (59.61 cm³)

Table C.4. Relative volumes of the liquid and vapor phases as a function of pressure at 130°F (54°C) (CO₂ concentration = 40 mole percent).

Pressure (psig)	Total Volume (cm ³)	*Relative Volume (cm ³ /cm ³)	Phase Volume (cm ³)		Observations
			Liquid	Vapor	
4,486	70.04	0.967	70.04	0.00	single phase
3,987	70.61	0.975	71.61	0.00	single phase
3,486	71.21	0.983	71.21	0.00	single phase
2,986	71.97	0.993	71.97	0.00	single phase
2,525	72.93	1.007	not measureable	not measureable	two phase
2,430	73.73	1.018	60.46	4.69	two phase
2,351	74.58	1.029	67.32	7.26	two phase
1,986	80.99	1.118	61.84	19.15	two phase

*Defined as the ratio of the total volume to the saturation volume

Table C.5. Properties of the saturated fluid with 40 mole percent CO₂ at 130°F (54°C).

Saturation Pressure (psia)	2,585.000
Saturation Volume (cm ³)	72.450
Bulk Density (g/cm ³)	0.697*
Gravimetric Density (g/cm ³)	0.693*
Swelling Factor	1.215**
Viscosity (cP)	0.270*

*Measured at 50 psi (345 kpa) above actual bubble point pressure

**Defined as the ratio of the saturation volume of CO₂/oil mixture to that of the virgin oil (59.61 cm³)

Table C.6. Relative volumes of the liquid and vapor phases as a function of pressure at 130°F (54°C) (CO₂ concentration = 60 mole percent).

Pressure (psig)	Total Volume (cm ³)	*Relative Volume (cm ³ /cm ³)	Phase Volume (cm ³)		Observations
			Liquid	Vapor	
4,986	70.42	0.957	70.42	0.00	single phase
4,487	71.18	0.968	71.18	0.00	single phase
3,987	72.05	0.980	72.05	0.00	single phase
3,487	73.03	0.993	73.03	0.00	single phase
3,076	74.01	1.006	74.01	0.00	single phase
2,914	74.67	1.015	44.55	30.12	two phase
2,776	75.46	1.026	43.60	31.86	two phase
1,987	85.48	1.162	46.83	38.65	two phase

*Defined as the ratio of the total volume to the saturation volume

Table C.7. Visual determination of the bubble point pressure using small pressure drops for the Anasazi oil with 60 mole percent CO₂ concentration.

Pressure (psig)	Observations
3,100	clear single phase
3,090	starting to cloud
3,075	opaque
3,060	two phase

Table C.8. Properties of the saturated fluid with 60 mole percent CO₂ at 130°F (54°C).

Graphical P _{sat} (psia)	3,176.000
Visual P _{sat} (psia)	3,100.000
Graphical V _{sat} (cm ³)	73.550
Bulk Density (g/cm ³)	0.725*
Swelling Factor	1.234**
Viscosity (cP)	0.215*

*Measured at 50 psi (345 kpa) above actual bubble point pressure

**Defined as the ratio of the saturation volume of CO₂/oil mixture to that of the virgin oil (59.61 cm³)

Table C.9. Relative volumes of the liquid and vapor phases as a function of pressure at 130°F (54° C) (CO₂ concentration = 75 mole percent).

Pressure (psig)	Total Volume (cm ³)	*Relative Volume (cm ³ /cm ³)	% Liquid	Observations
7,986	75.43	0.965	0.00	single phase
7,486	75.69	0.968	0.00	single phase
6,986	76.49	0.978	0.00	single phase
6,487	77.07	0.986	0.00	single phase
5,986	77.87	0.996	0.00	single phase
5,487	78.76	1.007	not measureable	two phase
4,987	79.72	1.019	1.25	two phase
4,486	80.90	1.035	4.94	two phase
3,986	82.36	1.053	10.32	two phase
3,486	84.05	1.075	16.42	two phase
2,986	86.43	1.105	21.75	two phase
2,486	90.46	1.157	26.86	two phase
2,036	98.23	1.256	29.83	two phase

*Defined as the ratio of the total volume to the saturation volume

Table C.10. Properties of the saturated fluid with 75 mole percent CO₂ at 130°F (54° C).

Visual P _{sat} (psia)	5,800.000
Saturation Volume (cm ³)	78.200
Bulk Density (g/cm ³)	0.805*
Swelling Factor	1.215**
Viscosity (cP)	0.210

*Measured at 50 psi (345 kpa) above actual bubble point pressure

**Defined as the ratio of the saturation volume of CO₂/oil mixture to that of the virgin oil (59.61 cm³)

